Unterschrift BetreuerIn

TECHNISCHE
UNIVERSITÄT
WIEN
Vienna University of Technology

DIPLOMARBEIT

STRESS-PROTECTIVE GENES FROM TARDIGRADES

ausgeführt am Institut für Chemie und Molekulare Biologie
der Universität Göteborg

unter der Anleitung von
Per Sunnerhagen
(University of Gothenburg)
&
Robert Mach
(TU Wien)

durch

Tobias Schierscher

June 8, 2020

Unterschrift StudentIn

Abstract

From obtained stress-resistant yeast clones expressing tardigrade genes, plasmids are isolated, transformed into *E. coli* and then back-transformed into naive yeast (*S. cerevisiae*). Plasmids conferring stress tolerance are sequenced and sequence homologs from other species are identified through BLAST search on the amino acid level. Patterns of cross-resistance to multiple stressors (heat stress, oxidative stress, hyperosmosis) are examined among the transformants using the Scan-O-Matic microbial colony growth screening press and by recording growth in liquid media using Bioscreen. It was shown that a tardigrade gene that codes for a serum paraoxonase/arylesterase 1 is enhancing the resistance of *S. cerevisiae* to heat stress and osmotic stress.

Contents

List of Abbreviations and Symbols

LB Luria-Bertani

MCS multiple cloning site

WT wild-type

RT room temperature

LiAc lithium acetate

DMSO dimethyl sulfoxide

ITIS Integrated Taxonomic Information System

TDP tardigrade-specific intrinsically disordered protein

HSP heat shock protein

Mthsp mitochondrial heat shock protein

LEA late embryogenesis abundant

IDP intrinsically disordered protein

CAHS cytoplasmic abundant heat soluble

SAHS secretory abundant heat soluble

MAHS mitochondrial abundant heat soluble

ROS reactive oxygen specie

YAC Yeast Artificial Chromosome

tTA tetracycline transactivator

TRE tetracycline response element

DOX doxycycline

OD optical density

BLAST Basic Local Alignment Search Tool

NCBI National Center for Biotechnology Information

EST expressed sequence tags

ORF open reading frame

PON paraoxonase

HDL high-density lipoprotein

LDL low-density lipoprotein

SEM scanning electron microscope

FTIR fourier-transform infrared spectroscopy

DSC Differential scanning calorimetry spectroscopy

ON overnight

amp ampicillin

EtBr ethidium bromide

PC positive control

ERCC8 DNA excision repair protein

CS cockayne syndrome

CSB cockayne syndrome type B

UV ultraviolet light

CTF chromosome transmission fidelity

CTF18-RFC CTF18-replication factor C

1 Introduction

1.1 Tardigrada

Tardigrada is a phylum of water-dwelling eight-legged segmented metazoans. The 0.1 mm to 1.2 mm large animal, was firstly described by German zoologist Goeze in 1773.[1] Tardigrada is Latin and means slow-moving, because of their appearance and clumsy way of moving they are often referred to as water bears. Tardigrades are considered aquatic because they need to be surrounded by water to permit gas exchange as well as to prevent uncontrolled desiccation.[2] They live worldwide in the sea, freshwater or in humid habitats on land, where they are especially found in moss and linches. Tardigrades are exceptional among metazoans because they are found in a broad range of extreme habitats such as mountain tops, deep sea, mud volcanoes and Antarctic.[3] Ramazzotti classified Tardigrada as a phylum in 1962.[4] Currently, there are approximately 1200 described species according to Integrated Taxonomic Information System (ITIS) Aforementioned, tardigrades need to be surrounded by water to be in their active, feeding and reproducing stage. Nevertheless, numerous species that invaded terrestrial environments, where they endure periods of dehydration by entering a stage of life called cryptobiosis. There are two main evolutionary lines within the phylum of Tardigrada, Eutardigrada and Heterotardigrada. While Eutardigrades are semi-terrestrial, Heterotardigrades consists of the order Echiniscoidea[5] and Arthrotardigrada[6], in which arthrotardigrades are only present in the ocean and echiniscoideans are limno-terrestrial.[7] Within the order of Echiniscoidea there are four families, the marine Echiniscoididae and three limno-terrestrial families (Echiniscidae, Carphanidae and Oreelidae). *Echiniscus testudo (E. testudo)* belongs to the family Echiniscidae and is distributed on all continents except Australia and Antarctica and was *E. testudo* firstly described by Doyère in 1840.[8] [9]

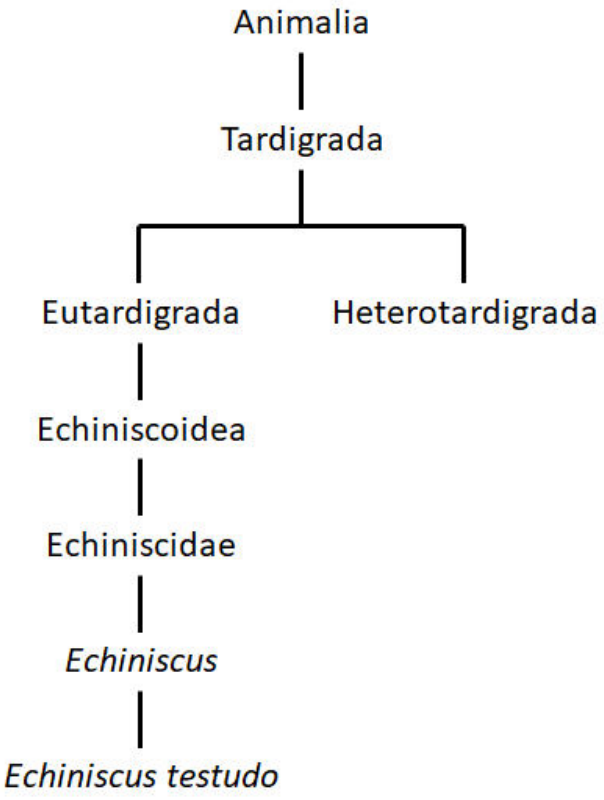

Figure 1.1: Tree of life of *E. testudo*

Cryptobiosis is characterized by a quick response to sudden environmental changes and is believed to be ametabolic.[7] [2] [10] All in all, limno-terrestrial tardigrades can enter cryptobiosis in response to five extreme conditions, namely these are: anhydrobiosis, cryobiosis, osmobiosis, anoxybiosis and chemobiosis. Among these stages, anhydrobiosis - the response to desiccation - is the best understood.[10] While entering anhydrobiosis tardigrades form a so-called "tun", which is a controlled packaging of organs, cells and cell organelles.[11] [12] Remarkably, tardigrade in the anhydrobiotic stage of live can survive a broad range of extreme environments, *e.g.*: temperatures from −253 °C up to 151 °C, pressures from the space vacuum up to 600 MPa and UV radiation up to 6000 Gy.[13] [14] [15] In figure 1.2 a scanning electron microscope (SEM) of *M. tardigradum* in the active form and after dehydration is shown.

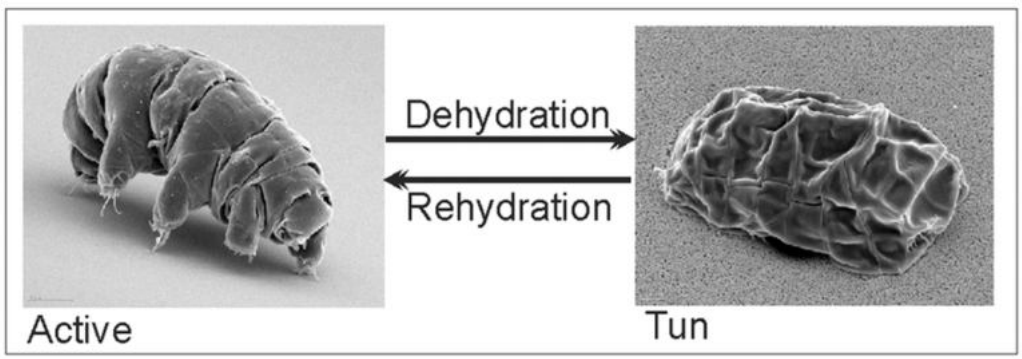

Figure 1.2: SEM images of *M. tardigradum* in the active stage and in the dehydrated state called tun[16]

1.1.1 Adaptions to Extreme Environments

The growth, survival and reproduction of organisms is strongly affected by stressful environmental conditions such as extreme pH, high or low salinity and temperature. These conditions may induce dormancy in form of various resting stages. One of these forms, cryptobiosis, is characterized by a quick response to sudden environmental changes. Another, slower form of dormancy is diapause, which occurs in species that live in habitats affected by seasonal changes.[7] Limno-terrestrial species exhibit cryptobiosis, which is a dormant state referred to as a reversible ametabolic state induced by unfavourable environmental conditions. Cryptobiosis is often executed by species living in limno-terrestrial habitats, that frequently dries or freezes, but also by species that experience large fluctuations in *e.g.* osmotic pressure and oxygen tension.[17] Among limno-terrestrial species there are four types of cryptobiosis occurring: dehydration (anhydrobiosis), low temperature (cryobiosis), lack of oxygen (anoxybiosis) and high salt concentration (osmobiosis).[2] Since anhydrobiosis is the best understood and described form of cryptobiosis, it is explained in more detail below.

1.1.2 Anhydrobiosis

Anhydrobiosis means "life without water" and is characterized by a desiccated state to withstand extreme fluctuations in water availability and temperature.[18] Beside tardigrades there are several other species performing anhydrobiosis, *e.g.* cyanobacteria, yeasts, linches, algae, mosses, some plant seeds and bacterial, fungal and protist spores. A slow rate of water loss seems to be essential to allow molecular changes to occur. Some organisms rely on their habitat to slowly dry out such as invertebrates living in moss or soil. Others, which live in a more exposed habitat such as linches, soil surfaces and aerial parts of plants, have developed mechanisms to keep the water loss rate as low as possible. This is possible by reducing the area through which water can be lost. As already mentioned, limno-terrestrial tardigrades are forming a tun, which is characterized by a contracted body and keeps the water loss rate as low as possible by reducing its surface. The mechanism of anhydrobiosis is illustrated in figure 1.3, it shows how crucial a low water loss rate is for tardigrades to survive desiccation.[7] Moreover, heat shock proteins (HSPs), which serve as molecular chaperones, and tardigrade-specific intrinsically disordered proteins (TDPs) are up-regulated and help to prevent the formation of damaging cellular compartments aggregates and is indispensable for surviving desiccation. In the state of anhydrobiosis adult tardigrades can spend long periods, from few months to several years. The longest documented survival time in anhydrobiosis has been reported for *E. testudo.*[19] Schill et al. (2008) investigated the desiccation tolerance in embryonic stages and they found that the humidity level and the developmental stage are both significant factors in determining successful hatch rates. In general, they described that the less developed the more sensitive tardigrades are to desiccation.[20]

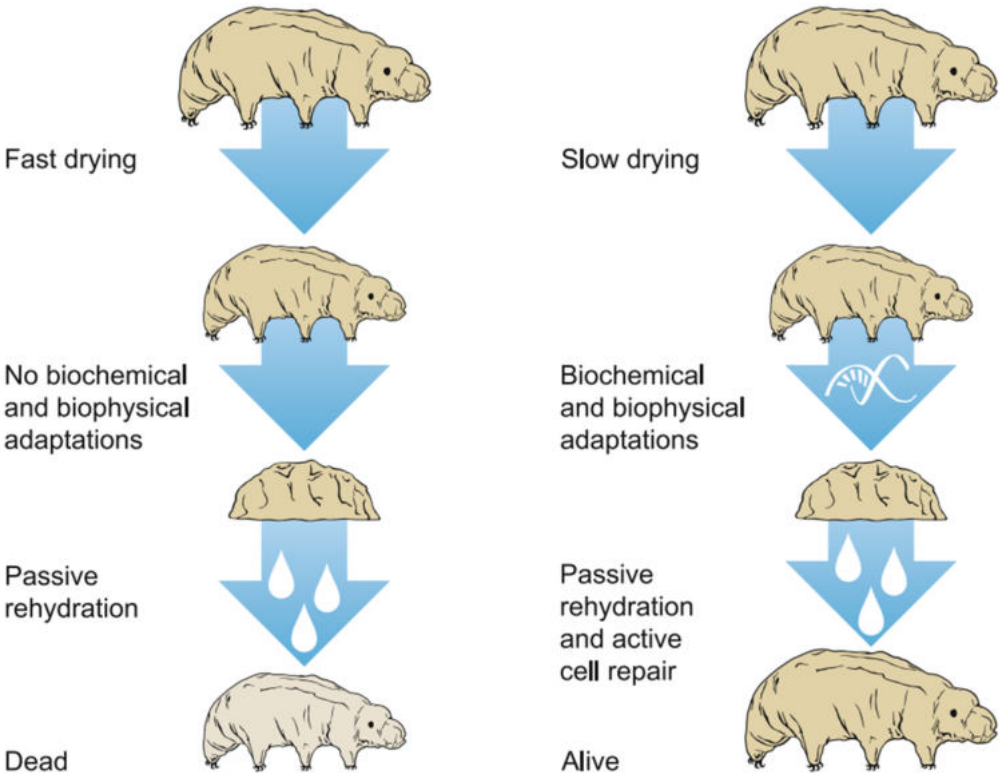

Figure 1.3: Effect of water loss rate on tardigrades during desiccation [7]

Heat Stress Proteins

Despite called HSP the induction is not only due to temperature effect but also to a whole other series of environmental stress factors. These proteins are highly conserved and ubiquitous in all organisms. [21] They play a crucial role in folding newly synthesized proteins, intracellular protection against protein-denaturing factors, folding/unfolding of damaged proteins, assembly of multiprotein complexes, transport/sorting of proteins into correct subcellular compartments, cell-cycle control and signalling and protection of cells against stress/apoptosis. [22] HSPs are classified based on their molecular weight: *hsp10, hsp40, hsp60, hsp70, hsp90*, etc. [22]

In embryos of the brine shrimp species *Artemia franciscana* large amounts of two small stress proteins,p26 and artemin, were found. [23] [24] p26 belongs to the small heat shock/α-crystallin protein family that has shown molecular chaperon activity *in vitro* and *in vivo*. [25] [26] Artemin, on the other hand, might play a role as a molecular chaperone for RNA. [27] Reuner et al. (2010) showed by creating several expressed sequence tagss (ESTs) of the eutardigrade *Milnesium tardigradum* that it possesses proteins that contain a small Hsp/α-crystalline domain, which are significantly up-regulated by heat stress. [28] The proteins are designated based on their molecular mass and occurrence in mitochondria as Mthsp19.5 and Mthsp17.2. Moreover, the library contained the coding sequence for HSP10 (chaperonin) and HSP60, which are found in the mitochondrion and cytoplasm and act as a chaperone and functional regulator, respectively. [28] Schill et al. (2004) showed that in *M. tardigradum* three isoforms of Hsp70 are up-regulated during a heat shock. [29] However, only isoform 2 was significantly induced in the transitional stage between the active and cryptobiotic stage and is found in the anhydrobiotic stage. [29] It has already been shown that RNA is accumulated in prokaryotic and eukaryotic cells during anhydrobiosis. Yeast studies showed that Hsp70 does not protect the yeast from dehydration stress during desiccation. [30] Thus, Hsp70 is probably only translated after rehydration to fold newly

synthesized protein and does not protect the cell during desiccation.

Metabolites for Cell Protection

Loss of intracellular water results in massive damage of proteins and membranes, that results mostly in cell death. Proteins and membranes compensate the loss of hydrogen bonds with water by hydrogen bonding with other molecules, which can lead to irreversible conformational changes and results in loss of enzyme activity and phase transition of membranes.[31] [32] Therefore, molecular interactions are controlled by replacing lost hydrogen bonds with reversible molecular interactions. The water replacement and the vitrification hypotheses describe how these molecular interactions are controlled by the cell.

The water replacement was firstly described by Webb et al. (1965), the hypothesis suggests that proteins interact with free hydroxyl groups of sugar molecules during and after removal of water.[33] In the hydrated state the phosphatidylcholine headgroup of the phospholipids is associated with 10 water molecules. When water is removed, the packaging density of the phosphatidylcholine headgroups increases, leading to increased van der Waals interactions between the hydrocarbon chains. As a result, the glass transition temperature (T_g) increases significantly (up to 70 °C) and thus the lipid layer is in the rubbery state at room temperature.[34] It has been shown that T_g decreases when the water content is increased.[35] The problem of this transition state is that the lipid bilayer becomes leaky especially during dehydrating. T_g is not affected until all water is removed and is not leaky when the temperature is above T_g during dehydration.[34] [36] In contrast, when membranes are dried in the presence of trehalose, the sugar molecules prevent interactions between the hydrocarbon chains by "replacing" water. Consequently, T_g is not increasing as much as it does without trehalose, which means that the system can be hydrated at lower temperatures.[34] It is well known that in *S. cerevisiae* trehalose is essential for survival after long-term desiccation.[37] [38] However, Hengherr et. al (2008) showed the trehalose level in tardigrades are rather low compared to the ones in yeasts.[39] In addition to that, they demonstrated that the trehalose level did not increase during desiccation in the heterotardigrades *E. testudo*.

The vitrification hypothesis proposes that a mixture of accumulate non-reducing sugars and highly hydrophilic proteins enter a glassy state during dehydration and thereby immobilize membranes and macromolecules preventing them from denaturation, coagulation, and disintegration. Moreover, this glassy state greatly reduces the reaction kinetics. Above T_g but below the eutectic point of the constituents, the product is in a highly viscous state leading to a transformation of an unstable amorphous liquid into a meta-stable amorphous solid state. Differential scanning calorimetry spectroscopy (DSC) and fourier-transform infrared spectroscopy (FTIR) were used to prove the water replacement and vitrification hypotheses and that trehalose plays an essential role during desiccation.[40] But how can tardigrades survive desiccation even though they do not accumulate trehalose? It has been shown that TDPs and late embryogenesis abundant (LEA) proteins are up-regulated during desiccation and may play a crucial role.[41]

Tardigrade-Specific Intrinsically Disordered Proteins

Despite the well-known lock-and-key model, that describes proteins as highly structured molecules determined by the amino acid sequence, many protein functions do not require a unique structure.[42]

In plants, the expression of hydrophilic and disordered proteins, in particular LEA proteins, is associated with water stress. LEA proteins were first identified in plants during seed development, where they accumulate to high concentrations in embryo tissues before desiccation.[43] These small proteins are ubiquitous in land plants, but also occur in bacteria and yeast, and most of them belong to the "hydrophilins" family, a group of highly hydrophilic intrinsically disordered proteins (IDPs) characterized by a biased amino composition enriched in glycine and other small residues that favors a flexible conformation in aqueous solutions.[44] [45] However, tardigrades express predominantly TDPs, such as cytoplasmic abundant heat soluble (CAHS), and secretory abundant heat soluble (SAHS) proteins, which are secreted or localized in most intracellular compartments, except the mitochondrion.[46] There is a special heat-soluble protein that is localized in mitochondria (mitochondrial abundant heat soluble (MAHS) protein). It has been shown that these TDPs are constitutively expressed at high levels or induced during desiccation in tardigrade species such as *Hypsibius dujardini* and *Paramacrobiotus richtersi*.[41]

DNA Damage during Anhydrobiosis

DNA is a preferred biological target of reactive oxygen species (ROSs), as shown later ROSs is formed spontaneously from chemical degradation of various substances in the metabolism and has negative effects on proteins, membranes and DNA. Since the metabolism is shut down during anhydrobiosis energy-dependant repair systems cannot be activated, which leads to an accumulation of DNA damage. Thus, it is indispensable for tardigrades to remove ROS to protect their DNA.

1.2 Yeast as a Model System

In this study the budding yeast *Saccharomyces cerevisiae (S. cerevisiae)* was used as a model system. Despite having a more complex genetic than bacteria (containing 3.5 times more DNA than *Escherichia coli (E. coli)*) *S. cerevisiae* is a popularly used model system and shares a lot of properties *e.g.* rapid growth, dispersed cell, the ease of replica plating and mutant isolation, a well-defined genetic system, and a highly versatile DNA transformation system. Another important fact is that this *S. cerevisiae* is non-pathogenic, cheap, and easy and fast to cultivate *in vitro* in the laboratory. Furthermore, the development of DNA transformation has made *S. cerevisiae* accessible to gene cloning and genetic engineering. It is possible to introduce plasmids, either as replicating molecules or by integration into the genome. The integrative recombination proceeds exclusively via homologous recombination and has led to well established techniques for direct replacement of genetically engineered DNA sequences into their normal chromosome locations. Thus, mutations can be introduced easily and has contributed toward understanding protein function *in vivo*.

In addition, *S. cerevisiae* have been valuable for studies of other organisms using the two-hybrid screening system for detection of protein-protein interactions, Yeast Artificial Chromosomes (YACs) for cloning large DNA fragments and expression system for preparation of heterologous proteins.[47]

A lot of shuttle vectors for *S. cerevisiae* and *E. coli* are commercially available. In this study, YC-type (centromeric) shuttle expression vector pCM188 (ATCC$^{(R)}$ 87660^{TM}) was used to express heterologous proteins in *S. cerevisiae* (see the map of pCM188 at supplementary material).[48] It makes use of the Tet-Off system, where a tetracycline transactivator (tTA), a fusion protein of *E. coli*, tetracycline repressor and the activation domain of VP16 (Herpes Simplex) binds at the specific tetracycline operator sequences, placed upstream of a CMV promoter. Several repetitive TetO sequences with

a minimal promoter is called a tetracycline response element (TRE). Binding of tTA to TRE leads to the expression of the gene of interest. However, when tetracycline or its more stable analogous doxycycline (DOX) is present, it binds tTA and it is incapable of binding to the TRE sequences, hence the transactivation of the gene of interest is repressed.

2 Aim and Motivation

Tardigrades have shown unique proteins that enhance resistance to several stress conditions including UV radiation, heat stress and oxidative stress. In this study a novel approach was chosen to find tardigrade unique proteins that enhances resistance. While other approaches are based on bioinformatic tools to pull out new genes, by comparing expressed sequence tags in unstressed and stressed tardigrade species to identify upregulated genes, this approach is based on a functional shotgun approach. Therefore, an EST of *E. testudo* was constructed and transformed into *S. cerevisiae* BY4741 to obtain a library full with transformed *S. cerevisiae* BY4741 containing *E. testudo* genes. The library was screened to different stress conditions and if enhanced growth was visible, the clone was isolated. Subsequently, the plasmid was extracted, sequenced, and checked if the gene is originating from *E. testudo*.

The goal of this project is to verify the original stress resistance, but also to identify cross-resistance. Furthermore, more In this project already identified stress conferring clones were tested again in order to confirm the original stress-resistance but also to find cross-resistance to other stress factors.
The aim is to screen for tardigrade unique proteins that can find use in medical and industrial applications. For instance, TDPs could be used to preserve biological materials, such as tissues for transplantations, blood for transfusion, semen for artificial insemination, micro-organisms for type cultures, seeds for germination and certain articles of food.[2] Furthermore, it is very likely that tardigrades have unique proteins that prevent damage to DNA and repair damaged DNA. Those proteins are probably involved in the desiccation/radiation tolerance of tardigrades and can be interesting for space research.[49]

3 Materials and Methods

3.1 Materials

3.1.1 Equipment

Following is a list of materials used during the project (without quantities of usage).

- Pipettes for handling liquids
  - Single pipettes: 10 µL, 20 µL, 100 µL, 1000 µL - *Eppendorf AG*
  - Multichannel pipette: 100 µL - *Eppendorf AG*
  - Serological pipettes: 10 mL, 25 mL, 50 mL - *Eppendorf AG*
- Micro-reaction tubes: 0.2 mL, 1.5 mL - *Eppendorf AG*
- Reaction tubes: 15 mL, 50 mL - *SARSTEDT AG & Co. KG*
- Petri dishes: 92 x 16 mm - *SARSTEDT AG & Co. KG*
- Scan-o-matic
  - 200 SBS format plus plates - *Singer*
  - RePads: 96 long, 1536 short - *Singer*
  - HDA RoToR robot - *Singer*
  - Epson Perfection V700 PHOTO scanners - *Epson Corporation*
- Gel electrophoresis
  - PowerPac^{TM} Basic Power Supply - *Bio-Rad Laboratories, Inc.*
  - Sub-Cell GT Cell - *Bio-Rad Laboratories, Inc.*
- Bioscreen C
  - Honeycomb plate
  - E1-ClipTip Equalizer 8-ch 10-300 l Pipette
  - Bioscreen C MBR

3.1.2 Chemicals

- NaCl - ACS, ISO, Reag. Ph Eur - *Merck KGaA*
- Yeast extract granulated - *Merck KGaA*
- Tryptone - *Merck KGaA*

- KCl - $\geq$ 99% - *Sigma-Aldrich*
- $MgSO_4 \cdot 7\,H_2O$ - ACS, Reag. Ph Eur - *Merck KGaA*
- $MgCl_2 \cdot 6\,H_2O$ - ACS, Reag. Ph Eur - *Merck KGaA*
- D(+)-glucose anhydrous - ACS - *VWR International*
- Peptone - *Merck KGaA*
- Adenine hemisulfate salt - $\geq$ 99% - *Sigma-Aldrich*
- Succinic acid - $\geq$ 99% - *Sigma-Aldrich*
- NaOH - EMSURE$^{(R)}$ - *Merck KGaA*
- $(NH_4)_2SO_4$ - ACS, ISO, Reag. Ph Eur - *Merck KGaA*
- Difco^{TM} yeast nitrogen base w/o amino acids and ammonium sulfate - LOT5341888 - *Becton, Dickinson and Company*
- CSM DROP-OUT: -URA - LOTFM0120/9974 - *Formedium Ltd*
- Na_2HPO_4 - ACS, Reag. Ph Eur - *Merck KGaA*
- KH_2PO_4 - *Merck KGaA*
- PIPES - $\geq$ 99% - *Duchefa Farma B.V.*
- $CaCl_2 \cdot 2\,H_2O$ - ACS - *Scharlau*
- Poly(ethylene glycol) - average Mn 3350 - *Sigma-Aldrich*
- $C_2H_3LiO_2 \cdot 2\,H_2O$ - *AppliChem Panreac ITW companies*
- Salmon Sperm DNA Solution - *Invitrogen*
- DOX hydrochloride - *Sigma-Aldrich*
- Anhydrotetracycline hydrochloride - *Abcam*
- H_2O_2 - 30 % - *Sigma-Aldrich*
- ampicillin (amp) sodium salt - *Sigma-Aldrich*
- Difco^{TM} Agar - *Becton, Dickinson and Company*

3.2 Media and Buffers

- LB-medium:	1 % NaCl 1 % tryptone 0.5 % yeast extract
- SOB-medium:	2 % tryptone 0.5 % yeast extract 10 mM NaCl 2.5 mM KCl 10 mM $MgCl_2$ 10 mM $MgSO_4$
- SOC-medium:	SOB-medium + 2 % glucose
- YPAD:	1 % yeast extract 2 % peptone 2 % glucose 0.004 % adenine sulfate
- 10 x YNB:	100 g L^{-1} succinic acid 60 g L^{-1} NaOH 50 g L^{-1} $(NH_4)_2SO_4$ 19 g L^{-1} YNB
- 10 x CSM-URA:	7.7 g L^{-1} CSM-URA
- YNB-URA media:	1 x YNB 1 x CSM-URA 2 % glucose
- 10 x PBS (pH 7.4):	1.37 M NaCl 0.027 M KCl 0.1 M Na_2HPO_4 0.018 M KH_2PO_4
- TAE-buffer (pH 8.0)	40 mM tris base 20 mM acetic acid 1 mM EDTA sodium dihydrat
- Transformation buffer (pH 6.7):	0.01 M PIPES 0.015 M $CaCl_2$ 0.25 M KCl 0.055 M $MnCl_2$
- Transformation mix :	240 µL 50 % PEG 3350 36 µL 1 M LiAc 50 µL 2 mg mL^{-1} ss-DNA 33 µL H_2O

3.3 Methods

3.3.1 Strains

In this study *S. cerevisiae* BY4741 was used. BY4741 is part of a set of deletion strains derived from S288C in which commonly used selectable marker genes were deleted in order to minimize homology to the corresponding marker genes in commonly used vectors without significantly affecting adjacent gene expression.[50] In the following the genotype of the used strains are shown:

WT: MATa his3Δ1 leu2Δ0 met15Δ0 ura3Δ0
PC: MATa his3Δ1 leu2Δ0 met15Δ0 ura3Δ0 pdr5Δ

Miyahara et al. showed that PDR5 mutants have increased sensitivity to NaCl, LiCl and $MgCl_2$, it is proposed that Pdr5 contributes to cation resistance by regulating cellular cation homeostasis under ionic stress conditions. Furthermore, Pdr5 has a detoxifying effect on yeast cells.[51] [52]

3.3.2 Screening

The library was screened for hyperosmotic stress (1.5 M KCl in the growth media), hyperosmotic and ionic toxicity (1.2 M NaCl in the growth media), oxidative stress (H_2O_2 in the growth media) and heat stress (at 42 °C). Colonies were picked, cultured and stored at −80 °C.

3.3.3 Growth Conditions

Bacterial Growth Conditions

E. coli strain NEB10-beta was used to amplify the empty plasmid pCM188 and the ones containing cDNA sequences in the multiple cloning site (MCS). Transformed NEB10-beta cells were selected on Luria-Bertani (LB) media plates containing 100 µg mL^{-1} amp and were grown at 37 °C overnight (ON). Obtained colonies were grown in liquid LB media supplemented with 100 µg mL^{-1} amp ON at 37 °C and 200 rpm. Plasmid extraction was performed using GeneJET Plasmid Miniprep Kit from Thermo Fisher Scientific.

Yeast Growth Conditions

S. cerevisiae BY4741 was used to amplify the empty plasmid pCM188 and those containing cDNA sequences and thus, grown in YNB-URA media at 30 °C and 200 rpm if needed. Native *S. cerevisiae* BY4741 was grown in YPD to perform subsequent transformation at the same condition as stated before. Plasmid extraction was performed using Zymoprep™ Yeast Plasmid Miniprep II.

3.3.4 Transformation

Bacterial Transformation

Competent NEB10-beta cells were prepared according to H. Inoue et al. (1990)[53]. Briefly, NEB10-beta was streaked on LB media and incubated ON at 30 °C. The next day a single colony was picked and inoculated in 5 mL SOB media and incubated for 4 h to an optical density (OD) of 0.66. The culture was diluted to an OD of OD 0.01 with a total volume of 250 mL and incubated at 17 °C and 225 rpm. Before harvesting, the culture was put on ice for 15 min. After, the culture was harvested by centrifuging for 10 min at 2456 xg and 4 °C. Subsequently, 80 mL of Transformation Buffer was added

to the pellet and suspended by flicking and inverting the tube. The culture was further incubated on ice for another 10 min. The culture was pelleted by centrifuging at the same conditions as before. The pellet was suspended in 20 mL Transformation buffer, 1.5 mL dimethyl sulfoxide (DMSO) was added and incubated on ice for another 10 min. The cell suspension was aliquoted in 1 mL in CryoTubes™ and immediately frozen in liquid nitrogen. Finally, they were stored at −150 °C for a few days and then transferred to −80 °C.

For the transformation competent NEB10-beta cells were thawed on ice and circa 50 ng plasmid DNA was added to 50 µL competent cells. After 40 min incubation on ice, heat shock was performed at 42 °C for 60 s. Afterwards, the mixture was put on ice for at least 5 min, 450 µL SOC medium was added and incubated at 37 °C for 45 min. After the incubation, 100 µL of the culture was plated on LB plates containing 100 µL amp and incubated ON at 37 °C.

Yeast Transformation

Yeast *S. cerevisiae* transformation was performed according to the LiAc/SS carrier DNA/PEG method as described by Gietz at al. (2007).[54] Briefly, *S. cerevisiae* BY4741 was incubated ON at 30 °C and 200 rpm. The next day, the culture was diluted to an OD of 0.1 and incubated to an OD of around 0.4 at 30 °C and 200 rpm. The culture was centrifuged for 5 min with 3000 G and the pellet was washed with 25 mL water. Subsequently, the pellet was suspended in 1 mL 100 mM lithium acetate (LiAc) and incubated for 12 min at 30 °C. The suspension was aliquoted to 100 µL and centrifuged for 1 min with 20 600 G. The pellet was suspended in 359 µL transformation mix and 1 µL of plasmid DNA was added. The transformation mix was first incubated for 30 min at 30 °C and then heat shocked for 30 min at 42 °C. Afterwards, the transformation mix was centrifuged for 1 min and 20 600 G and resuspended in 1 mL water. A dilution of 1:10 was prepared and 100 µL was plated on a YNB-URA plate. The plate was incubated at 30 °C for 2 days.

3.3.5 Agarose Gel Electrophoresis

All agarose gel electrophoresis were performed with 1 % (w/v) agarose gel in 1x TAE buffer containing 0.5 µg mL^{-1} ethidium bromide (EtBr) and run at 90 V for 70 min.

3.3.6 Phenotypic Characterization

To obtain the phenotypes of the clones, several different tests were performed. On the one hand the stressor was supplemented into the Agar-plates and clones were shocked with the stressor. The conducted steps are described in the following.

3.3.6.1 Resistance Test

First, wild-type (WT) and clones were streaked on YNB-URA plates and incubated for 2 to 3 days at 30 °C. Colonies were picked and inoculated in 2 mL YNB-URA medium and incubated ON. Then, the ON culture was diluted to an OD of 0.2 and incubated. After 5 hours, the OD was measured and diluted if necessary. Afterwards, 1:10, 1:100 and 1:1000 dilutions were prepared in a 96-well plate using YNB-URA supplemented with 2 µg mL^{-1} DOX. Eventually, a spot assay was performed on YNB-URA plates using a replicator and the plates were incubated for 2 to 3 days at 30 °C, unless other indicated.

3.3.6.2 Survival Test

Heat Stress by Spot assay

WT and clones were streaked on YNB-URA plates and incubated for 2 to 3 days at 30 °C. Colonies were picked and inoculated in 2 mL YNB-URA medium and incubated ON. Then, the ON culture was diluted to an OD of 0.2 and incubated. After 5 hours, the OD was measured and diluted if necessary. 0.5 mL of the culture was transferred to an 1.5 mL Eppendorf tube and incubated for 1 h and 300 rpm at 45 °C, 46 °C, 47 °C and 48 °C, respectively. Afterwards, 1:10, 1:100, and 1:1000 dilutions were prepared in a 96-well plate using YNB-URA supplemented with 2 µg mL^{-1} DOX. Finally, a spot assay was performed on YNB-URA plates using a replicator and the plates were incubated at 30 °C for 2 to 3 days.

Oxidative Stress by Spot Assay

WT and clones were streaked on YNB-URA plates and incubated for 2 to 3 days at 30 °C. Colonies were picked and inoculated in 2 mL YNB-URA medium and incubated ON. Then, the ON culture was diluted to an OD of 0.2 and incubated. After 5 hours, the OD was measured and diluted if necessary. 0.5 mL of the culture was transferred to an 1.5 mL Eppendorf tube. Subsequently, H_2O_2 was added to a concentration of 2 mM, 3 mM, and 4 mM, and incubated for 2 h at 30 °C.Afterwards, 1:10, 1:100, and 1:1000 dilutions were prepared in a 96-well plate using YNB-URA supplemented with 2 µg mL^{-1} DOX. Finally, a spot assay was performed on YNB-URA plates using a replicator and the plates were incubated at 30 °C for 2 to 3 days.

3.3.7 Scan-o-matic

Clones were collected in 96-well plates and then pined onto YNB-URA and YNB-URA supplemented with 1 µg mL^{-1} anhydrotetracycline plates containing 2 % agar using 1536 positions. Thus, each well of the 96-well plate is present at 4 positions. The WT was pinned on every fourth position, hence it was present at 384 positions. Then, the plates are incubated for 3 days at 30 °C and was used as a pre-culture for further experiments. The pre-culture was pinned on new YNB-URA and YNB-URA supplemented with 1 µg mL^{-1} anhydrotetracycline plates, and on plates containing 1.5 M KCl - with and without 1 µg mL^{-1} anhydrotetracycline. The plates were incubated for 3 days, pictures were taken every 20 min.

3.3.8 Bioscreen

The growth in liquid media was recorded using the instrument called "Bioscreen C Analyzer". The machine is measuring the OD over time while it provides constant incubating temperature and linear shaking to assure homogeneity. The cultures were placed inside the analyzer in Honeycomb microplates. Colonies were inoculated in 5 mL YNB-URA and grown ON at 30 °C. A 10 fold concentrated dilution series of DOX were prepared and 30 µL were transferred to the Honeycomb microplates. 270 µL of the culture with an OD of 0.111 was added to each well. The plates were placed inside the Bioscreen C Analyzer and run at 30 °C and 40 °C, continuous shaking with slow speed and low amplitude, measurement interval of 20 min, just the filter at 420−580 nm and a lenght of 3 days.
Each culture was tested on a series of different DOX concentrations. The positive control, without DOX, was at the first four positions. The dilution series was added from the highest to the lowest concentration. Furthermore, 20 negative controls were included.

4 Results and Discussion

4.1 Initial Screening of T-HS and T-OX Clones

Clones isolated by heat stress are labeled with the abbreviation T-HS, the ones that are extracted by oxidative stress are labeled as T-OX in the following. The screening process was repeated to check if the extracted clones did not survive by chance. In addition, cross-resistance to heat, oxidative and osmotic stress was investigated. Since the repression of the gene of interest with DOX only had a slight or no effect, plates with supplemented DOX are not shown. To get a better overview only plates where an effect is visible are displayed here. The remaining plates can be found in the supplementary.

4.1.1 Heat Stress

4.1.1.1 Heat Shock

9. Plate

Figure 4.1 shows T-HS1, 4, 5, 6 and 8, that were treated at 46 °C for 1 h and grown on YNB-URA plates for 2 days at 30 °C. Compared to the control in figure 4.2 that were not treated and grown on YNB-URA plates for 2 days at 30 °C, T-HS1, 4, 5 and 6 show better survival rates than the WT.

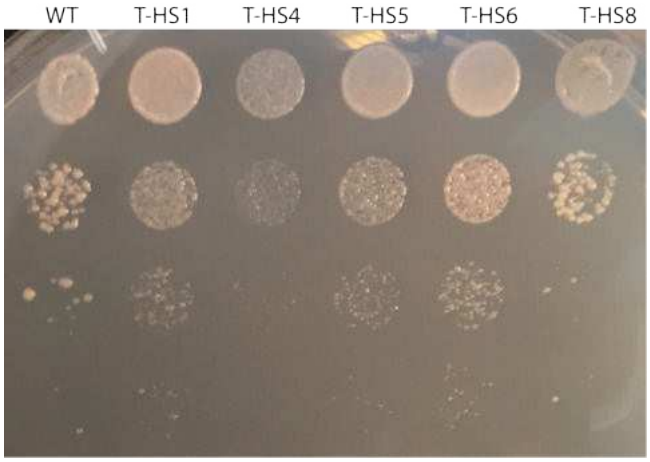

Figure 4.1: Cells treated at 46 °C for 1 h, plated on YNB-URA and grown at 30 °C for 48 h

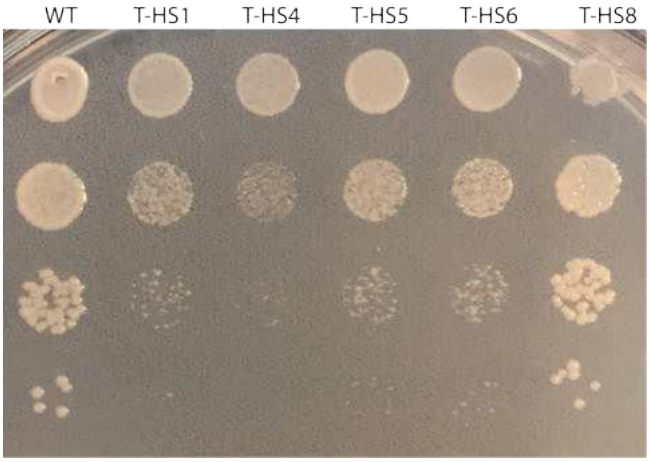

Figure 4.2: Control: Untreated cells plated on YNB-URA and grown at 30 °C for 48 h

Even though, the cells were heat-shocked at 48 °C for 1 h T-HS1, 4, 5 and 6 do not seem to be affected by the higher temperature, which is well visible when the treated cells were grown on YNB-URA at 30 °C for 3 days (figure 4.4).

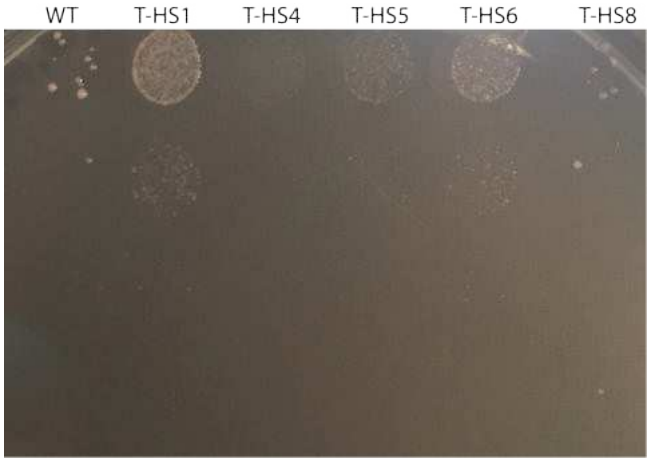

Figure 4.3: Cells treated at 48 °C for 1 h, plated on YNB-URA and grown at 30 °C for 48 h

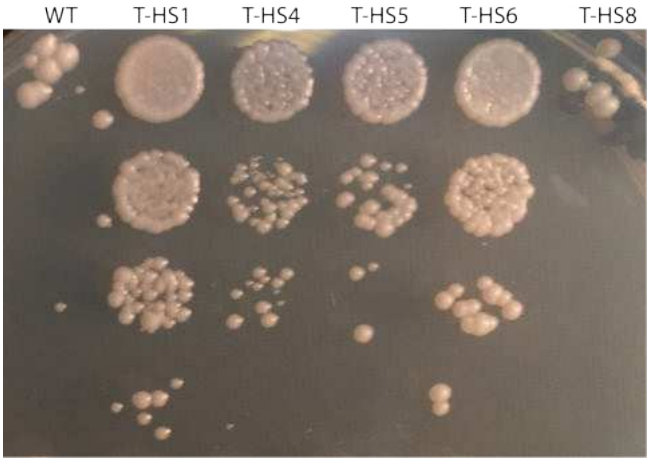

Figure 4.4: Cells treated at 48 °C for 1 h, plated on YNB-URA and grown at 30 °C for 72 h

11. Plate

In figure 4.5 heat stressed cells of T-HS18, T-HS20 and T-HS21 are shown. It is obvious that T-HS20 and T-HS21 are able to survive heat shock at 47 °C for 1 h better than the WT and T-HS18. Again the plates were incubated for a longer time and the survival effect is better visible after 72 h (visible in figure 4.7).

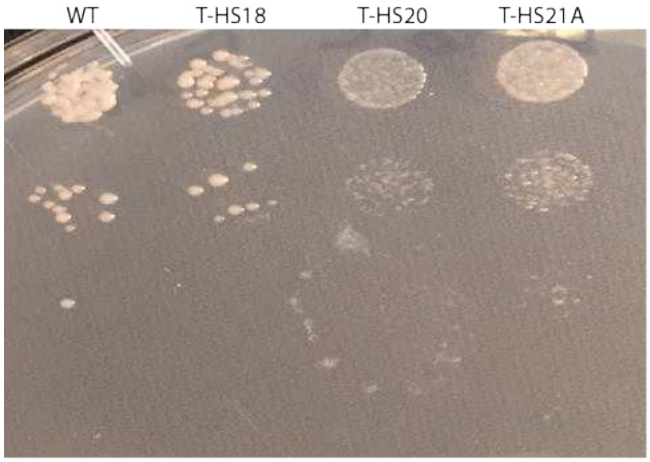

Figure 4.5: Cells treated at 47 °C for 1 h, plated on YNB-URA and grown at 30 °C for 48 h

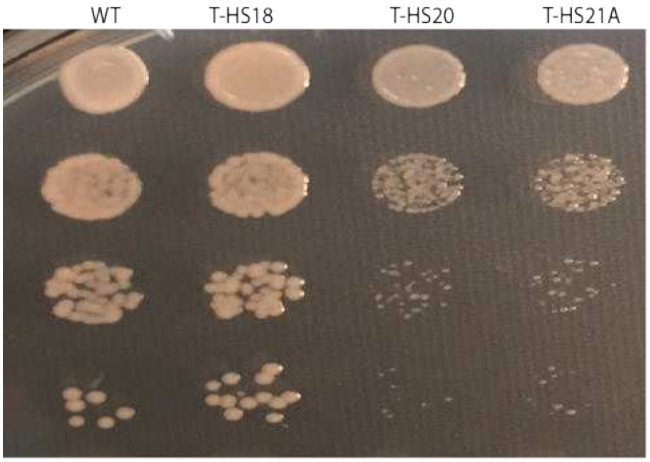

Figure 4.6: Control: Untreated cells plated on YNB-URA and grown at 30 °C for 48 h

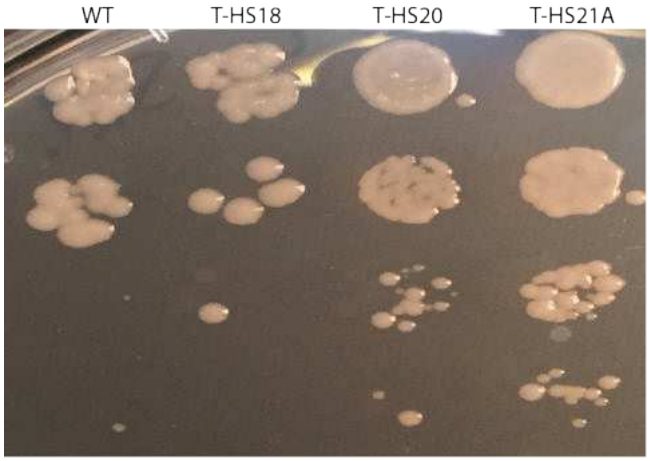

Figure 4.7: Cells treated at 47 °C for 1 h, plated on YNB-URA and grown at 30 °C for 72 h

4.1.1.2 Continuous Growth at 40 °C

To test if clones are able to grow at a higher temperature, cells were plated on YNB-URA ± 2 µg mL^{-1} DOX plates, wrapped up with parafilm and placed inside a bag to avoid drying out during incubation at 40 °C for a few days.

14. Plate

Figure 4.8 shows the continuous exposure to 40 °C of T-HS1, 4, 5, 6 and 8. T-HS1, 4, 6 and 8 show better growth than the WT. Interestingly is that when DOX was added to the media, the clones growth was enhanced, even though gene expression should be repressed under those conditions. Also the WT was growing better at 40 °C, when DOX was supplemented. It is well known that DOX disturbs mitochondrial proteostasis and that it can prolong lifespans of organisms.[55] The disruption only leads to a smaller yield when fermentable substrates are not available, which is not the case here since glucose was the C-source and can be anaerobically metabolised.[56] Thus, a main source of ROS formation - the oxidative pathway - is shut down when DOX is added, which might result in a higher yield. Furthermore, DOX has a radical-scavenging effect, it is able to directly scavenge superoxides, but not H_2O_2.[57]

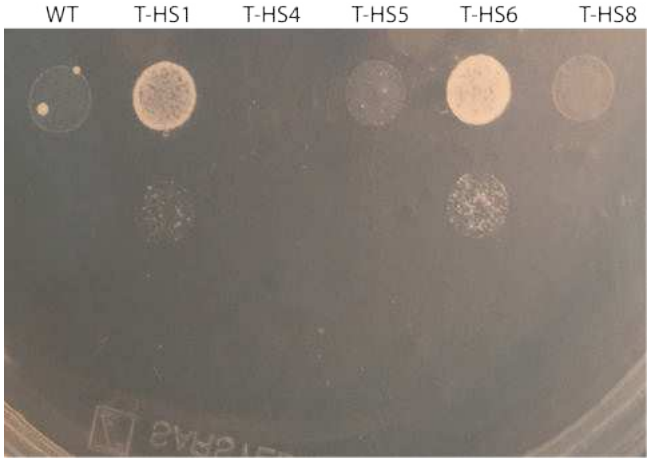

Figure 4.8: Cells plated on YNB-URA and grown for 5 days at 40 °C

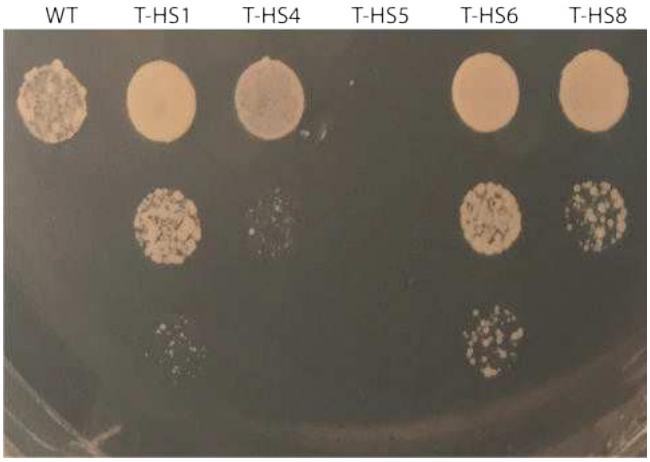

Figure 4.9: Cells plated on YNB-URA + 2 µg mL^{-1} DOX and grown for 5 days at 40 °C

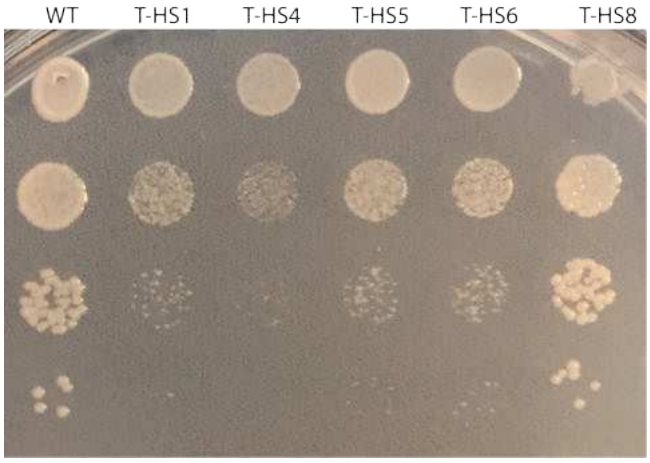

Figure 4.10: Control: Cells plated on YNB-URA and grown for 2 days at 30 °C

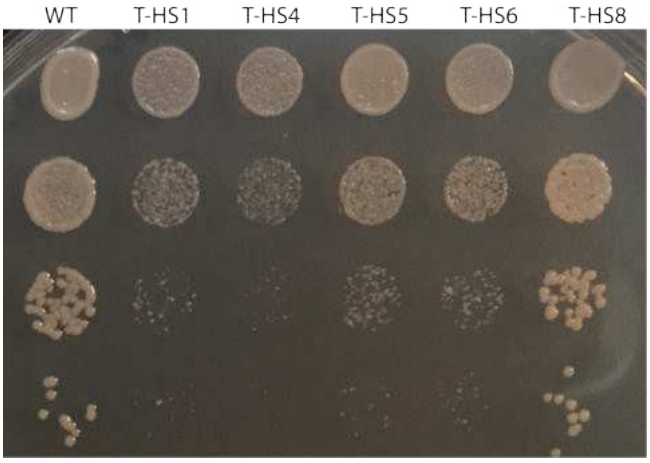

Figure 4.11: Control: Cells plated on YNB-URA + 2 µg mL^{-1} DOX and grown for 2 days at 30 °C

15. Plate

Figure 4.12 shows the growth of T-HS2, 3, 14 and 17 at 40 °C after 5 days. Compared to the WT, T-HS2 and 3 show significantly better growth, while T-HS17 only shows a slightly better growth under these conditions.

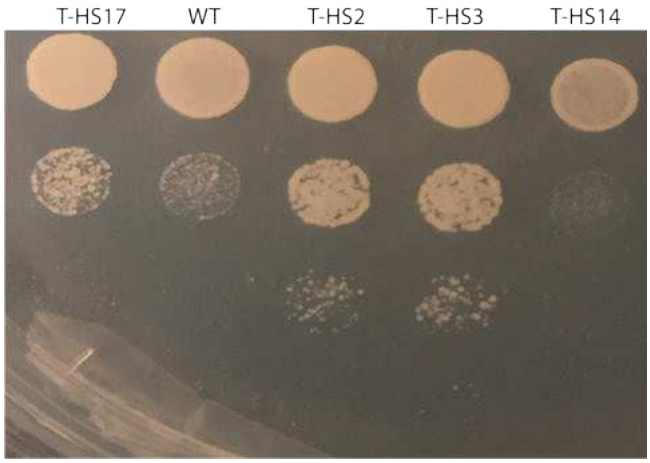

Figure 4.12: Cells plated on YNB-URA and grown for 5 days at 40 °C

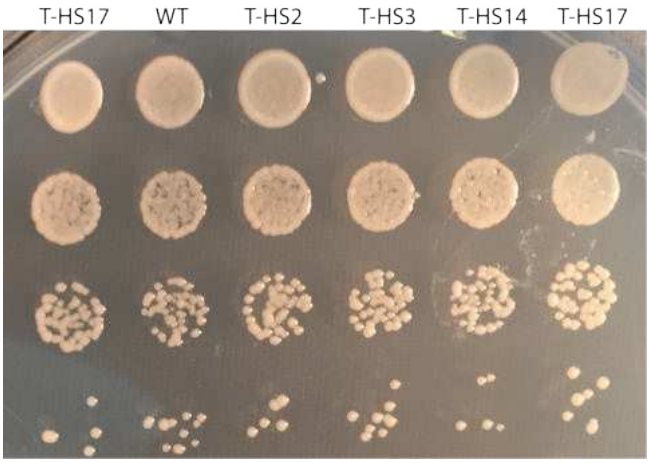

Figure 4.13: Control: Cells plated on YNB-URA and grown for 2 days at 30 °C

4.1.2 Oxidative Stress

Oxidative stress was only investigated by shock treatments, since when H_2O_2 was supplemented to an agar plate, the results were not reproducible.

17. Plate

Figure 4.14 shows the spot assay of T-OX41, 42, 43, 53 and 54 after exposing the cells to 4 mM H_2O_2 for 2 h. More cells of T-OX42 and 43 survived the oxidative shock than the WT.

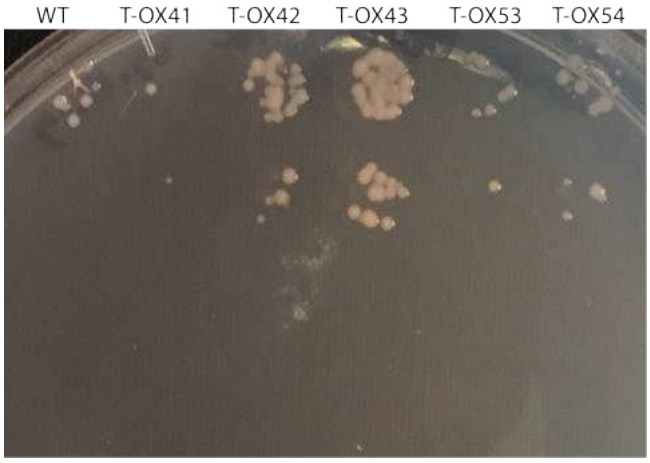

Figure 4.14: Cells treated with 4 mM H_2O_2, plated on YNB-URA and grown at 30 °C for 2 days

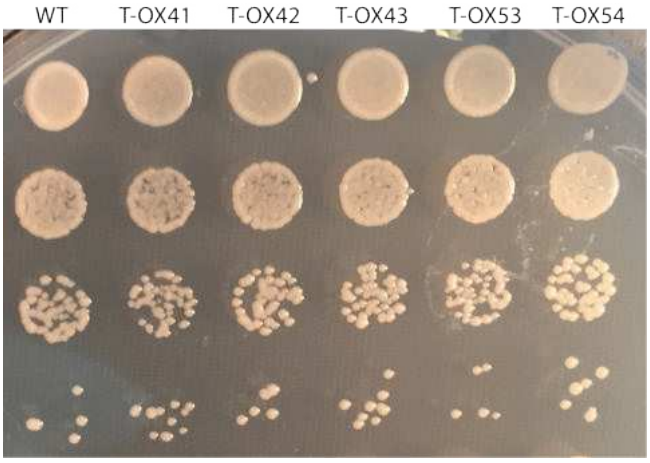

Figure 4.15: Control: Cells plated on YNB-URA and grown at 30 °C for 2 days

18. Plate

Figure 4.16 shows that T-HS1 was able to survive the 4 mM H_2O_2 shock better than the WT. All other clones shown on this plate were not able to withstand the oxidative shock.

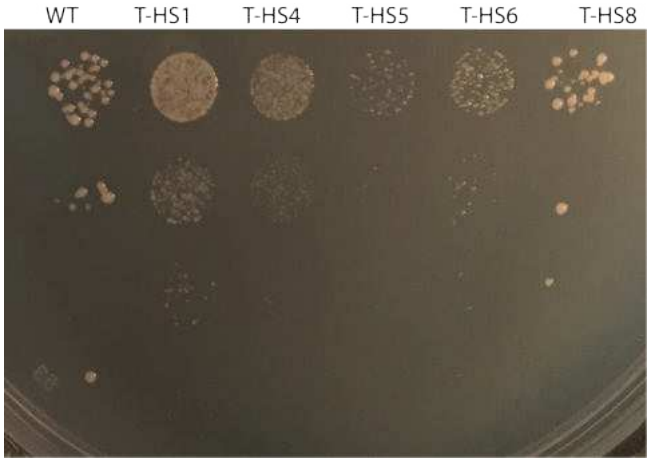

Figure 4.16: Cells treated with 4 mM H_2O_2, plated on YNB-URA and grown at 30 °C for 2 days

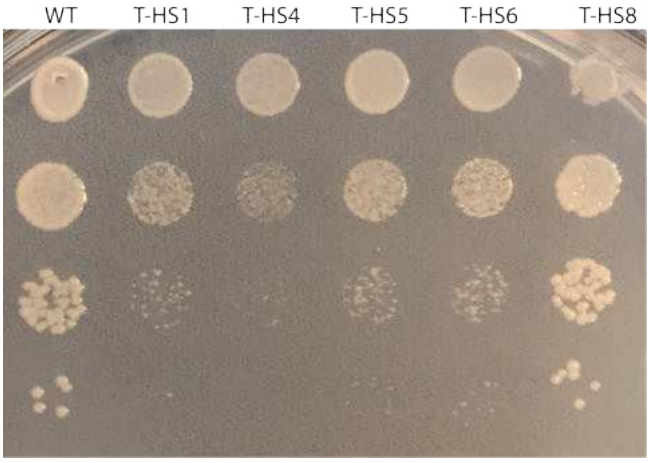

Figure 4.17: Control: Cells plated on YNB-URA and grown at 30 °C for 2 days

20. Plate

Figure 4.18 shows the WT T-HS18, 20 and 21A after exposing to 4 mM H_2O_2. T-HS20 and 21A show a higher survival rate than the WT.

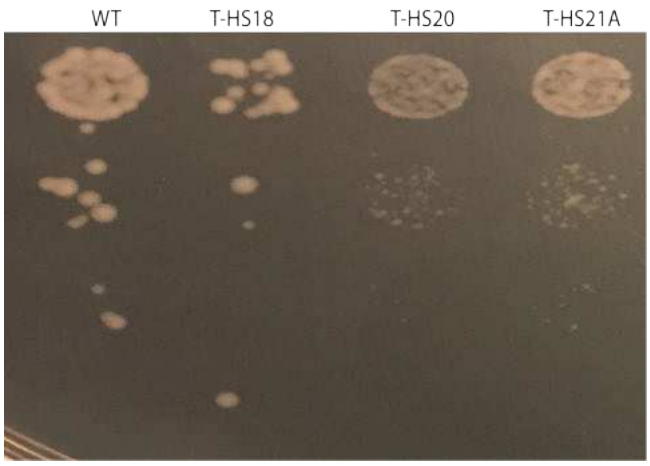

Figure 4.18: Cells treated with 4 mM H_2O_2, plated on YNB-URA and grown at 30 °C for 2 days

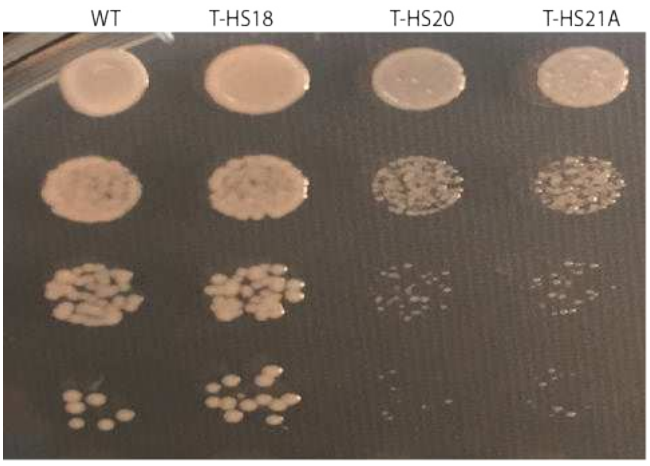

Figure 4.19: Control: Cells plated on YNB-URA and grown at 30 °C for 2 days

4.1.3 Summary of Initial Screening

In table 4.1 an overview of the initial screening can be seen. While most of the clones did not show any resistance, T-HS1 and T-HS21A show cross-resistance to heat and oxidative stress. However, to verify the resistances, the plasmid was extracted, purified and transformed into *S. cerevisiae* BY4741 *pdr5*Δ (positive control) and *S. cerevisiae* BY4741 (WT). Afterwards, the screening was repeated with the same conditions. Unfortunately, all of the phenotypes shown in table 4.1 could not be reproduced. T-HS1, 2, 3, 4, 6, 8, 20 and 21 did not show a correct restriction pattern, which was probably the reason why the secondary transformants did not show the same phenotypes any more. Even though, the transformation into *E. coli* was done a few times and the plasmid was extracted several times, the agarose gel always showed the same restriction pattern. Hence, it is not likely that the plasmid was rearranged and those clones were just false positives.

Table 4.1: Summary of Initial Screening

clone	1.2 M **NaCl**	1.5 M **KCl**	**heat shock**	40 °C	**H_2O_2 shock**
T-HS1	−	−	+	+	+
T-HS2	−	−	−	+	−
T-HS3	−	−	−	+	−
T-HS4	−	−	−	+	−
T-HS5	−	−	+	−	−
T-HS6	−	−	+	+	−
T-HS8	−	−	−	+	−
T-HS13	−	−	−	−	−
T-HS14	−	−	−	−	−
T-HS15	−	−	−	−	−
T-HS16	−	−	−	−	−
T-HS17	−	−	−	+	−
T-HS18	−	−	−	−	−
T-HS20	−	−	+	−	+
T-HS21A	−	−	+	+	+
T-OX41	−	−	−	−	−
T-OX42	−	−	−	−	+
T-OX43	−	−	−	−	+
T-OX44	−	−	−	−	−
T-OX45	−	−	−	−	−
T-OX51	−	−	−	−	−
T-OX52	−	−	−	−	−
T-OX53	−	−	−	−	−
T-OX54	−	−	−	−	−
T-OX61	−	−	−	−	−
T-OX62	−	−	−	−	−
T-OX65	−	−	−	−	−
T-OX66	−	−	−	−	−

4.2 Bioinformatic Analysis

T-HS1, 2, 3, 4, 6, and 21 did not show a proper restriction pattern, which should have a plasmid backbone at around 8000 bp and a smaller insert, this is probably why sequencing failed and blast results are not reliable. Sequencing was performed by Eurofins Genomics Tubeseq service and trimmed sequences were delivered. Based on the trimmed sequences, restriction sites of FD-BamH1 and FD-Pst1 were looked for and if present the sequences were modified by removing the 5' end and 3' end, respectively. Afterwards, Basic Local Alignment Search Tool (BLAST) from National Center for Biotechnology Information (NCBI) was used to find similar regions on the amino acid level (blastx).[58] Details about the length and quality of the reads as well as a summary of the best blastx hits can be found in table 6.1 to 6.4 in the supplementary. Blastx was conducted using default algorithm parameters and the database of "Non-redundant protein sequences (nr)".

T-HS1

Figure 4.20 shows an overview of the bioinformatic results of T-HS1.

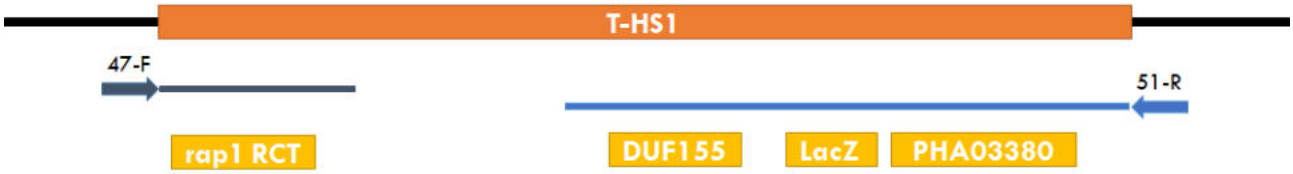

Figure 4.20: Overview of bioinformatic analysis of T-HS1; black = pCM188, orange = gene of interest, dark-blue = forward sequence - amplified with pCM188_47-F, light-blue = reverse sequence - amplified with pCM188_51-R, yellow = conserved region

T-HS1-pCM188_47-F shows a hypothetical protein as a hit that comes from *Pseudoalteromona spiscici* that is a bacteria occurring in the sea.[59] Using the tool, called CD-Search (Conserved Domain - Search) of NCBI conserved domains were investigated.[60] In table 6.5 conserved regions of T-HS1-pCM188_47-F and T-HS1-pCM188_51-R are shown. T-HS1-pCM188_47-F has a rap1_RCT super family domain, which is the C-terminal end of RAP1. Rap1 has the function to bind to DNA and act as a transcriptional factor in *S. cerevisiae*. Thus, it is likely that T-HS1-pCM188_47-F is a yeast contamination.

T-HS1-pCM188_51-R shows three conserved domains in its sequence. LacZ super family originates from *E. coli* and is typically used in vectors to perform blue-white screening and to quantify the expression level of plasmids.[61] However, pCM188 does not contain a LacZ coding site.[48] DUF155 super family is a "domain of unknown function". Furthermore, T-HS1-pCM188_51-R contains a PHA03380 super family, that occurs in transactivating tegument protein VP16, which is part of the vector pCM188 as well.[48]

T-HS2

BLAST results of T-HS2-pCM188_47-F shows a hit with Nuclear Hormone Receptor family of *Caenorhabditis elegans* (*C. elegans*), that has a conserved zinc-binding site. *C. elegans* is a free living transparent nematode.

T-HS2-pCM188_51-R shows a hit with an unnamed protein from *Pneumocystis jirovecii*, which has a conserved phosphate-binding site. Despite that the most similar proteins of T-HS2 show conserved regions, CD-Search was inconclusive. Moreover, no results were obtained by searching for similarities in the EST database of *E. testudo* (SRX448019), which indicates that this sequence does not originate from *E. testudo* and is probably a contamination.

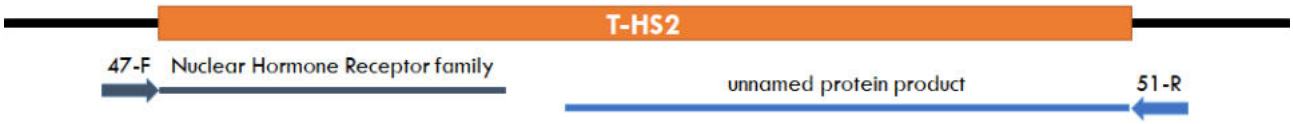

Figure 4.21: Overview of bioinformatic analysis of T-HS2; black = pCM188, orange = gene of interest, dark-blue = forward sequence - amplified with pCM188_47-F, light-blue = reverse sequence - amplified with pCM188_51-R

T-HS3

T-HS3-pCM188_51-R shows the same blastx results as T-HS1-pCM188_51-R. Moreover, conserved region search delivered similar results as T-HS1. T-HS3-pCM188_51-R - just as T-HS1 - contains conserved regions of lacZ and PHA03380 super families. T-HS3 also shows the same hit as T-HS1 in the EST database of *E. testudo*. Furthermore, T-HS1 and T-HS3 show high similarity when they are

aligned using the alignment tool of Clustal Omega, thus it is very likely that T-HS1 and T-HS3 are the same.[62]

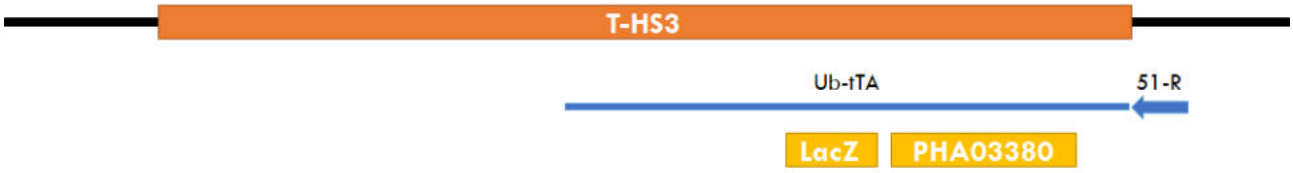

Figure 4.22: Overview of bioinformatic analysis of T-HS3; black = pCM188, orange = gene of interest, light-blue = reverse sequence - amplified with pCM188_51-R, yellow = conserved region

T-HS4

T-HS4-pCM188_47-F did not show any similarity while performing blastx search.

T-HS4-pCM188_51-R shows a hit with putative Troponin T form the tardigrade specie *H. dujardini*. Troponin T is a tropomyosin binding subunit of troponin, which is a complex, that is fulfilled with an inhibitory component of the actin-myosin interaction, troponin I and a Ca^{2+}-binding component.[63] In vertebrates phosphorylation/dephosphorylation of myosin regulatory light chain is the major mechanism to regulate actin-myosin interactions and troponin is predominantly expressed in striated muscles.[64] In tardigrades non-striated muscle cells are present throughout the whole body, most of them show smooth muscle-like morphology - actin filaments and myosin filaments are mostly aligned in parallel without striations.[65] Obinata et. al showed that a troponin I-like protein is co-localized with actin filaments in tardigrade non-striated muscle and suggest that troponin is involved in the contractile regulation of this muscle.[66] Thus, troponin is probably involved in the tun formation and therefore important to withstand extreme conditions. However, no study suggests enhanced resistance in *S. cerevisiae* due to troponin T over-expression.

The DNA sequence was blasted against an EST database of *E. testudo*. In figure 4.23 the red line illustrates sequences with a high identity to the EST database. Hence, T-HS4 originates from *E. testudo* and codes for troponin T.

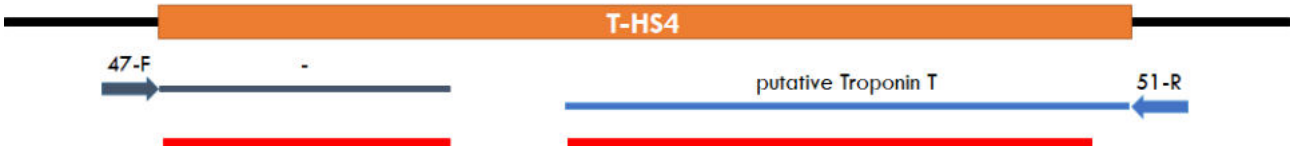

Figure 4.23: Overview of bioinformatic analysis of T-HS4; black = pCM188, orange = gene of interest, dark-blue = forward sequence - amplified with pCM188_47-F, light-blue = reverse sequence - amplified with pCM188_51-R, red = query cover with EST of *E. testudo*

T-HS5

T-HS5-pCM188_47-F and -pCM188_51-R do not show any similarities to any sequence. Furthermore, no conserved region was found.

However, forward and reverse sequences of T-HS5 show high query cover and identity with the EST database of *E. testudo*, which is highlighted in red in figure 4.24. Furthermore, forward and reverse sequenced showed an overlapping region. The sequences were merged using the online merger tool of EMBOSS.[67] The resulting sequence does not show any reasonable long open reading frame (ORF) and no conserved region.

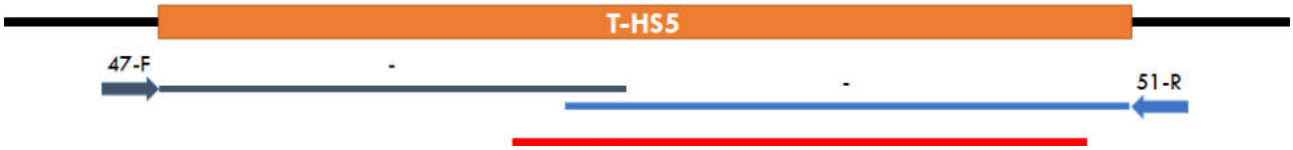

Figure 4.24: Overview of bioinformatic analysis of T-HS5; black = pCM188, orange = gene of interest, dark-blue = forward sequence - amplified with pCM188_47-F, light-blue = reverse sequence - amplified with pCM188_51-R, red = query cover with EST of *E. testudo*

T-HS13

Both, forward and reverse sequences, show similarities to trypsin-like proteases. Furthermore, a trypsin super family was found as a conserved region, which would fit to the blastx results of T-HS13. Moreover, the DNA sequences show high similarities to the EST database of *E. testudo*. Hence, it can be said that this gene originates from *E. testudo* and is a trypsin-like serine protease. Many of trypsin-like serine proteases are synthesized as inactive precursor zymogens that are cleaved during limited proteolysis to generate their active forms.[68] This enzyme is expressed to regulate blood coagulation.[68] The enzyme is also found in eutardigrada species like *H. dujardini* and *R. ramazzotti*. However, it is not known that trypsin-like serine protease enhances resistance, neither in tardigrades nor in *S. cerevisiae*. Despite having excellent quality and long reads, it is not possible to merge the sequences, because the insert is according to the agarose gel about 2400 bp long. Thus, an internal primer needs to be designed to get the full length of the insert and to get a full protein sequence.

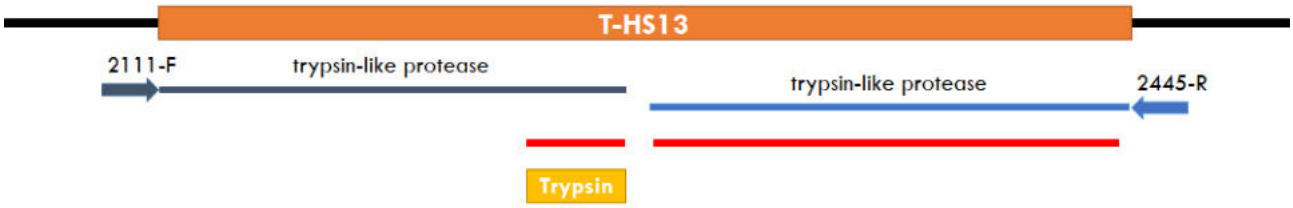

Figure 4.25: Overview of bioinformatic analysis of T-HS13; black = pCM188, orange = gene of interest, dark-blue = forward sequence - amplified with pCM188_2111-F, light-blue = reverse sequence - amplified with pCM188_2445-R, red = query cover with EST of *E. testudo*, yellow = conserved region

T-HS14

T-HS14-2430-R shows phosphoribosylaminoimidazole-succinocarboxamidesynthase as a best hit. This protein is conserved in eukaryotes, bacteria and archaea and is vital for living because it catalyzes a step in the biosynthesis of purines. Despite having blastx results, the sequences do not have any conserved region. T-HS14-2430-R shows high similarities with the EST of *E. testudo*, which can be seen in figure 4.26. T-HS14-2111-F and T-HS14-2430-R show an overlapping region, thus they were merged using the online merger tool EMBOSS.[67] The merged sequence shows no similarity, no conserved region and no reasonable long ORF.

Figure 4.26: Overview of bioinformatic analysis of T-HS14; black = pCM188, orange = gene of interest, dark-blue = forward sequence - amplified with pCM188_2111-F, light-blue = reverse sequence - amplified with pCM188_2430-R, red = query cover with EST of *E. testudo*

T-HS17

T-HS17-pCM188_47-F does not show any similarities. Furthermore, T-HS17-pCM188_47-F does not show conserved regions. But it has high similarities to the EST of *E. testudo* as it can be seen in figure 4.27.

Figure 4.27: Overview of bioinformatic analysis of T-HS17; black = pCM188, orange = gene of interest, dark-blue = forward sequence - amplified with pCM188_F-47, red = query cover with EST of *E. testudo*

T-OX41

T-OX41-2131-F and -2450-R show a dioxygenase as the best hit. Dioxygenases in general are enzymes that catalyze the transfer of electrons from a reductant to an oxidant. In this case, the gamma-butyrobetaine dioxygenase oxidizes gamma-butyrobetaine to L-carnitine, which is the last step of the biosynthesis of L-carnitine.

Conserved regions are shown in yellow in figure 4.28. Forward and reverse sequences show high similarities with the carnitine_bodg super family. Members of this family are gamma-butyrobetaine hydroxylase - as mentioned before - members of this family catalyze the last step in the conversion of L-lysine to L-carnitine. Many studies suggest that L-carnitine is a free radical scavenger that protects antioxidant enzymes from oxidative damage.[69] [70] However, this effect was not visible in this study. In figure 4.28 query cover with the EST database of *E. testudo* is shown in red.

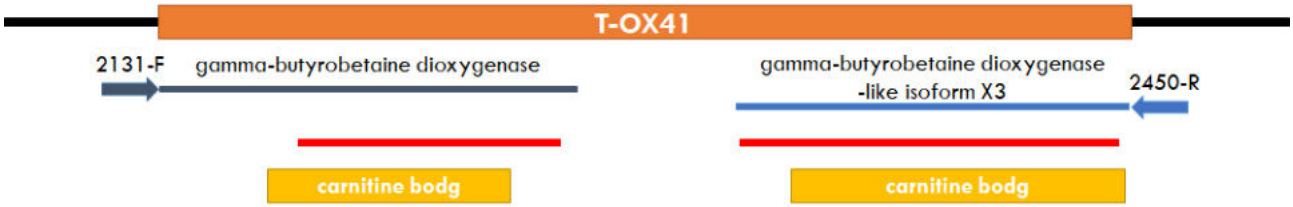

Figure 4.28: Overview of bioinformatic analysis of T-OX41; black = pCM188, orange = gene of interest, dark-blue = forward sequence - amplified with pCM188_2131-F, light-blue = reverse sequence - amplified with pCM188_2450-R, red = query cover with EST of *E. testudo*, yellow = conserved region

T-OX42

The best blastx hits only show hypothetical proteins. Other than that, a lot of myosin regulatory light chains were proposed, which is more likely to be the case. Due to the length of OXU27309.1, it is not likely that T-OX42 is coding for it, because the length of the insert is according to the agarose

gel 1300 bp. Moreover, the conserved region shows similarity to FRQ super family, which occurs in Ca^{2+}-binding proteins, which is also present in myosin regulatory light chains. Myosin regulatory light chain is important to contract muscles, which is crucial for tardigrades to form a tun.[71] However, there is no study that indicates enhanced resistance of *S. cerevisiaei* to environmental stress due to over-expression of myosin regulatory light chain. Figure 4.29 shows the alignment of T-OX42 with the EST database of *E. testudo*. Despite merging forward and reverse sequence, no reasonable long ORF was found.

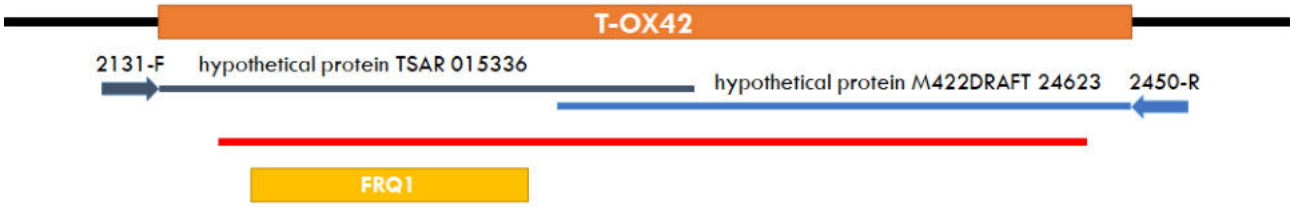

Figure 4.29: Overview of bioinformatic analysis of T-OX42; black = pCM188, orange = gene of interest, dark-blue = forward sequence - amplified with pCM188_2131-F, light-blue = reverse sequence - amplified with pCM188_2450-R, red = query cover with EST of *E. testudo*, yellow = conserved region

T-OX43

According to the best blastx hit T-OX43 seems to be a hypothetical protein of *R. varieornatus* with a length of 2276 aa, which does not fit to the length of the insert, which is about 1600 bp long, according to the agarose gel. It has been shown that RvY_05566 is coding for filamin-C, which is a Ca^{2+}-binding actin-bundling protein and is important for the cytoskeleton and muscle contraction.[68]
T-OX43-2131-F shows a specific hit for filamin-type immunoglobulin domains and in general a hit for filamin superfamily, which is shown in figure 4.30 Aforementioned, filamin is an actin-binding protein and plays an important role in the signal transduction in the cytoskeletons.

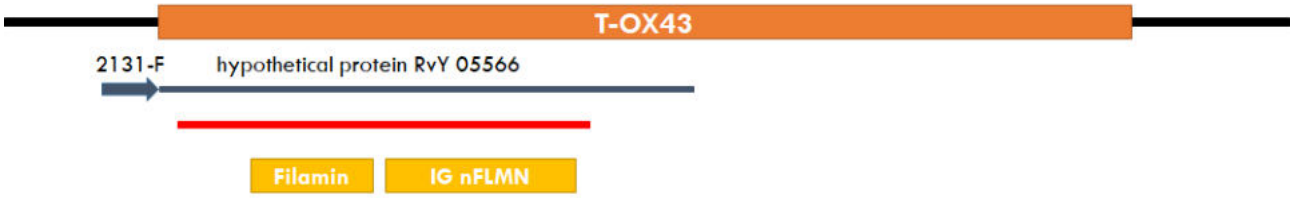

Figure 4.30: Overview of bioinformatic analysis of T-OX43; black = pCM188, orange = gene of interest, dark-blue = forward sequence - amplified with pCM188_2131-F, red = query cover with EST of *E. testudo*, yellow = conserved region

T-OX44

T-OX44 shows similar results as T-OX42. When they are aligned using Clustal Omega they show high similarities.[62] Hence, T-OX44 is likely the same as T-OX42.

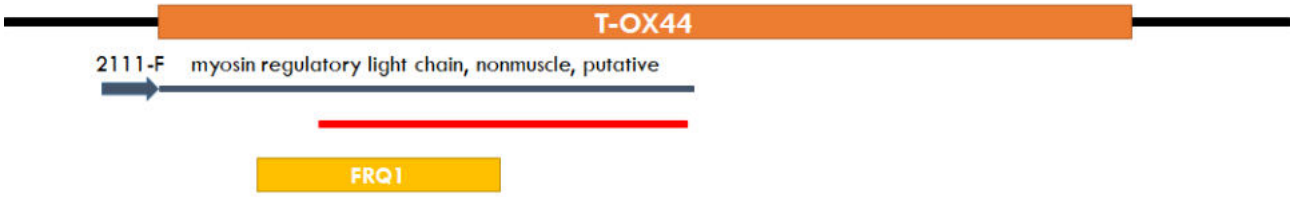

Figure 4.31: Overview of bioinformatic analysis of T-OX44; black = pCM188, orange = gene of interest, dark-blue = forward sequence - amplified with pCM188_2111-F, red = query cover with EST of *E. testudo*, yellow = conserved region

T-OX45

T-OX45 shows as a best hit the kelch repeat protein *Aspergillus vadensis* CBS 113365. Kelch proteins are proteins with normally five to seven kelch tandem repeats and are involved in protein-protein interactions. [72]

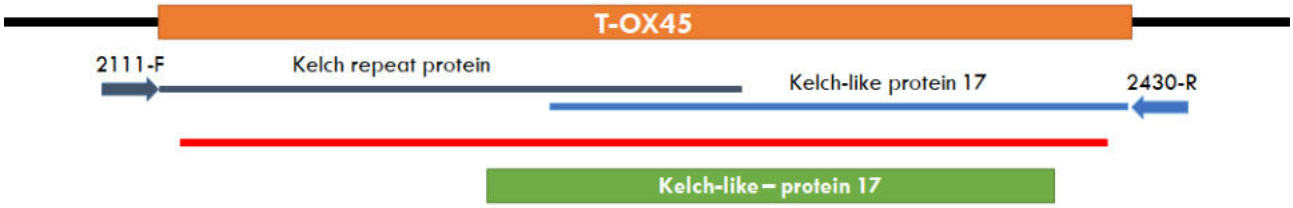

Figure 4.32: Overview of bioinformatic analysis of T-OX45; black = pCM188, orange = gene of interest, dark-blue = forward sequence - amplified with pCM188_2111-F, light-blue = reverse sequence - amplified with pCM188_2430-R, red = query cover with EST of *E. testudo*, green = ORF and corresponding protein

T-OX45-2111-F and 2430-R have a long overlapping region, thus they were merged, which resulted in a 1448 bp long sequence, which fits to the length on the agarose gel.

Table 4.2: ORF search of T-OX41-2131-F, label, strand, frame, start and stop position and resulting length in nt

label	strand	frame	start	stop	length \nt
ORF3	+	2	533	1285	753

Table 4.3: BLAST of found ORF; label, descrption, query cover in %, E value, percent identity in % and accession number

label	description	query cover \%	E value	per. id. \%	accession
ORF3	Kelch-like protein 17 [*Actinomadura* sp. 14C53]	49	3e-04	33.06	WP_138645565.1

Kelch-like protein 17 is microfilament protein and belongs to the complex of actin, that is found in the cytoplasm of almost all cells. They are often associated with microtubules and play a role in cytoskeletal function and mediate movement of the cell or the organelles within the cells. [73]

T-OX51

T-OX51-2131-F shows a hit with the adiponectin receptor protein 1-like *Ciona intestinalis*. Futhermore, T-OX51-2131-F shows a Haemolysin-III related conserved region, which is displayed in yellow in figure 4.33.

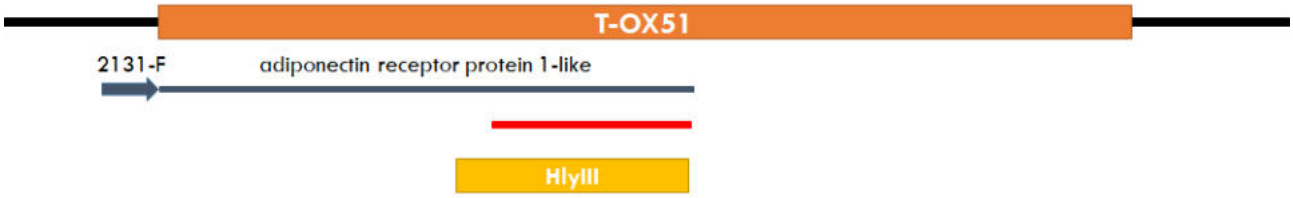

Figure 4.33: Overview of bioinformatic analysis of T-OX51; black = pCM188, orange = gene of interest, dark-blue = forward sequence - amplified with pCM188_2131-F, red = query cover with EST of *E. testudo*, yellow = conserved region

T-OX52

T-OX51-2111-F shows a hit with an unnamed protein product of *Mus musculus*. T-OX52-2430-R does not show any hit at all. Furthermore, the sequences do not show a conserved region.
However, when blasted against the EST database of *E. testudo* T-OX52-2430-R shows high similarity, which is shown in red in figure 4.34.

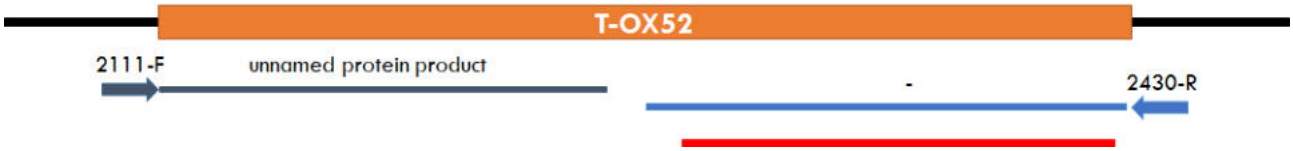

Figure 4.34: Overview of bioinformatic analysis of T-OX52; black = pCM188, orange = gene of interest, dark-blue = forward sequence - amplified with pCM188_2111-F, light-blue = reverse sequence - amplified with pCM188_2430-R, red = query cover with EST of *E. testudo*

T-OX53

T-OX53-2131-F shows a hit with a hypothetical protein of *R. varieornatus* and is probably an adenylate kinase.[68] Furthermore, T-OX53-2430-R has a conserved region of the ZM super family. This region is a short motif of 26 amino acids present in an alpha-actinin-binding proteins. Figure 4.35 also shows the alignment to the EST database of *E. testudo* - both forward and reverse sequence show high similarities.

Figure 4.35: Overview of bioinformatic analysis of T-OX53; black = pCM188, orange = gene of interest, dark-blue = forward sequence - amplified with pCM188_2111-F, light-blue = reverse sequence - amplified with pCM188_2430-R, red = query cover with EST of *E. testudo*, yellow = conserved region

T-OX62

T-OX62-2131-F and T-OX62-2430-R have high similarity with the charged multivesicular body protein

5-like from *Eurytemora affinis*. Charged multivesicular body protein 5 is according to UniProt: "a peripherally associated component of the endosomal s sorting required for transport complex III, that is involved in mulitvesicular bodies formation".[74] Furthermore, conserved regions were found, both sequences showed a Snf7 super family. According to the agarose gel the insert is about 1000 bp long. Thus, the forward and reverse sequence showed a long overlapping region. The sequences were merged using the online merger tool EMBOSS and we obtained a sequence with a length of 1014 bp.

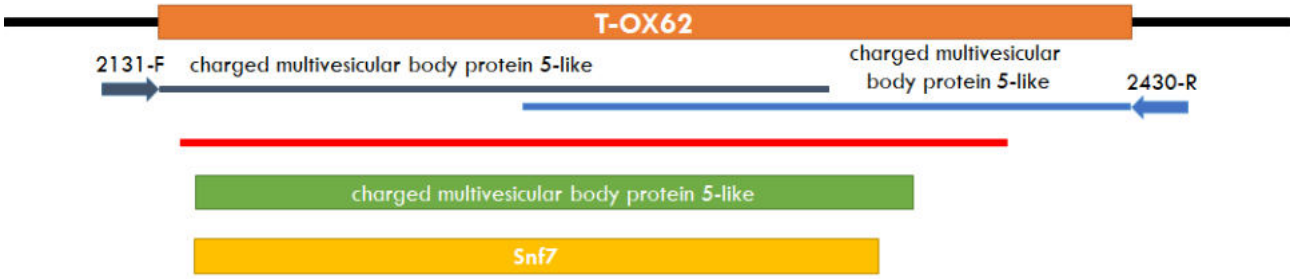

Figure 4.36: Overview of bioinformatic analysis of T-OX62; black = pCM188, orange = gene of interest, dark-blue = forward sequence - amplified with pCM188_2131-F, light-blue = reverse sequence - amplified with pCM188_2430-R, red = query cover with EST of *E. testudo*, yellow = conserved region

An ORF with a length of 223 aa was found and it has high similarity with the charged multivesicular body protein 5-like of *Eurytemora affinis*.

Table 4.4: ORF search of T-OX41-2131-F, label, strand, frame, start and stop position and resulting length in nt

label	strand	frame	start	E stop	length \nt
ORF2	+	3	69	740	672

Table 4.5: BLAST of found ORF; label, description, query cover in %, E value, percent identity in % and accession

label	description	query cover \%	E value	per. id. \%	accession
ORF2	charged multivesicular body protein 5-like [*Eurytemora affinis*]	99	5e-106	67.42	XP_023332328.1

T-OX65

As figure 4.37 shows, T-OX65 shows a hit with chromosome transmission fidelity protein 8 homologue of *Diabrotica virgifera virgifera*. However, no conserved region was found, but the sequence shows high similarity to the EST database of *E. testudo*.

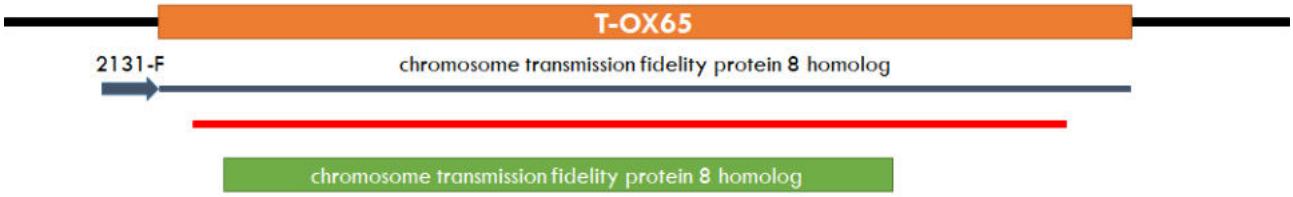

Figure 4.37: Overview of bioinformatic analysis of T-OX65; black = pCM188, orange = gene of interest, dark-blue = forward sequence - amplified with pCM188_2131-F, red = query cover with EST of *E. testudo*, green = ORF

Despite failed reverse sequencing an ORF with a length of 180 aa was found. T-OX65-ORF1 has an orthologous chromosome transmission fidelity protein 8 homolog in *Diabrotica virgifera virgifera*. Transmission fidelity protein 8 homolog is involved in sister chromatid cohesion and fidelity of chromosome transmission. Moreover, it is part of the cell nuclear antigen loader complexes CTF18-replication factor C (CTF18-RFC), that binds to single stranded and primed DNAs and has weak ATPase activity that is stimulated in the presence of primed DNA, replication protein A and proliferating cell nuclear antigen. Beside catalyzing ATP-dependent loading of proliferating cell nuclear antigen onto primed and gapped DNA, it also interacts with DNA Polymerase η, which coordinates DNA repair, recombination and chromosome cohesion reactions with replication fork progression. [75] [76]

Table 4.6: ORF search of T-OX65-2131-F, label, strand, frame, start and stop position and resulting length in nt

label	strand	frame	start	E stop	length \nt
ORF1	+	3	138	680	543

Table 4.7: BLAST of found ORF; label, description, query cover in %, E value, percent identity in % and accession

label	description	query cover \%	E value	per. id. \%	accession
ORF1	chromosome transmission fidelity protein 8 homolog [*Diabrotica virgifera virgifera*]	55	1.4	30.48	XP_028139461.1

T-OX66

Figure 4.37 shows an overview of the bioinformatic analysis of T-OX66. Blastx results suggest that T-OX66 is coding for a short-chain dehydrogenase/reductase family 42E member 1. Moreover, T-OX66 has a NADBRossmann conserved region. However, it is not known that short-chain dehydrogenase/reductase family 42E member 1 is enhancing stress resistance. Forward and reverse sequences were merged and a 1621 bp long sequence was obtained. An ORF with a length of 411 aa was found and BLAST search showed strong similarity to short-chain dehydrogenase/reductase family 42E member 1 of *Danio rerio*.

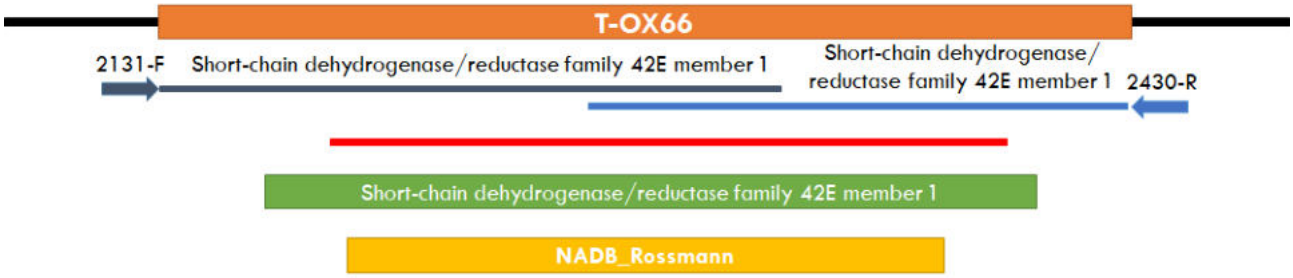

Figure 4.38: Overview of bioinformatic analysis of T-OX66; black = pCM188, orange = gene of interest, dark-blue = forward sequence - amplified with pCM188_2131-F, red = query cover with EST of *E. testudo*, green = ORF

Table 4.8: ORF search of T-OX66-merged label, strand, frame, start and stop position and resulting length in nt

label	strand	frame	start	E stop	length \nt
ORF3	+	3	252	1487	1236

Table 4.9: BLAST of found ORF; label, description, query cover in %, E value, percent identity in % and accession

label	description	query cover \%	E value	per. id. \%	accession
ORF3	Short-chain dehydrogenase/reductase family 42E member 1 [*Danio rerio*]	86	2e-84	38.04	A8DZE7.1

Short-chain dehydrogenase/reducatase is one of the hugest enzyme superfamilies with circa 46000 members.[77] Short-chain dehydrogenase/reductase family 42E member 1 has a 3β-hydroxysteroid dehydrogenase activity and therefore is responsible for the biosynthesis of all classes of hormonal steroids.[78]

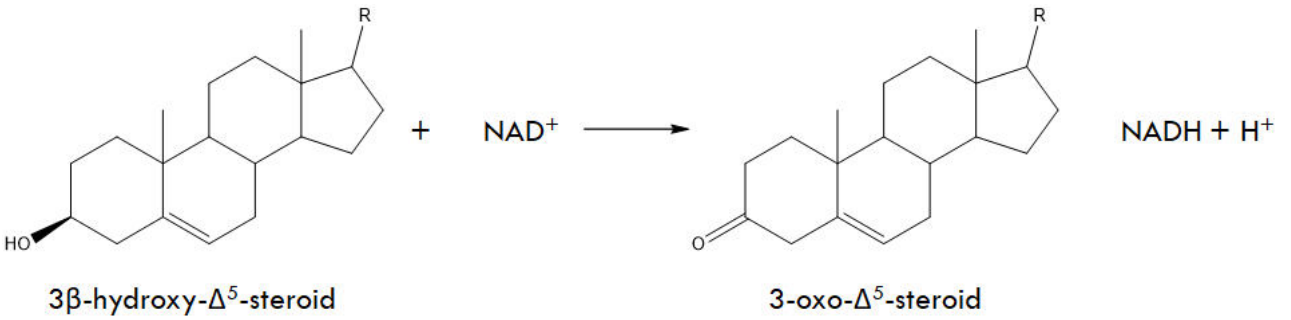

Figure 4.39: Reaction mechanism that is catalyzed by 3β-hydroxysteroid dehydrogenase

P1E6

P1E6 shows a hit with inositol oxygenase, which is an enzyme that is part of the catabolism of myo-inositol resulting in glucoronic acid.[79] More evidence that P1E6 is coding for an inositol oxygenase

is shown in table 6.15, where the conserved region of P1E6 is shown. Young et al. (2004) showed that glucuronic acid induced the synthesis of HSP70 and that cells pretreated with glucuronic acid were significantly more tolerant to heat shock and H_2O_2 stress.[80] It is also known that to high levels of glucuronic acid leads to apoptosis because glucuronic acid induces the generation of ROS.[80] However, no enhanced resistance was found when P1E6 was exposed to heat shock or oxidative stress. The reason could be that the myo-inositol level is just too low to form enough glucuronic acid to enhance resistance. The failure of higher survival rates could also be that too much glucuronic acid was synthesized and hence cell death was due to the toxic effect of glucuronic acid. Nevertheless, the first explanation seems to be more realistic since the survival pattern on the agar plate did not show much difference to the WT.

Figure 4.40: Overview of bioinformatic analysis of P1E6; black = pCM188, orange = gene of interest, dark-blue = forward sequence - amplified with pCM188_2131-F, red = query cover with EST of *E. testudo*, green = ORF

P1E8

P1E8 codes for a DNA excision repair protein ERCC-8 (ERCC8). Both, forward and reverse sequences, show conserved regions of the WD40 super family. In the merged sequence there are six WD40 repeats present, normally there are seven WD40 repeats present that allow ligand or protein-protein interactions.

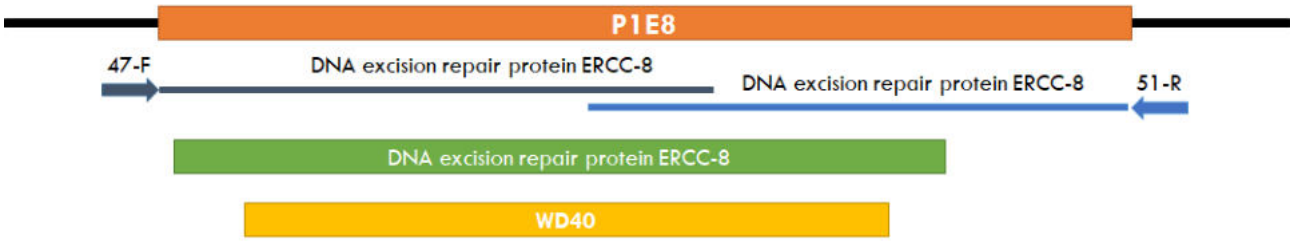

Figure 4.41: Overview of bioinformatic analysis of P1E8; black = pCM188, orange = gene of interest, dark-blue = forward sequence - amplified with pCM188_2131-F, red = query cover with EST of *E. testudo*, green = ORF

Table 4.10: ORF search of P1E8-merged label, strand, frame, start and stop position and resulting length in nt

label	strand	frame	start	E stop	length \nt
ORF3	+	2	38	1384	1347

Table 4.11: BLAST of found ORF; label, description, query cover in %, E value, percent identity in % and accession

label	description	query cover \%	E value	per. id. \%	accession
ORF3	DNA excision repair protein ERCC-8 [*Lingula anatina*]	90	2e-49	29.44	XP_013402995.1

DNA excision repair protein ERCC-8 interacts with the cockayne syndrome type B (CSB) and p44 proteins, the latter being a subunit of the RNA polymerase II transcription factor II.[81] Deletion of ERCC8 is associated leads to the cockayne syndrome (CS) which is an accelerated ageing disorder characterized by photo-sensitivity.[82] ultraviolet light (UV) induces the formation of covalent bondages between pyrimidine base pairs.[83] Pyrimidine base pairs can inhibit polymerases and is thereafter causing misreading during transcription and replication.[83] Figure 4.42 shows the UV mediated reaction that leads to the thymine dimer. CSB proteins are involved in transcription-coupled nucleotide excision repair, that divides the thymine dimer again.[82]

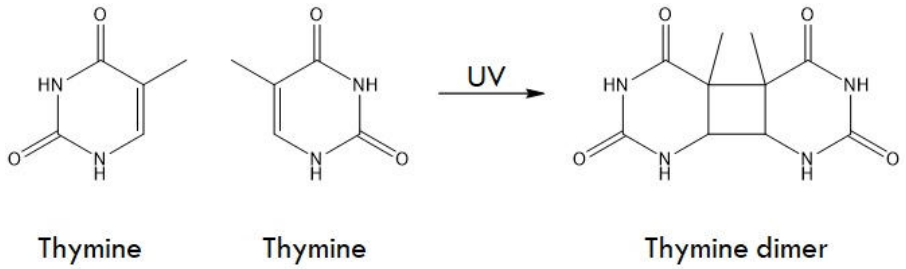

Figure 4.42: Reaction mechanism that leads to thymine dimers

4.3 P1E5

Scan-o-matic

Scan-o-matic is a method to measure the growth of a single colony on an agar plate. Scan-o-matic is written in Phyton (2.7). The protocol of Zackrisson et. al (2006) was followed to analyze the growth curves.[84]

In the following growth curves of P1E5 compared to the WT and the positive control (PC) are shown. In figures 4.43 to 4.46 P1E5-1 has the same background as the PC and P1E5-2 the same as WT. Figure 4.43 shows that the WT has a higher colony size than the corresponding clone P1E5-2. However, the opposite effect is visible when PDR5 is deleted (PC and P1E5-1). Generally, strains without the PDR5 gene do not have such high yields. Moreover, P1E5-2 has a slight higher yield when grown YNB-URA + 1.5 M KCl without supplemented DOX. The fact that P1E5-2 grows worse than the WT, could be that the protein that is encoded by the plasmid is toxic to *S. cerevisiaei*.

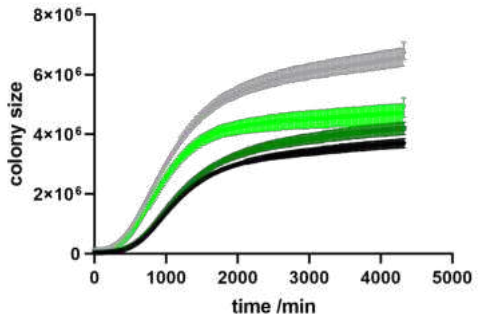

Figure 4.43: Growth curves of PC, P1E5-1, WT and P1E5-2 grown on YNB-URA

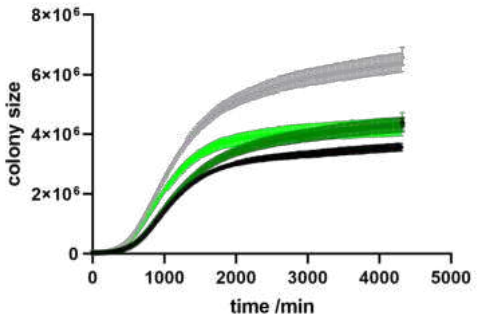

Figure 4.44: Growth curves of PC, P1E5-1, WT and P1E5-2 grown on YNB-URA + 2 µg mL^{-1} DOX

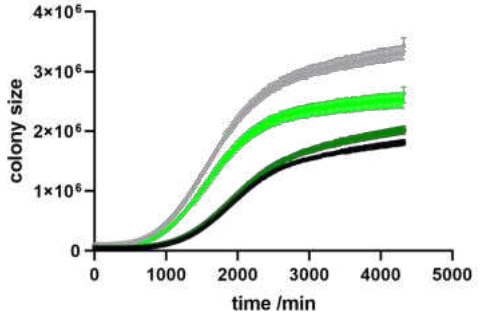

Figure 4.45: Growth curves of PC, P1E5-1, WT and P1E5-2 grown on YNB-URA + 1.5 M KCl

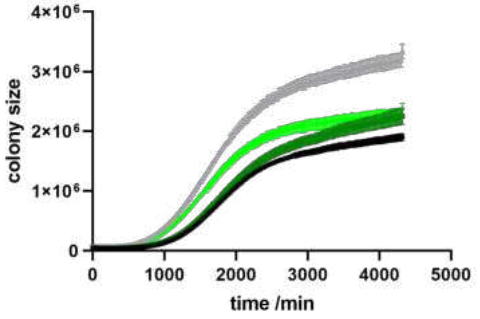

Figure 4.46: Growth curves of PC, P1E5-1, WT and P1E5-2 grown on YNB-URA + 1.5 M KCl + 2 µg mL^{-1} DOX

Bioinformatic Analysis

blastx result shows that P1E5 encodes for a serum paraoxonase/arylesterase 2 originated from *Strongylocentrotus purpuratus* and *R. varieornatus*, respectively. However no conserved region was found, neither in the forward and reverse nor the merged sequence. Table 4.12 shows a summary of the ORF search. The result is a 392 aa long protein sequence that has high similarities with serum paraoxonase/arylesterase 1 from *Strongylocentrotus purpuratus*. However, the protein sequence does not show any conserved region, even though the blast hit shows a Str_synth super family and a SGL super family.

Figure 4.47: Overview of bioinformatic analysis of P1E5; black = pCM188, orange = gene of interest, dark-blue = forward sequence - amplified with pCM188_2131-F, red = query cover with EST of *E. testudo*, green = ORF

Table 4.12: ORF search of P1E5-merged: label, strand, frame, start and stop position and resulting length in nt

label	strand	frame	start \nt	E stop \nt	length \nt
ORF2	+	2	188	1366	1179

Table 4.13: BLAST of found ORF; label, description, query cover in %, E value, percent identity in % and accession number

label	description	query cover \%	E value	per. id. \%	accession
ORF2	serum paraoxonase/arylesterase 1 [*Strongylocentrotus purpuratus*]	94	1e-37	29.66	XP_030843757.1

In humans there are three forms of paraoxonases known, paraoxonase 1 (PON1), paraoxonase (PON)2, and PON3. PON1 is a Ca^{2+} dependent enzyme, with a central tunnel that contains two Ca^{2+} ions. The Ca^{2+} ion located deeper within the tunnel has a critical role in the conformational stability of PON1. The other Ca^{2+} ion has a catalytic role and is indispensable for substrate positioning and ester bond activation. Furthermore, three helices are located above the active site, where two of them have their function in PON1-high-density lipoprotein (HDL) interactions. It has been shown that PON1 prevents accumulation of lipoperoxides in low-density lipoprotein (LDL) by metabolizing oxidative damage of LDL.[85] PON2 is capable of hydrolyzing lactones and a number of aromatic carboxylic acid esters. Figure 4.48 shows the reaction mechanism of PON1.

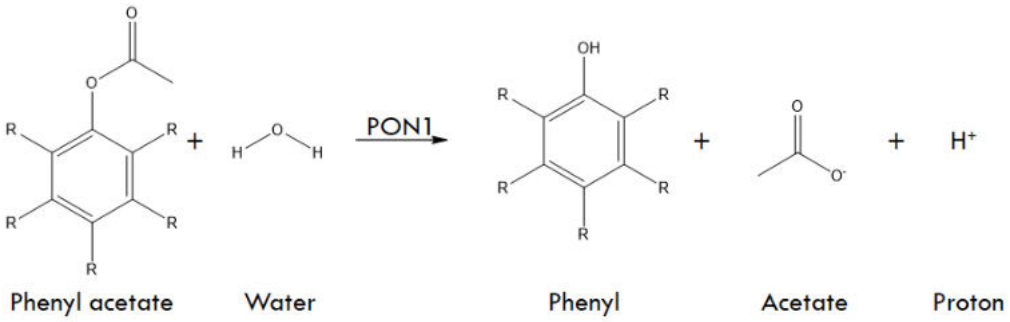

Figure 4.48: reaction mechanism of PON1

Cross resistance

To test cross resistance of P1E5, P1E5 and pCM188 was transformed in *S. cerevisiaei* BY4741. Afterwards, both strains were grown overnight in YNB-URA and YNB-URA + 2 µg mL^{-1} DOX, plated on YNB-URA and YNB-URA + 2 µg mL^{-1} DOX plates and grown at 40 °C for four days. The same overnight culture was also plated on YNB-URA + 1.4 M NaCl and YNB-URA 1.4 M NaCl + 2 µg mL^{-1} dox. Furthermore, the cultures were heat-shocked at 47 °C for 1 h and shocked with 4 mM H_2O_2 for 2 h. However, no effect was visible when grown on 1.4 M NaCl, which is why the plates are not shown here. As it can be seen in figures 4.49 and 4.51 P1E5-2 is not able to grow on YNB-URA plates at 40 °C at all. But when P1E5-2 is grown on YNB-URA + 2 µg mL^{-1}, it is able to grow only when the

preculture was grown in YNB-URA without DOX (figures 4.50 and 4.52. In other words, when gene expression is allowed in the pre-culture, P1E5-2 is able to grow at 40 °C but only when gene expression is shut down during the incubation.

Figure 4.49: P1E5-2 and WT grown in YNB-URA overnight, plated on YNB-URA and grown at 40 °C for 4 days

Figure 4.50: P1E5-2 and WT grown in YNB-URA + 2 µg mL^{-1} DOX overnight, plated on YNB-URA and grown at 40 °C for 4 days

Figure 4.51: P1E5-2 and WT grown in YNB-URA overnight, plated on YNB-URA + 2 µg mL^{-1} DOX and grown at 40 °C for 4 days

Figure 4.52: P1E5-2 and WT grown in YNB-URA + 2 µg mL^{-1} DOX overnight, plated on YNB-URA + 2 µg mL^{-1} DOX and grown at 40 °C for 4 days

Bioscreen C

OD was measured over time and the data was pre-processed using PRECOG.[86] Before, background subtraction and calibration that transform raw optical densities into population sizes, PRECOGG filters raw optical densities in three steps. First, a sliding window one-dimensional median filter takes three consecutive data values into account and replaces the middle value with the median of all three data points. Moreover, edge cropping is avoided by padding (filling the gap by cloning the endpoints). Median filters are commonly used to minimize the impact of high amplitude noise at single time points, while preserving the overall data characteristics. Afterwards, PRECOG employs a one-dimensional mean filter in a sliding window of three values to get rid of low amplitude but high-frequency noises. Therefore, the middle value is replaced by the mean over the three values in the series. The result is that also correct values are adjusted. Finally, a monotonicity filter is applied. This filter step sweeps each data series and enforces data monotonicity by replacing any value lower than its predecessor with the predecessor itself. The third filtering step is restricted to removing or reducing abnormalities in

collapsing curves.[87] In figure 4.53 an example of processed data is shown. WT is shown in black, while P1E5-2 is shown in green. Red symbols highlight OD values that were used to calculate the yield. As shown below it is obvious that P1E5-2 can grow better at 42 °C than the WT in YNB-URA media supplemented with 0.031 25 µg mL^{-1} DOX.

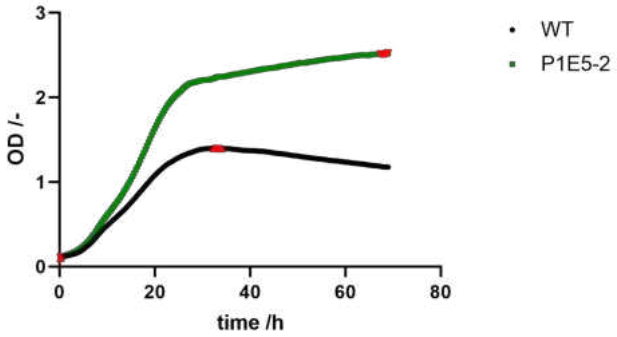

Figure 4.53: growth curves of WT (black) and P1E5-2 (green) grown in YNB-URA supplemented with 0.031 25 µg mL^{-1}; red symbols highlight what OD value was used to calculate the yield

Since earlier experiments showed, that the level of expression has probably an effect on the resistance, nine different DOX concentrations were investigated. As it can be seen in figure 4.55 no effect is visible when paraoxonase is overexpressed (0 µg mL^{-1} DOX). Furthermore, when paraoxonase expression is repressed strongly by DOX at 8 µg mL^{-1}, 4 µg mL^{-1}, 2 µg mL^{-1} and 1 µg mL^{-1} no difference in yields is visible. Garì et. al (1997) demonstrated that 1 µg mL^{-1} is already enough to shut down gene expression in pCM171 completely. pCM171 is almost the same as pCM188 (has the same amount of tetO-operator). However, pCM171 contains a LacZ coding site instead of a MCS and has another genetic marker.[48] This effect is also visible here, as soon as the DOX concentration drops below 1 µg mL^{-1} P1E5-2nd-2 shows better yields at 42 °C. Interestingly, the lower the DOX concentration the better the yield. Hence, P1E5 does not affect the growth However, there is still a lot to investigate, since there is no maximum of the curve, thus the best DOX concentration is still unknown.

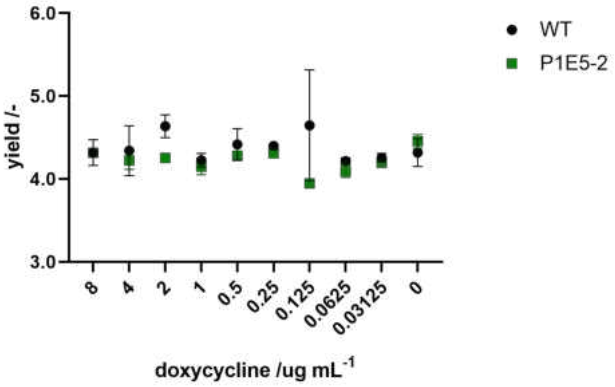

Figure 4.54: Yield: WT and P1E5-2 grown at 30 °C

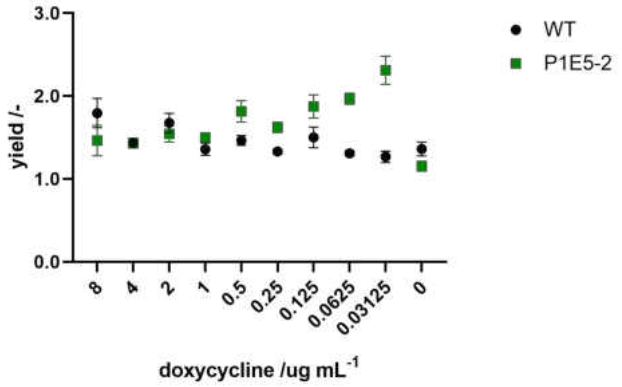

Figure 4.55: Yield: WT and P1E5-2 grown at 42 °C

5 Conclusion and Future Perspectives

To conclude, we found a clone (P1E5) that definitively has a positive effect on the growth at certain conditions, including osmotic and heat stress. A Bioscreen experiments was performed to quantify resistance to 42 °C and showed that resistance is dependant on the level of gene expression which was controlled by DOX. It was shown that the best yield was achieved with a DOX concentration of 0.031 25 µg mL^{-1}. However, there was no maximum of the yield, which leaves the question open if lower concentration of DOX would even show better results. Since other experiments were performed with 2 µg mL^{-1} DOX, it is likely that the effect of P1E5 under other stress conditions was not seen, because the the gene expression was either too high or not present at all. Therefore, other stress experiments need to be repeated at lower DOX concentration, but first it would be the best to find the optimal DOX concentration by performing more Bioscreen C experiments. Furthermore, it was shown that P1E5 is coding for a serum paraoxonase/arylesterase 1 and originates from *E. testudo*. Even though, the reverse sequence has not the best quality it was possible to merge forward and reverse sequences and obtain a sequence that fits perfectly to the agarose gel and an ORF that fits to the length of other paraoxonase/arylesterases 1. However, the reverse sequence still needs to be improved. Moreover, P1E5 can be transformed into other organisms, *e.g. Yarrowia lipolytica, Kluyveromyces lactis* and *Pichia pastori*, to check if it shows the same characteristic resistance in those organisms. Furthermore, to investigate whether the expression of P1E5 activates stress responses on their own, in the absence of an external stress, it could be co-expressed with a fluorescence tagged protein chaperon (Hsp104-GFP). The clone could then be examined for accumulation of protein aggregates by microscopy.

Even tough, a lot of clones with a resistance was found in the first round of screening, the second round of screening was inconclusive. Therefore, it is likely that a lot of false positives were found. Moreover, T-HS1, 2, 3, 4 and 21 did not show a proper restriction site. However, it is unlikely that the plasmid was rearranged during the transformation into *E. coli* because the pattern was the same for several extracted plasmids.

Moreover, a bunch of other stresses could be tested, *e.g.* UV radiation and copper. It has been shown that a *E. testudo* seems to be able to enter chemobiosis in response to high copper concentrations.[88] Therefore, it would be interesting to investigate into this stress condition, since chemobiosis is still unexplored and it is not known what proteins are responsible to enhance resistance to toxic chemicals such as copper.

References

[1] Charles Bonnet and Johann August Ephraim Goeze. *Herrn Karl Bonnets Abhandlungen aus der Insektologie /*, volume 1. Halle :Bey J.J. Gebauers Wittwe und Joh. Jac. Gebauer,, 1773. https://www.biodiversitylibrary.org/bibliography/47534 — Translation of: Traité d'insectologie.

[2] David Keilin. The leeuwenhoek lecture - the problem of anabiosis or latent life: history and current concept. *Proceedings of the Royal Society of London. Series B - Biological Sciences*, 150(939):149–191, 1959.

[3] Tardigrades (water bears). `https://serc.carleton.edu/microbelife/topics/tardigrade/index.html`. Accessed: 2019-10-28.

[4] G. Ramazzotti. Il phylum tardigrada. *Memorie dell'Istituto Italiano di Idrobiologia, Pallanza*, 16:1–595, 1962.

[5] F. Richters. *Tardigrada*. Handbuch der Zoologie, 1926.

[6] E. Marcus. *Zur anatomie und ökologie mariner tardigraden*. Zoologische Jahrbücher Abteilung für Systematik, Ökologie und Geographie der Tiere, 1927.

[7] Ralph O. Schill, editor. *Water Bears: The Biology of Tardigrades*. 2018.

[8] S.J. McInnes. Zoogeographic distribution of terrestrial/freshwater tardigrades from current literature. *Journal of Natural History*, 28(2):257–352, 1994.

[9] M.L. Doyère. Memorie sur les tardigrades. 1840.

[10] James Clegg. Cryptobiosis—a peculiar state of biological organization. *Comparative biochemistry and physiology. Part B, Biochemistry molecular biology*, 128:613–24, 05 2001.

[11] John H. Crowe and K. A. Madin. Anhydrobiosis in tardigrades and nematodes. *Transactions of the American Microscopical Society*, 93(4):513–524, 1974.

[12] J. H. CROWE. The physiology of cryptobiosis in tardigrades. *Mem. Ist. Ital. Idrobiol.*, 32:37–59, 1975.

[13] Daiki Horikawa. *Survival of Tardigrades in Extreme Environments: A Model Animal for Astrobiology*, volume 21, pages 205–217. 08 2012.

[14] Kunihiro Seki and Masato Toyoshima. Preserving tardigrades under pressure. *Nature*, 395, 10 1998.

[15] K. I. Jönsson, Elke Rabbow, Ralph Schill, Mats Harms-Ringdahl, and Petra Rettberg. Tardigrades survive exposure to space in low earth orbit. *Current biology : CB*, 18:R729–R731, 10 2008.

[16] Elham Schokraie, Agnes Hotz-Wagenblatt, Uwe Warnken, Marcus Frohme, Frank Förster, Thomas Dandekar, Steffen Hengherr, Ralph Schill, and Martina Schnölzer. Proteomic analysis of tardigrades: Towards a better understanding of molecular mechanisms by anhydrobiotic organisms. *PloS one*, 5:e9502, 03 2010.

[17] N. Møbjerg, K. A. Halberg, A. Jørgensen, D. Persson, M. Bjørn, H. Ramløv, and R. M. Kristensen. Survival in extreme environments – on the current knowledge of adaptations in tardigrades. *Acta Physiologica*, 202(3):409–420, 2011.

[18] David A. Wharton. Anhydrobiosis. *Current Biology*, 25(23):R1114 – R1116, 2015.

[19] Aslak Jorgensen, Nadja Mobjerg, and Reinhardt M. Kristensen. Molecular study of the tardigrade Echiniscus testudo (Echiniscidae) reveals low DNA sequence diversity over a large geographical area. *JOURNAL OF LIMNOLOGY*, 66(1):77–83, 2007. 10th International Symposium on Tardigrada, Catania, ITALY, JUN 18-23, 2006.

[20] R. O. Schill and G. B. Fritz. Desiccation tolerance in embryonic stages of the tardigrade. *Journal of Zoology*, 276(1):103–107, 2008.

[21] S LINDQUIST. THE HEAT-SHOCK RESPONSE. *ANNUAL REVIEW OF BIOCHEMISTRY*, 55:1151–1191, 1986.

[22] Zihai Li and Pramod Srivastava. Heat-shock proteins. *Current Protocols in Immunology*, 58(1):A.1T.1–A.1T.6, 2003.

[23] Jack DE GRAAF, Reinout AMONS, and Wim MÖLLER. The primary structure of artemin from artemia cysts. *European Journal of Biochemistry*, 193(3):737–741, 1990.

[24] James S. Clegg, Susan A. Jackson, and Alden H. Warner. Extensive intracellular translocations of a major protein accompany anoxia in embryos of artemia franciscana. *Experimental Cell Research*, 212(1):77 – 83, 1994.

[25] James Clegg. Embryos of artemia franciscana survive four years of continuous anoxia: The case for complete metabolic rate depression. *The Journal of experimental biology*, 200:467–75, 02 1997.

[26] Ping Liang, Reinout Amons, James S. Clegg, and Thomas H. MacRae. Molecular characterization of a small heat shock/-crystallin protein in encysted artemia embryos. *Journal of Biological Chemistry*, 272(30):19051–19058, 1997.

[27] A.H Warner, R.T Brunet, T.H MacRae, and J.S Clegg. Artemin is an rna-binding protein with high thermal stability and potential rna chaperone activity. *Archives of Biochemistry and Biophysics*, 424(2):189 – 200, 2004.

[28] Andy Reuner, Steffen Hengherr, Frank Förster, Detlev Arndt, Richard Reinhardt, Thomas Dandekar, Marcus Frohme, Franz Brümmer, and Ralph Schill. Stress response in tardigrades: Differential gene expression of molecular chaperones. *Cell Stress and Chaperones, epub-epub (2009)*, 15, 07 2010.

[29] Ralph O. Schill, Günther H. B. Steinbrück, and Heinz-R. Köhler. Stress gene (hsp70) sequences and quantitative expression in milnesium tardigradum (tardigrada) during active and cryptobiotic stages. *Journal of Experimental Biology*, 207(10):1607–1613, 2004.

[30] Irina Guzhova, Irina Krallish, Galina Khroustalyova, Boris Margulis, and Alexander Rapoport. Short communication. *Process Biochemistry*, 43(10):1138–1141, 2008.

[31] John F. Carpenter, Lois M. Crowe, and John H. Crowe. Stabilization of phosphofructokinase with sugars during freeze-drying: characterization of enhanced protection in the presence of divalent cations. *Biochimica et Biophysica Acta (BBA) - General Subjects*, 923(1):109 – 115, 1987.

[32] John H. Crowe, Samuel B. Leslie, and Lois M. Crowe. Is vitrification sufficient to preserve liposomes during freeze-drying? *Cryobiology*, 31(4):355 – 366, 1994.

[33] R Bather, S Webb, and T Cunningham. Evidence for the role of bound water and partial desiccation in carcinogenesis. *Nature*, 207:30–2, 08 1965.

[34] John Crowe, James Clegg, and Lois Crowe. *Anhydrobiosis: the water replacement hypothesis*, pages 440–455. 01 1998.

[35] Evgenyi Shalaev, George Zografi, and Peter Steponkus. Occurrence of glass transitions in long-chain phosphatidylcholine mesophases. *The journal of physical chemistry. B*, 114:3526–33, 02 2010.

[36] S B Leslie, E Israeli, B Lighthart, J H Crowe, and L M Crowe. Trehalose and sucrose protect both membranes and proteins in intact bacteria during drying. *Applied and Environmental Microbiology*, 61(10):3592–3597, 1995.

[37] Dean Calahan, Maitreya Dunham, Chris DeSevo, and Douglas E. Koshland. Genetic analysis of desiccation tolerance in saccharomyces cerevisiae. *Genetics*, 189(2):507–519, 2011.

[38] Hugo Tapia, Lindsey Young, Douglas Fox, Carolyn R. Bertozzi, and Douglas Koshland. Increasing intracellular trehalose is sufficient to confer desiccation tolerance to saccharomyces cerevisiae. *Proceedings of the National Academy of Sciences*, 112(19):6122–6127, 2015.

[39] Steffen Hengherr, Arnd G. Heyer, Heinz-R. Köhler, and Ralph O. Schill. Trehalose and anhydrobiosis in tardigrades – evidence for divergence in responses to dehydration. *The FEBS Journal*, 275(2):281–288, 2008.

[40] Minoru Sakurai, Takao Furuki, Ken-ichi Akao, Daisuke Tanaka, Yuichi Nakahara, Takahiro Kikawada, Masahiko Watanabe, and Takashi Okuda. Vitrification is essential for anhydrobiosis in an african chironomid, polypedilum vanderplanki. *Proceedings of the National Academy of Sciences*, 105(13):5093–5098, 2008.

[41] Thomas C. Boothby, Hugo Tapia, Alexandra H. Brozena, Samantha Piszkiewicz, Austin E. Smith, Ilaria Giovannini, Lorena Rebecchi, Gary J. Pielak, Doug Koshland, and Bob Goldstein. Tardigrades use intrinsically disordered proteins to survive desiccation. *Molecular Cell*, 65(6):975 – 984.e5, 2017.

[42] Peter E. Wright and H. Jane Dyson. Intrinsically disordered proteins in cellular signalling and regulation. *Nature Reviews Molecular Cell Biology*, 16(1):18–29, JAN 2015.

[43] Glenn Galau, Niddhi Bijaisoradat, and D.Wayne Hughes. Accumulation kinetics of cotton late embryogenesis-abundant mrnas and storage protein mrnas: Coordinate regulation during embryogenesis and the role of abscisic acid*1. *Developmental biology*, 123:198–212, 10 1987.

[44] William D. McCubbin, Cyril M. Kay, and Byron G. Lane. Hydrodynamic and optical properties of the wheat germ em protein. *Canadian Journal of Biochemistry and Cell Biology*, 63(8):803–811, 1985.

[45] A Garay-Arroyo, JM Colmenero-Flores, A Garciarrubio, and AA Covarrubias. Highly hydrophilic proteins in prokaryotes and eukaryotes are common during conditions of water deficit. *JOURNAL OF BIOLOGICAL CHEMISTRY*, 275(8):5668–5674, FEB 25 2000.

[46] Sae Tanaka, Junko Tanaka, Yoshihiro Miwa, Daiki D. Horikawa, Toshiaki Katayama, Kazuharu Arakawa, Atsushi Toyoda, Takeo Kubo, and Takekazu Kunieda. Novel mitochondria-targeted heat-soluble proteins identified in the anhydrobiotic tardigrade improve osmotic tolerance of human cells. *PLOS ONE*, 10(2):1–15, 02 2015.

[47] FRED SHERMAN. An introduction to the genetics and molecular biology of the yeast saccharomyces cerevisiae. *The Encyclopedia of Molecular Biology and Molecular Medicine*, 01 1997.

[48] Eloi Garí, Lidia Piedrafita, Martí Aldea, and Enrique Herrero. A set of vectors with a tetracycline-regulatable promoter system for modulated gene expression insaccharomyces cerevisiae. *Yeast (Chichester, England)*, 13:837–48, 07 1997.

[49] K. I. Jönsson. Radiation tolerance in tardigrades: Current knowledge and potential applications in medicine. *Cancers*, 11:1333, 09 2019.

[50] Carrie Brachmann, Adrian Davies, Gregory Cost, Emerita Caputo, Joachim Li, Philip Hieter, and Jef Boeke. Designer deletion strains derived from saccharomyces cerevisiae s288c: A useful set of strains and plasmids for pcr-mediated gene disruption and other applications. *Yeast (Chichester, England)*, 14:115–32, 01 1998.

[51] Kohji Miyahara, Masaki Mizunuma, Dai Hirata, Eiko Tsuchiya, and Tokichi Miyakawa. The involvement of the saccharomyces cerevisiae multidrug resistance transporters pdr5p and snq2p in cation resistance. *FEBS letters*, 399:317–20, 01 1997.

[52] G Leppert, Raymond Mcdevitt, S Falco, T Dyk, M Ficke, and John Golin. Cloning two multiple drug resistance loci of saccharomyces cerevisiae by gene amplification. *Genetics*, 125:13–20, 06 1990.

[53] Hiroaki Inoue, Hiroshi Nojima, and Hiroto Okayama. High efficiency transformation of escherichia coli with plasmids. *Gene*, 96(1):23 – 28, 1990.

[54] R. Gietz and Robert Schiestl. High-efficiency yeast transformation using the liac/ss carrier dna/peg method. *Nature protocols*, 2:31–4, 02 2007.

[55] Norman Moullan, Laurent Mouchiroud, Xu Wang, Dongryeol Ryu, Evan G. Williams, Adrienne Mottis, Virginija Jovaisaite, Michael V. Frochaux, Pedro M. Quiros, Bart Deplancke, Riekelt H. Houtkooper, and Johan Auwerx. Tetracyclines disturb mitochondrial function across eukaryotic models: A call for caution in biomedical research. *Cell Reports*, 10(10):1681 – 1691, 2015.

[56] George Clark-Walker and Anthony Linnane. In vivo differentiation of yeast cytoplasmic and mitochondrial protein synthesis with antibiotics. *Biochemical and biophysical research communications*, 25:8–13, 11 1966.

[57] Dahn Clemens, Michael Duryee, Cleo Sarmiento, Andrew Chiou, Jake McGowan, Carlos Hunter, Sarah Schlichte, Jun Tian, Lynell Klassen, James O'Dell, Geoffrey Thiele, Ted Mikuls, Matthew Zimmerman, and Daniel Anderson. Novel antioxidant properties of doxycycline. *International Journal of Molecular Sciences*, 19:4078, 12 2018.

[58] Stephen F. Altschul, Warren Gish, Webb Miller, Eugene W. Myers, and David J. Lipman. Basic local alignment search tool. *Journal of Molecular Biology*, 215(3):403 – 410, 1990.

[59] G Gauthier, M Gauthier, and Richard Christen. Phylogenetic analysis of the genera alteromonas, shewanella, and moritella using genes coding for small-subunit rrna sequences and division of the genus alteromonas into two genera, alteromonas (emended) and pseudoalteromonas gen. nov., and proposal of twelve new species combinations. *International journal of systematic bacteriology*, 45:755–61, 11 1995.

[60] Ncbi conserved domain search. `https://www.ncbi.nlm.nih.gov/Structure/cdd/wrpsb.cgi`. Accessed: 2020-10-05.

[61] Michael Koenen, U Rüther, and B Müller-Hill. Immunoenzymatic detection of expressed gene fragments cloned in the lac z gene of e. coli. *The EMBO journal*, 1:509–12, 02 1982.

[62] Clustal omega. `https://www.ebi.ac.uk/Tools/msa/clustalo/`. Accessed: 2020-10-05.

[63] Iwao Ohtsuki, Koscak Maruyama, and Setsuro Ebashi. Regulatory and cytoskeletal proteins of vertebrate skeletal muscle. *Advances in protein chemistry*, 38:1–67, 02 1986.

[64] William Gerthoffer. Actin cytoskeletal dynamics in smooth muscle contraction. *Canadian journal of physiology and pharmacology*, 83:851–6, 11 2005.

[65] B. Walz. Zur feinstruktur der muskelzellen des pharynx-bulbus von tardigraden. *Cell and Tissue Research*, 140:389–399, 09 1973.

[66] Takashi Obinata, Kanako Ono, and Shoichiro Ono. Detection of a troponin i-like protein in non-striated muscle of the tardigrades (water bears). *Bioarchitecture*, 1:96–102, 03 2011.

[67] Emobss - merger. `http://www.bioinformatics.nl/cgi-bin/emboss/merger`. Accessed: 2020-10-05.

[68] Takuma Hashimoto, Daiki Horikawa, Yuki Saito, Hirokazu Kuwahara, Hiroko Kozuka-Hata, Tadasu Shin-I, Yohei Minakuchi, Kazuko Ohishi, Ayuko Motoyama, Tomoyuki Aizu, Atsushi Enomoto, Koyuki Kondo, Sae Tanaka, Yuichiro Hara, Shigeyuki Koshikawa, Hiroshi Sagara, Toru Miura, Shin-ichi Yokobori, Kiyoshi Miyagawa, and Takekazu Kunieda. Extremotolerant tardigrade genome and improved radiotolerance of human cultured cells by tardigrade-unique protein. *Nature Communications*, 7:12808, 09 2016.

[69] Graziela Ribas, Carmen Vargas, and Moacir Wajner. L-carnitine supplementation as a potential antioxidant therapy for inherited neurometabolic disorders. *Gene*, 533, 10 2013.

[70] Bor-Jen Lee, Jun-Shuo Lin, Yi-Chin Lin, and Ping-Ting Lin. Effects of l-carnitine supplementation on oxidative stress and antioxidant enzymes activities in patients with coronary artery disease: A randomized, placebo-controlled trial. *Nutrition journal*, 13:79, 08 2014.

[71] James Stull, Kristine Kamm, and Rene Vandenboom. Myosin light chain kinase and the role of myosin light chain phosphorylation in skeletal muscle. *Archives of biochemistry and biophysics*, 510:120–8, 02 2011.

[72] Conserved region: Kelch. `https://www.ncbi.nlm.nih.gov/Structure/cdd/sd00038`. Accessed: 2020-10-05.

[73] Ncbi: Mesh. `https://www.ncbi.nlm.nih.gov/mesh/?term=kelch+protein+17`. Accessed: 2020-03-07.

[74] Uniprot: Charged multivesicular body protein 5. `https://www.uniprot.org/uniprot/Q9NZZ3`. Accessed: 2020-10-05.

[75] Vladimir Bermudez, Yoshimasa Maniwa, Inger Tappin, Keiko Ozato, Kyoko Yokomori, and Jerard Hurwitz. The alternative ctf18-dcc1-ctf8-replication factor c complex required for sister chromatid cohesion loads proliferating cell nuclear antigen onto dna. *Proceedings of the National Academy of Sciences of the United States of America*, 100:10237–42, 10 2003.

[76] Yasushi Shiomi, Chikahide Masutani, Fumio Hanaoka, Hiroshi Kimura, and Toshiki Tsurimoto. A second proliferating cell nuclear antigen loader complex, ctf18-replication factor c, stimulates dna polymerase activity. *The Journal of biological chemistry*, 282:20906–14, 08 2007.

[77] Bengt Persson, Yvonne Kallberg, James Bray, Elspeth Bruford, Stephen Dellaporta, Angelo Favia, Roser Gonzàlez-Duarte, Hans Jörnvall, Kathryn Kavanagh, Natalia Kedishvili, Michael Kisiela, Edmund Maser, Rebekka Mindnich, Sandra Orchard, Trevor Penning, Janet Thornton, Jerzy Adamski, and Udo Oppermann. The sdr (short-chain dehydrogenase/reductase and related enzymes) nomenclature initiative. *Chemico-biological interactions*, 178:94–8, 12 2008.

[78] Y Lachance, Van Luu-The, C Labrie, J Simard, M Dumont, Y Launoit, Sylvain Guérin, G Leblanc, and Fernand Labrie. Characterization of human 3-hydroxysteroid dehydrogenase/5-4 isomerase gene. *The Journal of biological chemistry*, 265:20469–75, 12 1990.

[79] L. Hankes, W. Politzer, Oscar Touster, and Laurens Anderson. Myo-inositol catabolism in human pentosurics: the predominant role of the glucuronate-xylulose-pentose phosphate pathway. *Annals of the New York Academy of Sciences*, 165:564 – 576, 03 2007.

[80] Young-Mee Kim, Hee-Jung Kim, Eun Song, and Kong-Joo Lee. Glucoronic acid is a novel inducer of heat shock response. *Molecular and cellular biochemistry*, 259:23–33, 05 2004.

[81] Ncbi: Ercc excision repair 8. `https://www.ncbi.nlm.nih.gov/gene?Db=gene&Cmd=ShowDetailView&TermToSearch=1161`. Accessed: 2020-20-05.

[82] Anneke Hoffen, Adayapalam Natarajan, Lynne Mayne, Albert Zeeland, Leon Mullenders, and Jaap Venema. Deficient repair of the transcribed strand of active genes in cockayne's syndrome cells. *Nucleic acids research*, 21:5890–5, 01 1994.

[83] David Goodsell. The molecular perspective: Ultraviolet light and pyrimidine dimers. *Stem cells (Dayton, Ohio)*, 19:348–9, 02 2001.

[84] Martin Zackrisson, Johan Hallin, Lars-Göran Ottosson, Peter Dahl, Esteban Fernandez-Parada, Erik Ländström, Luciano Fernandez-Ricaud, Petra Kaferle, Andreas Skyman, Simon Stenberg, Stig Omholt, Uros Petrovic, Jonas Warringer, and Anders Blomberg. Scan-o-matic: High-resolution microbial phenomics at a massive scale. *G3 (Bethesda, Md.)*, 6, 07 2016.

[85] Mike Mackness, Sharon Arrol, and Paul Durrington. Paraoxonase prevents accumulation of lipoperoxides in low-density lipoprotein. *FEBS letters*, 286:152–4, 08 1991.

[86] Luciano Fernandez-Ricaud, Olga Kourtchenko, Martin Zackrisson, Jonas Warringer, and Anders Blomberg. Precog: A tool for automated extraction and visualization of fitness components in microbial growth phenomics. *BMC Bioinformatics*, 17, 06 2016.

[87] Luciano Fernandez-Ricaud, Olga Kourtchenko, Martin Zackrisson, Jonas Warringer, and Anders Blomberg. Precog: A tool for automated extraction and visualization of fitness components in microbial growth phenomics. *BMC Bioinformatics*, 17, 06 2016.

[88] Thomas Hygum, Dannie Fobian, Maria Kamilari, Aslak Jørgensen, Morten Schiøtt, Martin Grosell, and Nadja Møbjerg. Comparative investigation of copper tolerance and identification of putative tolerance related genes in tardigrades. *Frontiers in Physiology*, 8, 02 2017.

[89] pcm188 (atcc® 87660™). `https://www.lgcstandards-atcc.org/~/media/Attachments/9/0/6/E/1717.ashx`. Accessed: 2019-10-28.

6 Supplementary

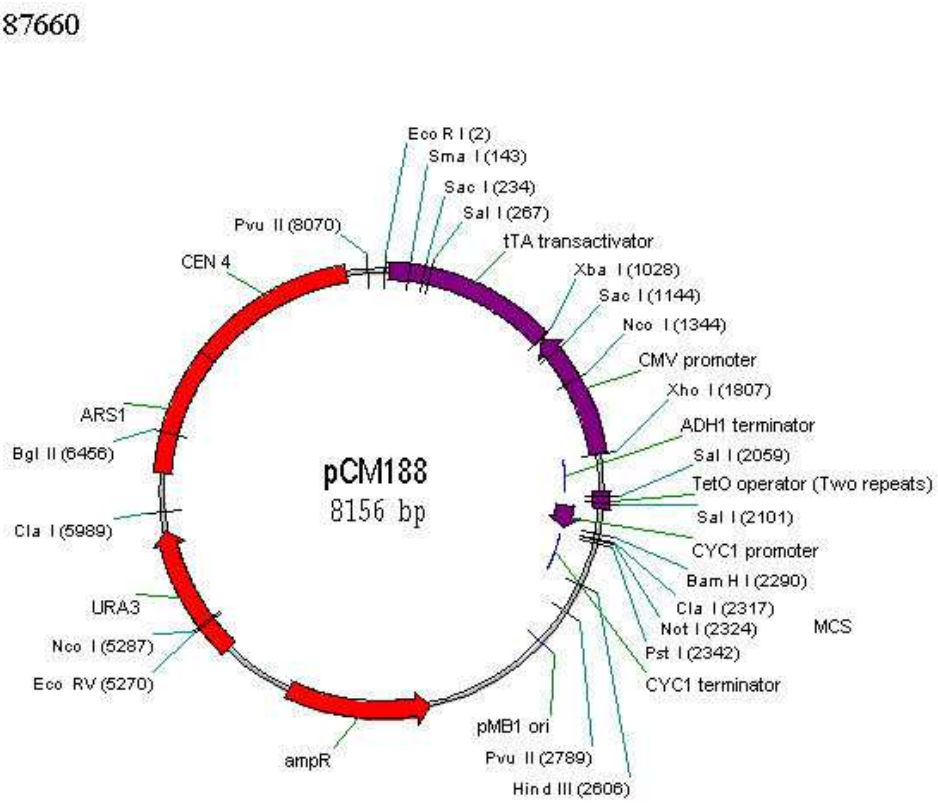

Figure 6.1: Vector map of pCM188 [89]

6.1 Plates

6.1.1 Osmotic Stress

6.1.1.1 Sodium Chloride

1. Plate

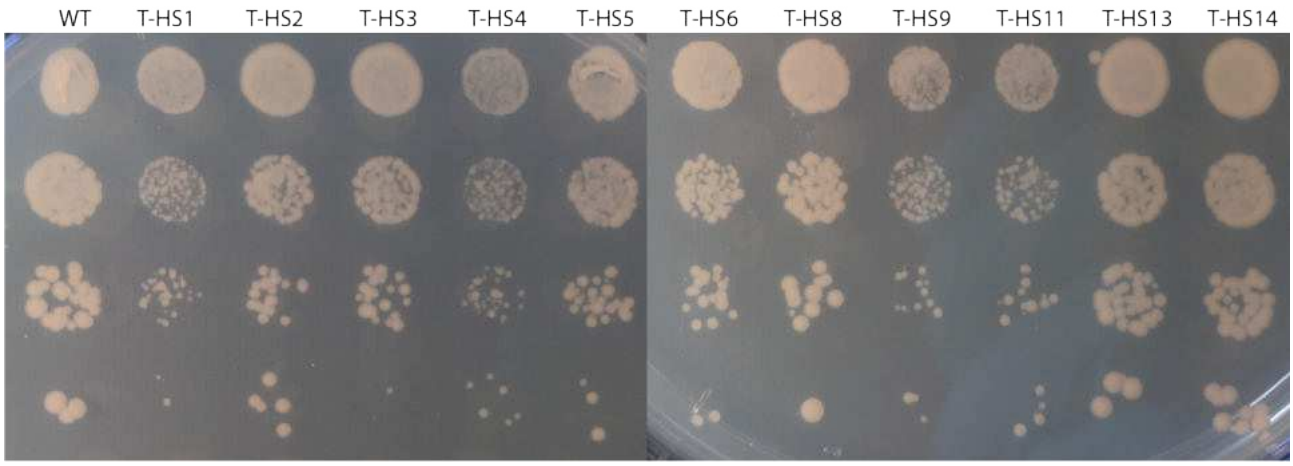

Figure 6.2: Cells plated on YNB-URA supplemented with 1.2 M NaCl and grown at 30 °C for 72 h

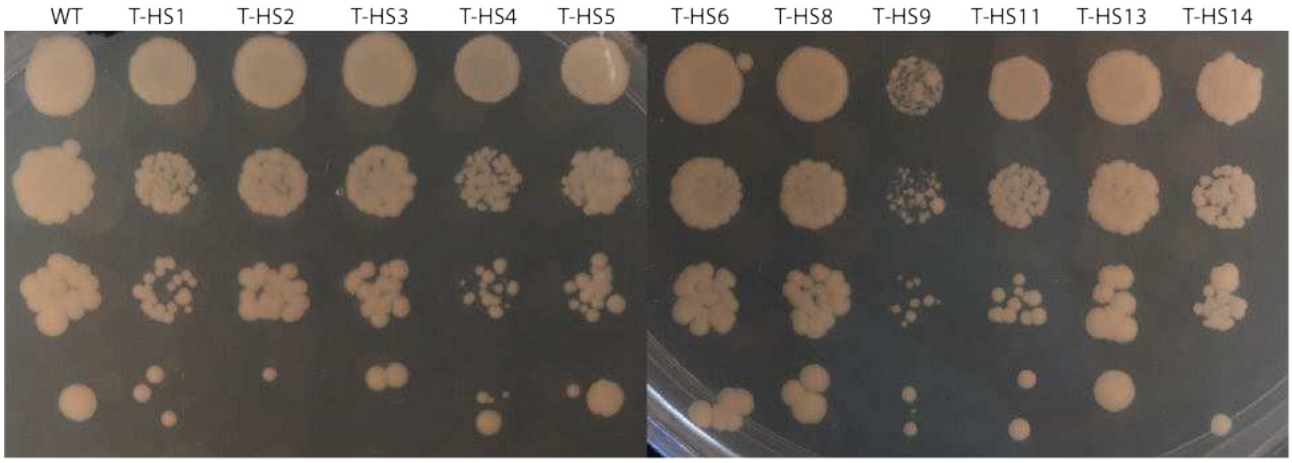

Figure 6.3: Control: cells plated on YNB-URA and grown at 30 °C for 72 h

2. Plate

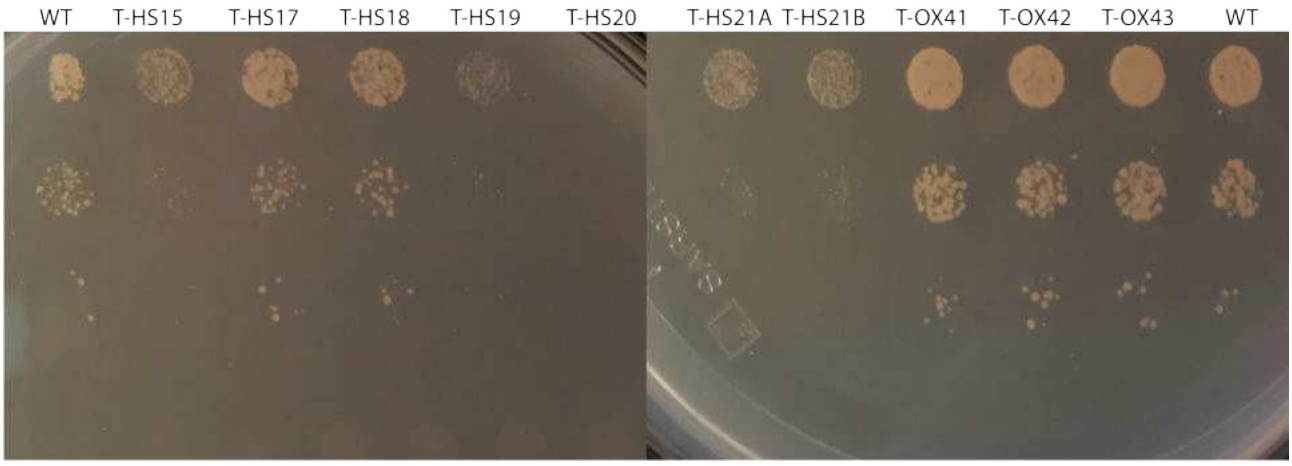

Figure 6.4: Cells plated on YNB-URA supplemented with 1.2 M NaCl and grown at 30 °C for 72 h

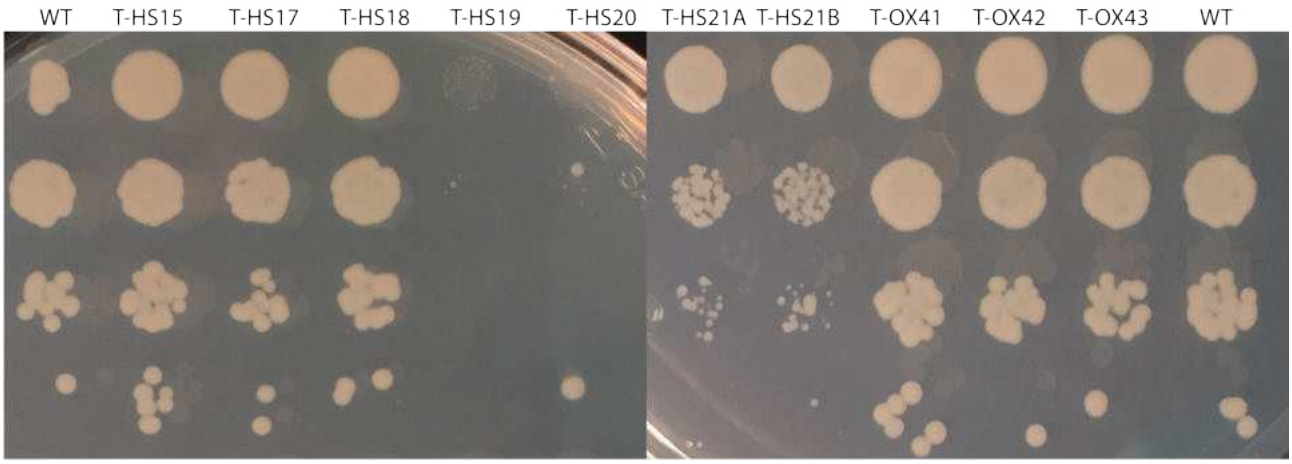

Figure 6.5: Control: cells plated on YNB-URA and grown at 30 °C for 72 h

3. Plate

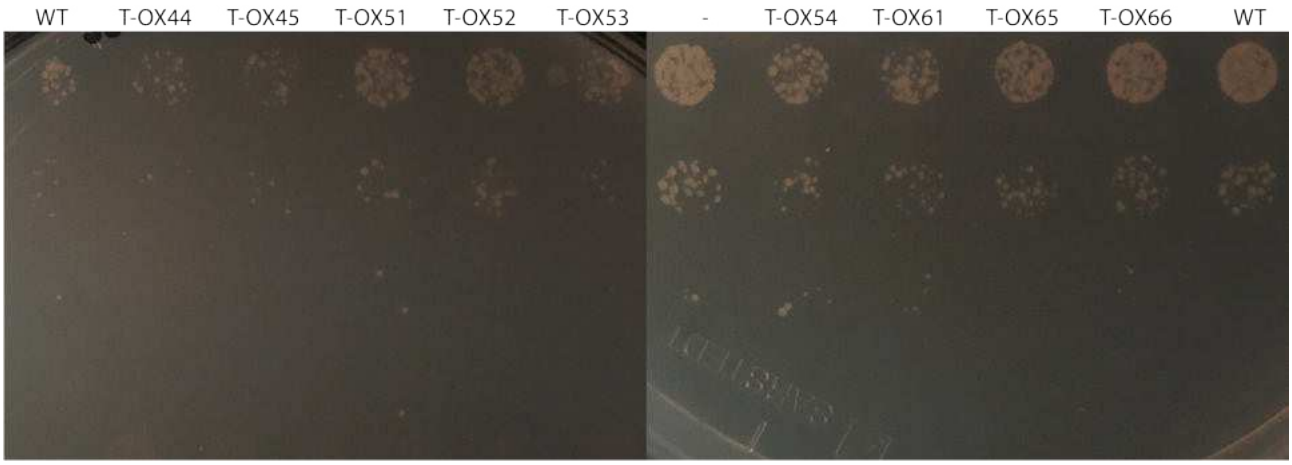

Figure 6.6: Cells plated on YNB-URA supplemented with 1.2 M NaCl and grown at 30 °C for 72 h

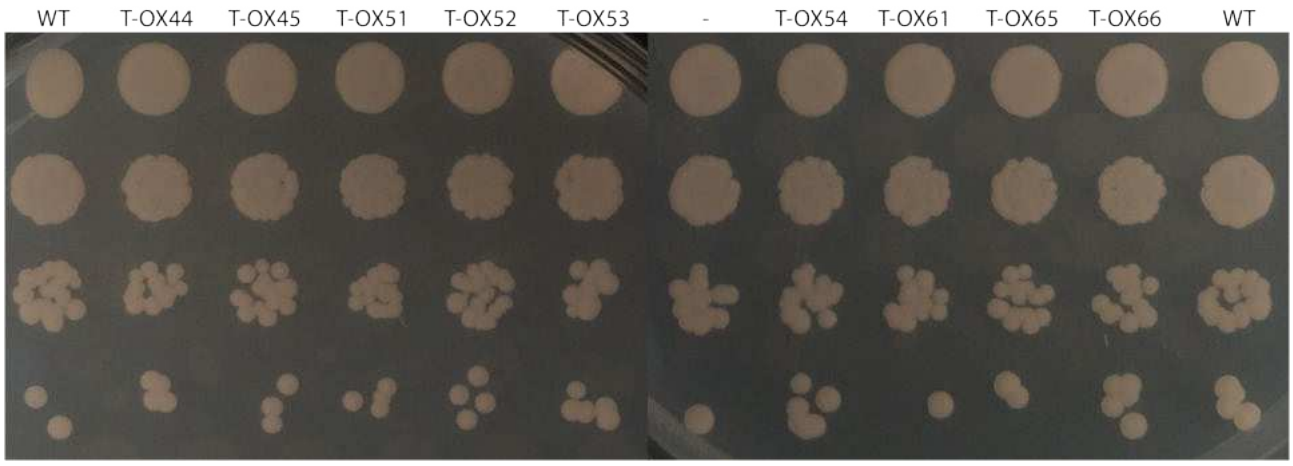

Figure 6.7: Control: cells plated on YNB-URA and grown at 30 °C for 72 h

6.1.1.2 Potassium Chloride

4. Plate

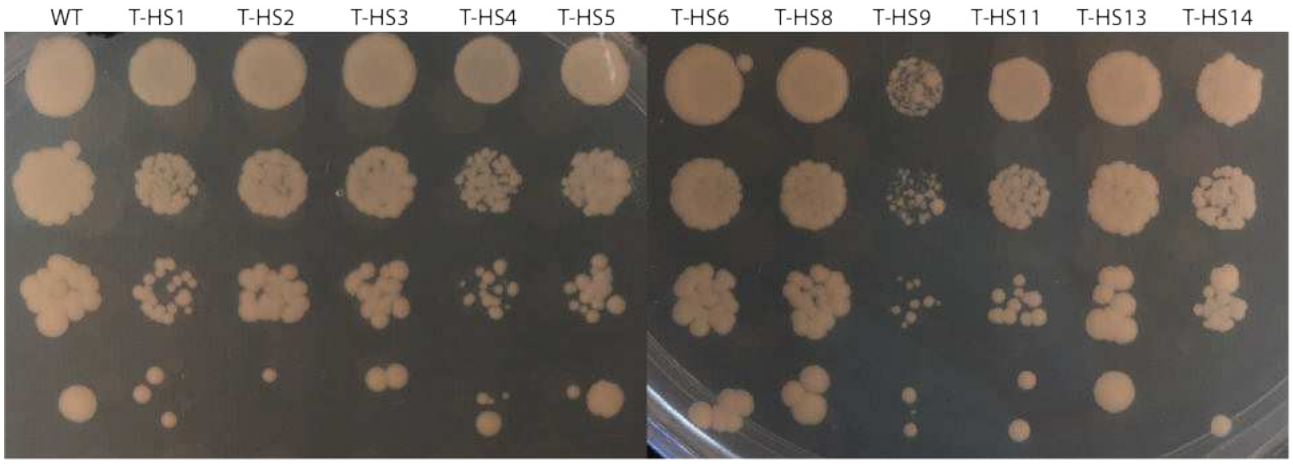

Figure 6.8: Control: cells plated on YNB-URA and grown at 30 °C for 72 h

5. Plate

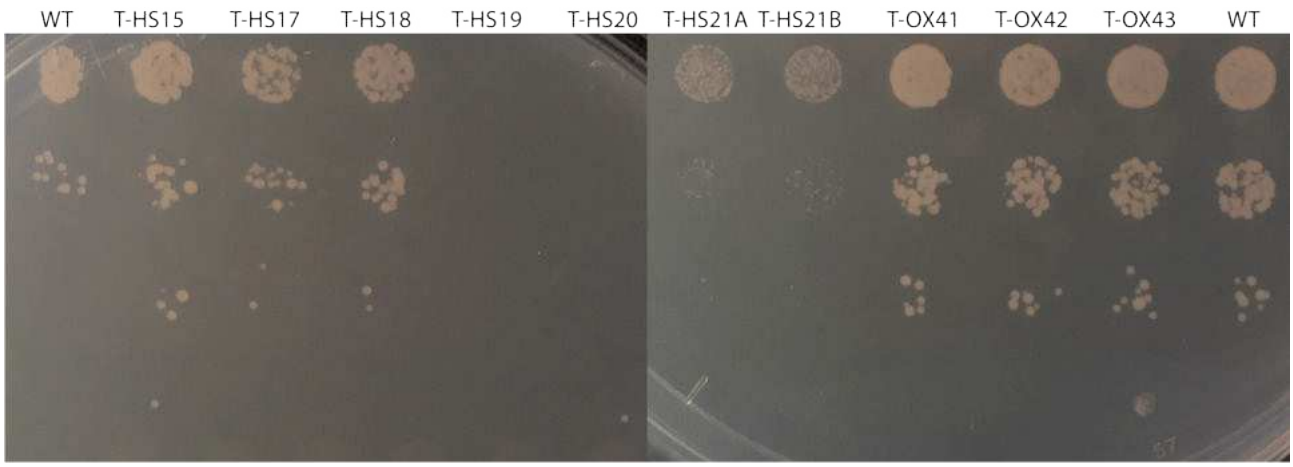

Figure 6.9: Cells plated on YNB-URA supplemented with 1.5 M KCl and grown at 30 °C for 72 h

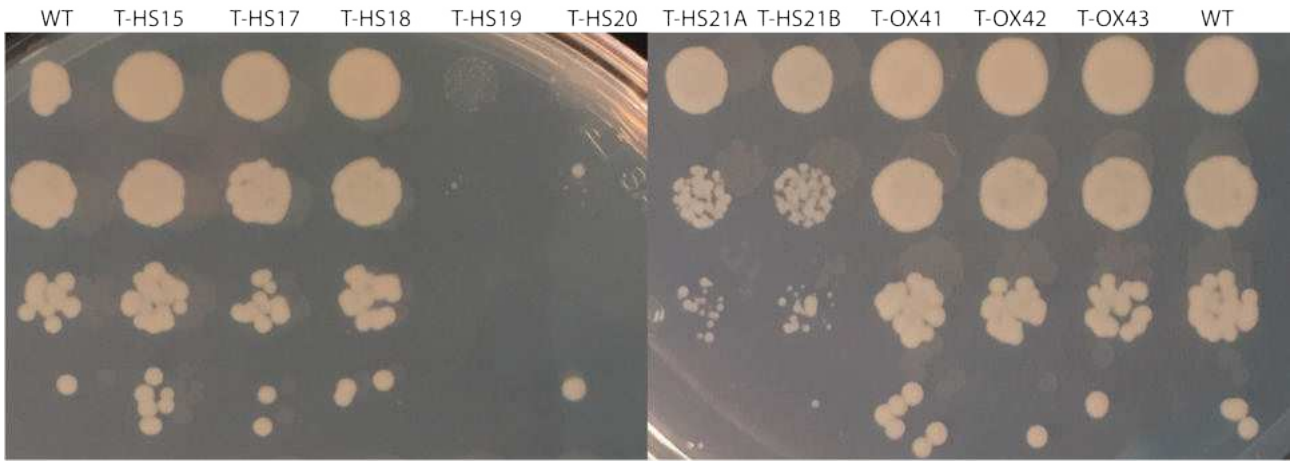

Figure 6.10: Control: cells plated on YNB-URA and grown at 30 °C for 72 h

6. Plate

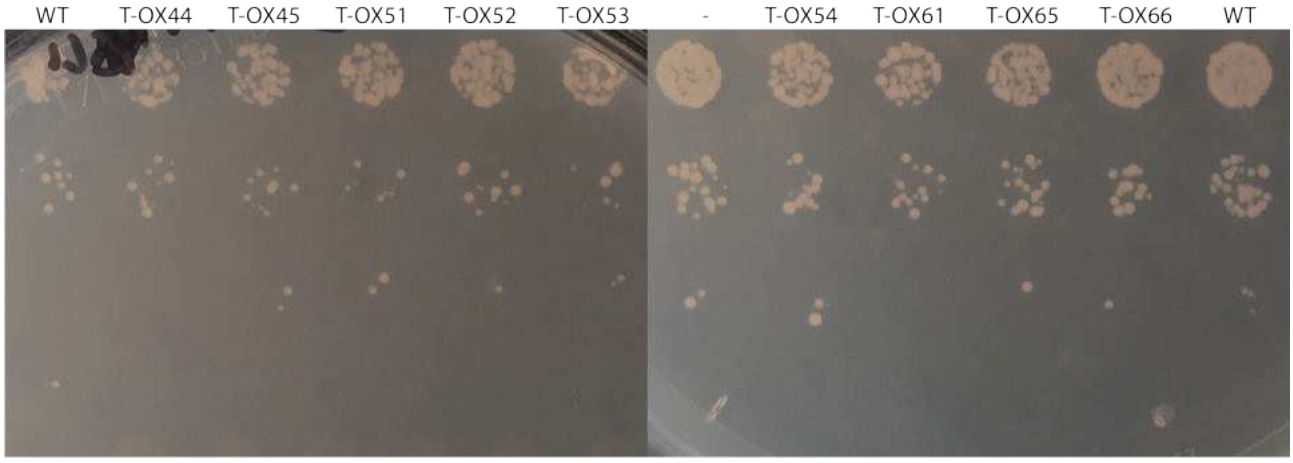

Figure 6.11: Cells plated on YNB-URA supplemented with 1.5 M KCl and grown at 30 °C for 72 h

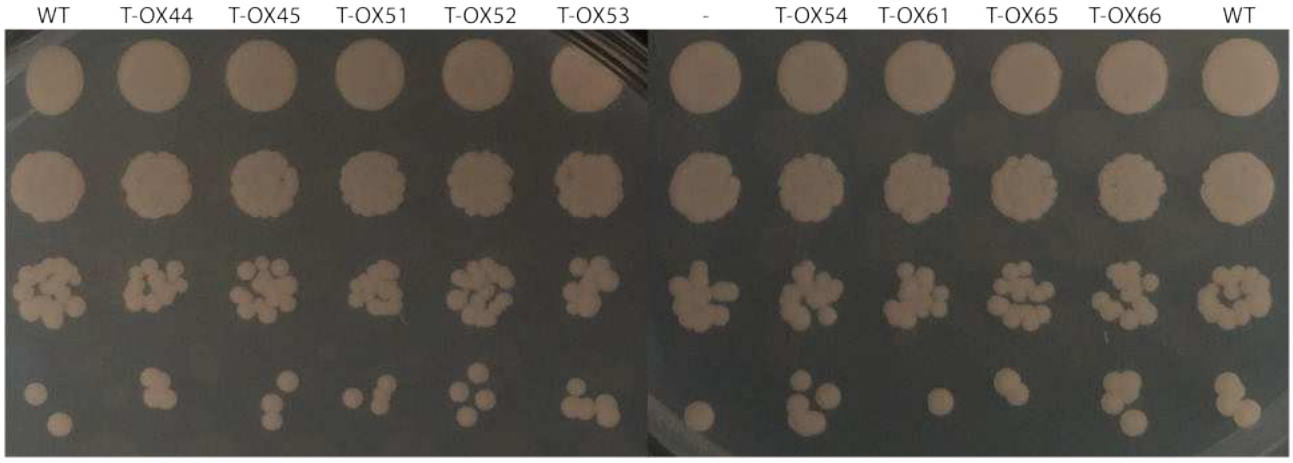

Figure 6.12: Control: cells plated on YNB-URA and grown at 30 °C for 72 h

6.1.2 Heat Stress

6.1.2.1 Heat Shock

7. Plate

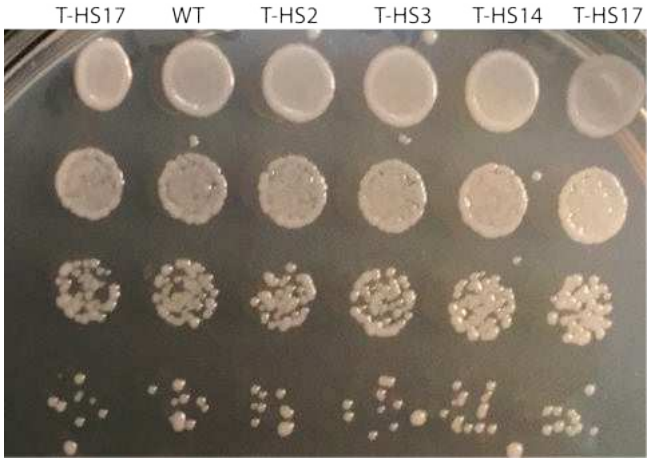

Figure 6.13: Cells treated at 44 °C for 1 h, plated on YNB-URA and grown at 30 °C for 48 h

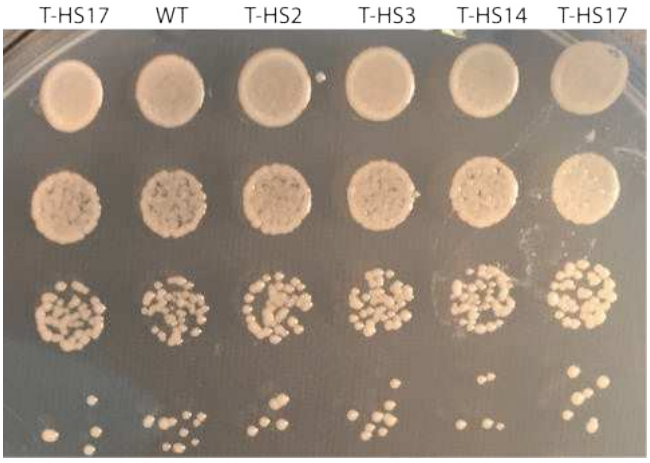

Figure 6.14: Control: untreated cells plated on YNB-URA and grown at ¡30 °C for 48 h

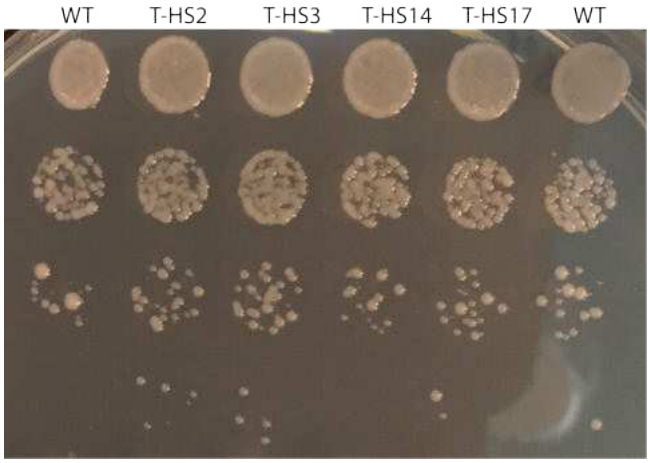

Figure 6.15: Cells treated at 46 °C for 1 h, plated on YNB-URA and grown at 30 °C for 48 h

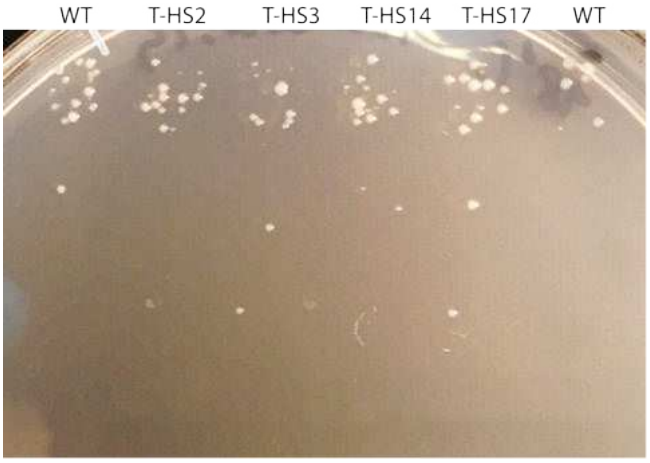

Figure 6.16: Cells treated at 46 °C for 1 h, plated on YNB-URA and grown at 30 °C for 48 h

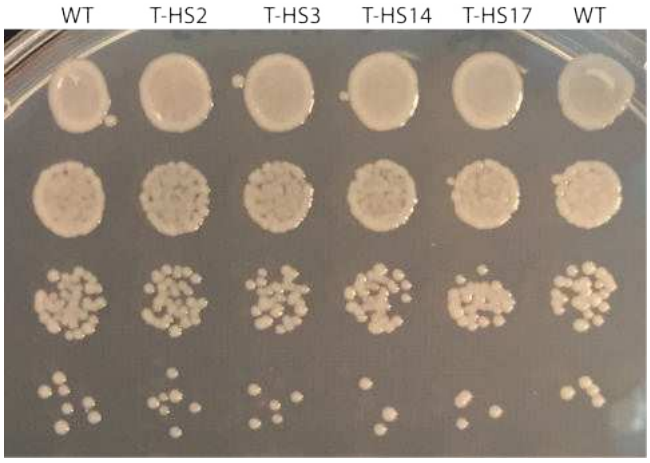

Figure 6.17: Control: untreated cells plated on YNB-URA and grown at ¡30 °C for 48 h

8. Plate

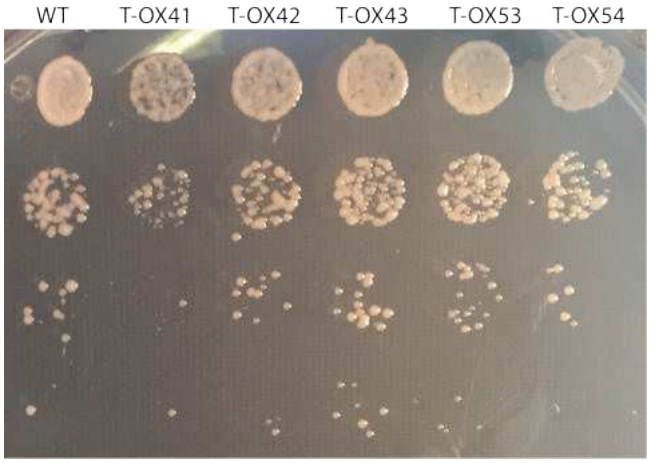

Figure 6.18: Cells treated at 46 °C for 1 h, plated on YNB-URA and grown at 30 °C for 48 h

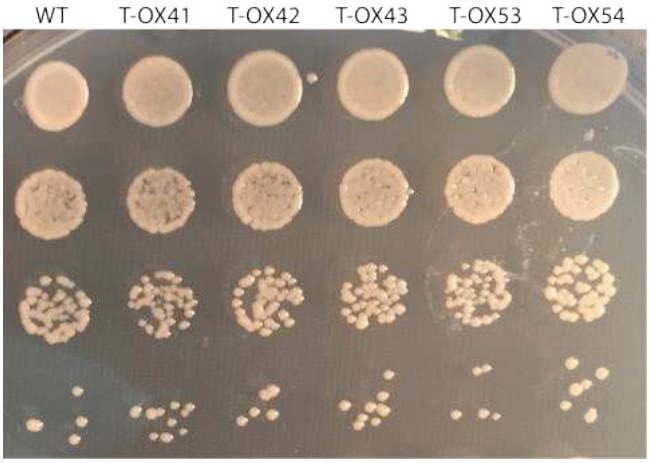

Figure 6.19: Control: untreated cells plated on YNB-URA and grown at 30 °C for 48 h

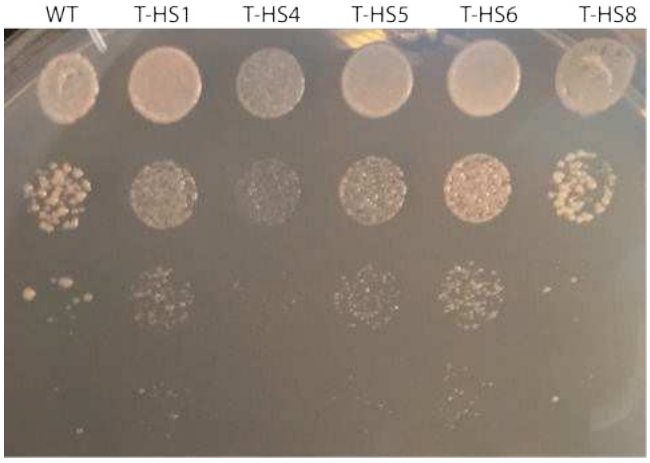

Figure 6.20: Cells treated at 46 °C for 1 h, plated on YNB-URA and grown at 30 °C for 48 h

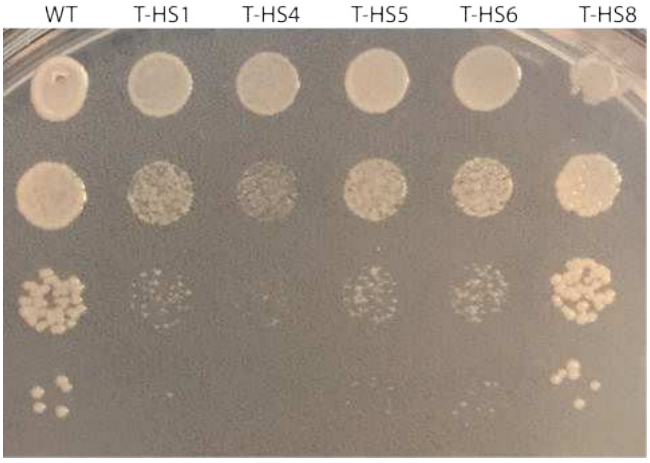

Figure 6.21: Control: untreated cells plated on YNB-URA and grown at 30 °C for 48 h

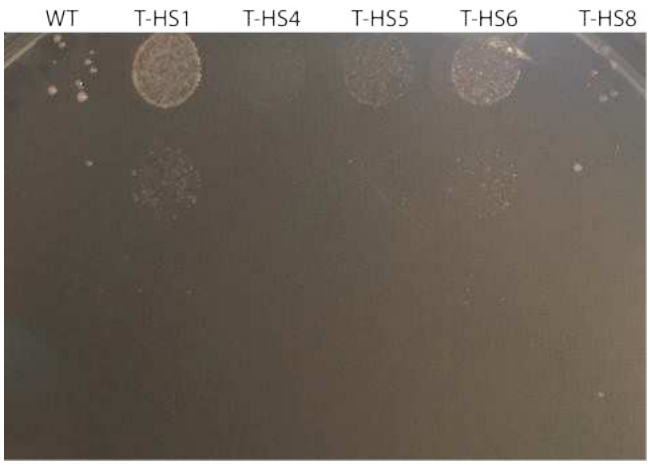

Figure 6.22: Cells treated at 46 °C for 1 h, plated on YNB-URA and grown at 30 °C for 48 h

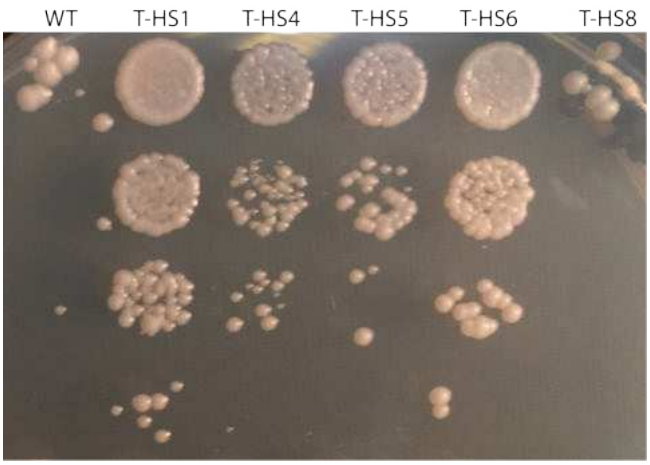

Figure 6.23: Cells treated at 46 °C for 1 h, plated on YNB-URA and grown at 30 °C for 72 h

10. Plate

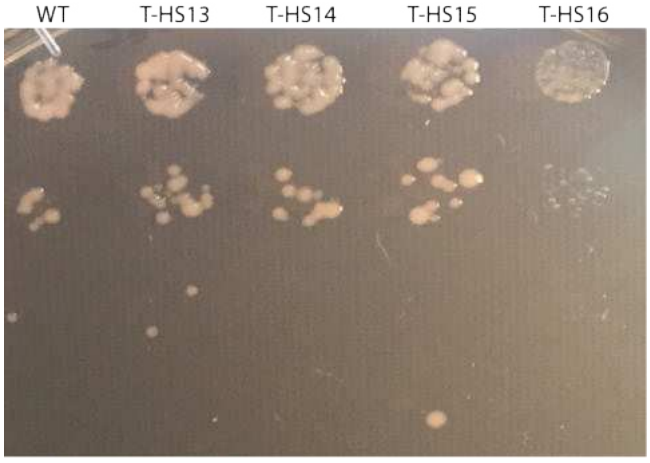

Figure 6.24: Cells treated at 47 °C for 1 h, plated on YNB-URA and grown at 30 °C for 48 h

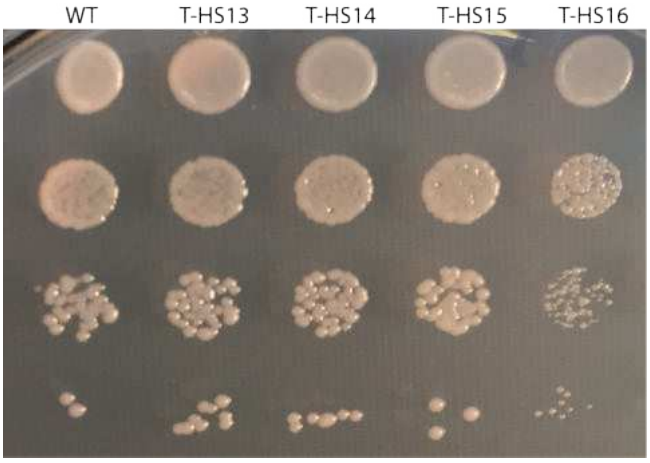

Figure 6.25: Control: untreated cells plated on YNB-URA and grown at 30 °C for 48 h

11. Plate

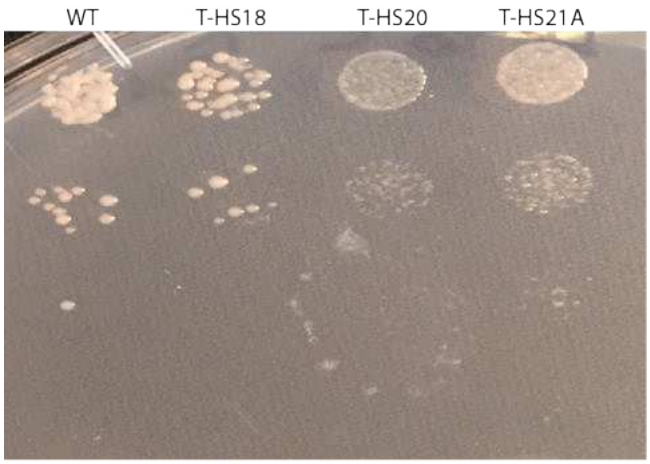

Figure 6.26: Cells treated at 47 °C for 1 h, plated on YNB-URA and grown at 30 °C for 48 h

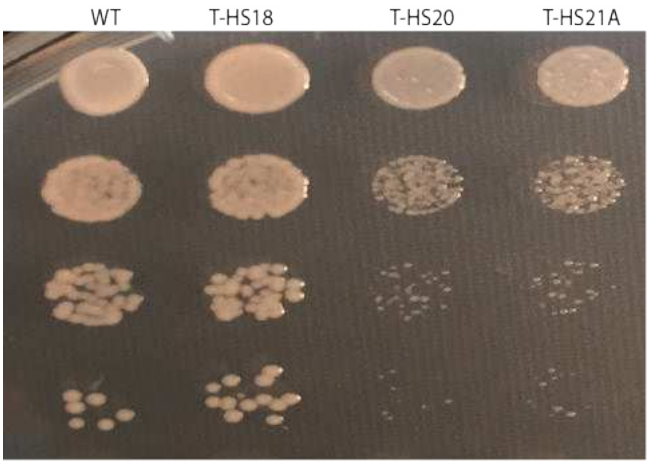

Figure 6.27: Control: untreated cells plated on YNB-URA and grown at 30 °C for 48 h

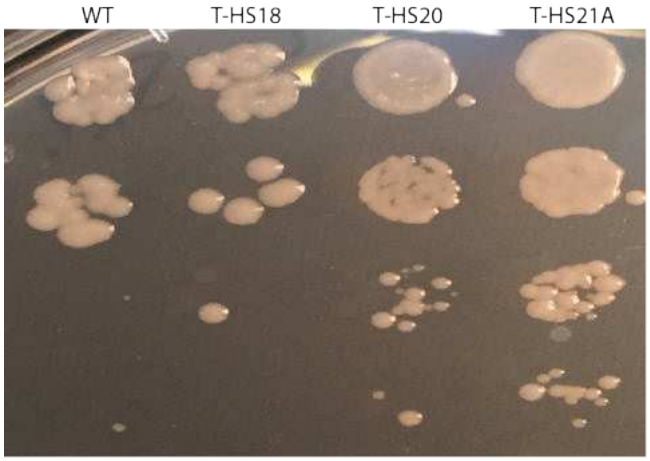

Figure 6.28: Cells treated at 47 °C for 1 h, plated on YNB-URA and grown at 30 °C for 72 h

12. Plate

Figure 6.29: Cells treated at 47 °C for 1 h, plated on YNB-URA and grown at 30 °C for 48 h

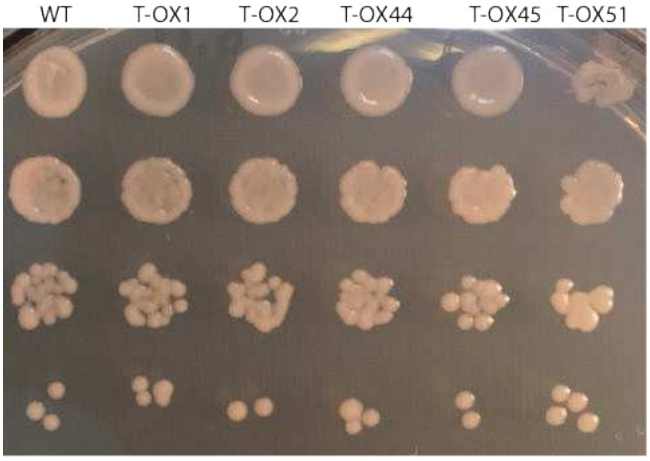

Figure 6.30: Control: untreated cells plated on YNB-URA and grown at 30 °C for 48 h

13. Plate

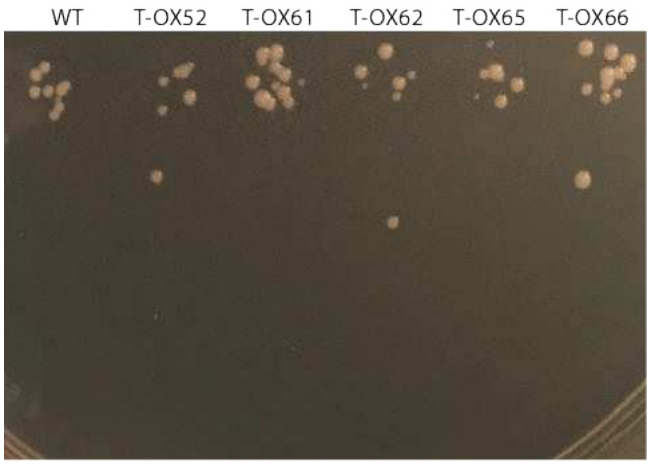

Figure 6.31: Cells treated at 47 °C for 1 h, plated on YNB-URA and grown at 30 °C for 48 h

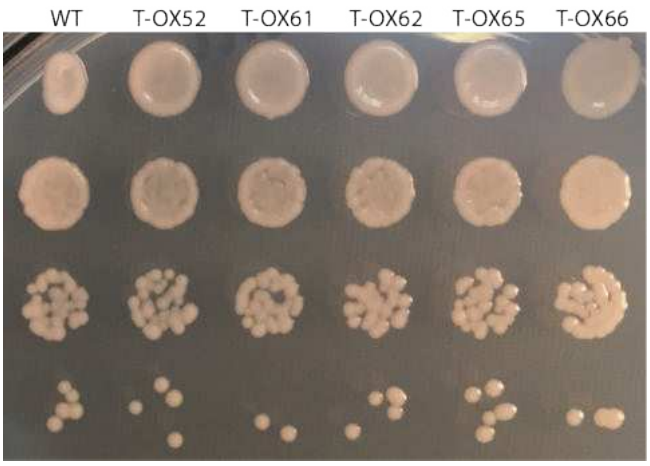

Figure 6.32: Control: untreated cells plated on YNB-URA and grown at 30 °C for 48 h

6.1.2.2 Continuous Growth at 40 °C

14. Plate

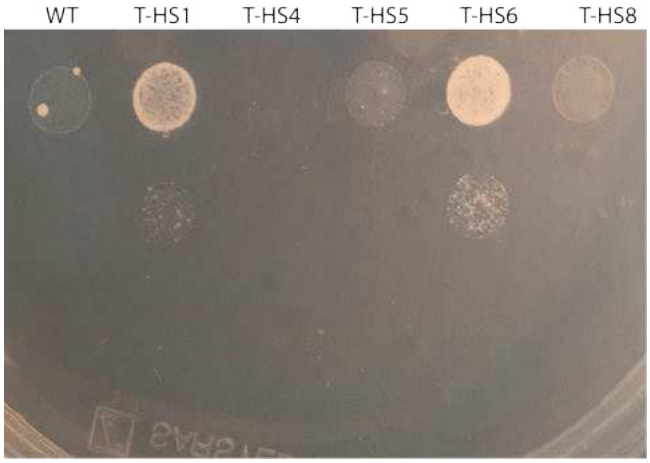

Figure 6.33: Cells plated on YNB-URA and grown for 5 days at 40 °C

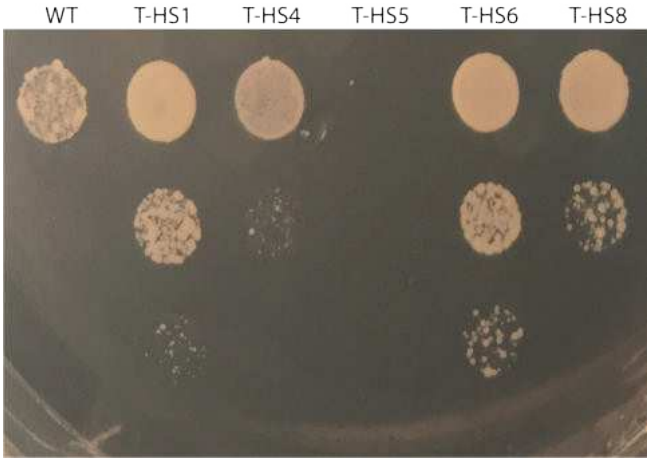

Figure 6.34: Cells plated on YNB-URA + 2 µg mL^{-1} DOX and grown for 5 days at 40 °C

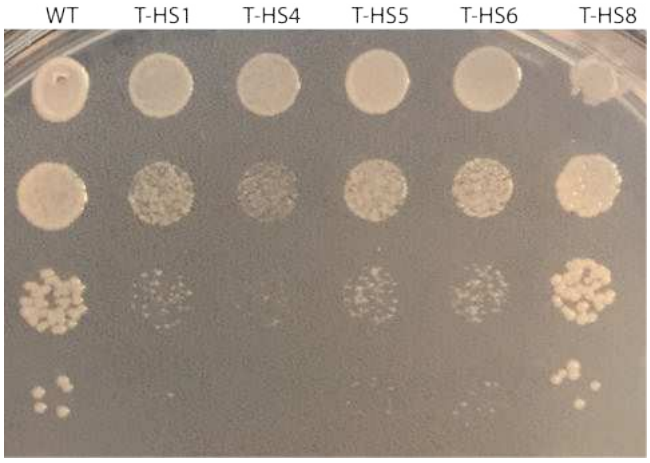

Figure 6.35: Cells plated on YNB-URA and grown for 2 days at 30 °C

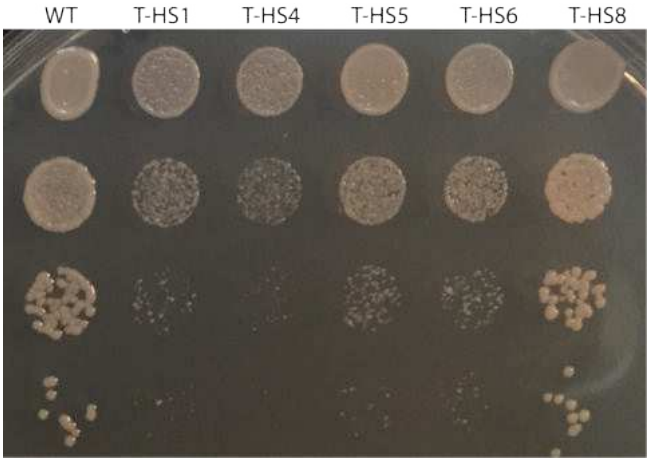

Figure 6.36: Cells plated on YNB-URA + 2 µg mL^{-1} DOX and grown for 2 days at 30 °C

15. Plate

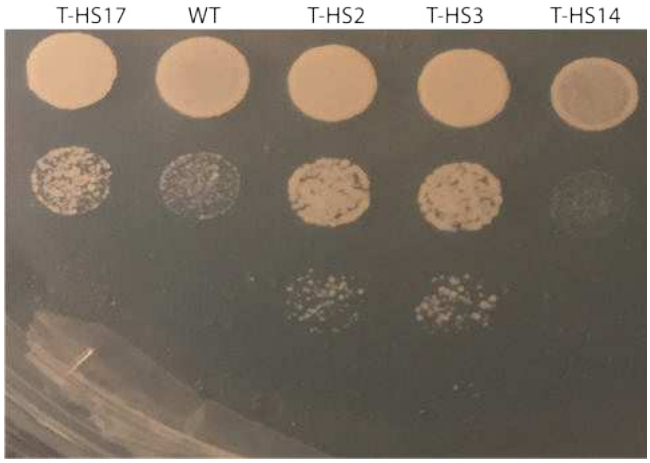

Figure 6.37: Cells plated on YNB-URA and grown for 5 days at 40 °C

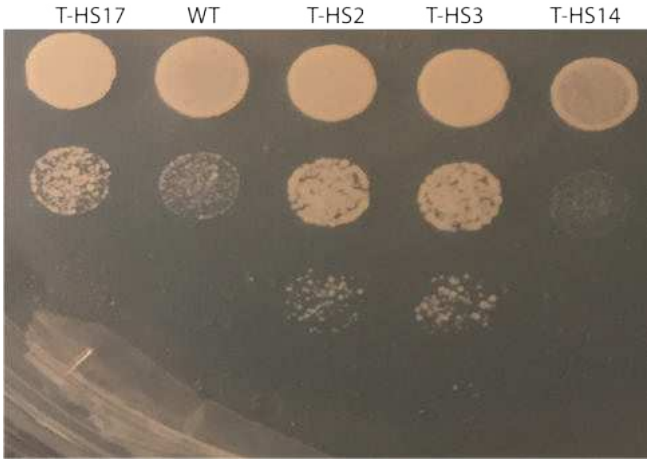

Figure 6.38: Cells plated on YNB-URA and grown for 2 days at 30 °C

6.1.3 Oxidative Stress

16. Plate

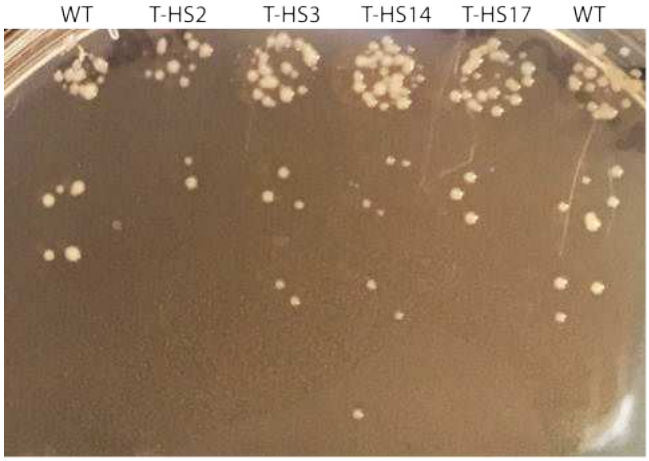

Figure 6.39: Cells treated with 4 mM H_2O_2, plated on YNB-URA and grown at 30 °C for 2 days

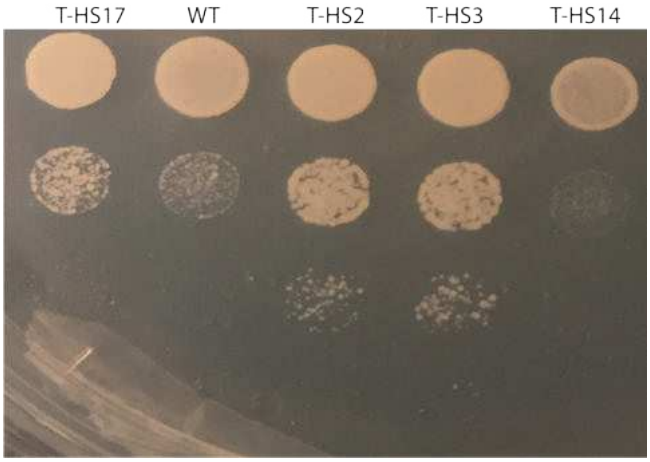

Figure 6.40: Control: cells plated on YNB-URA and grown at 30 °C for 2 days

17. Plate

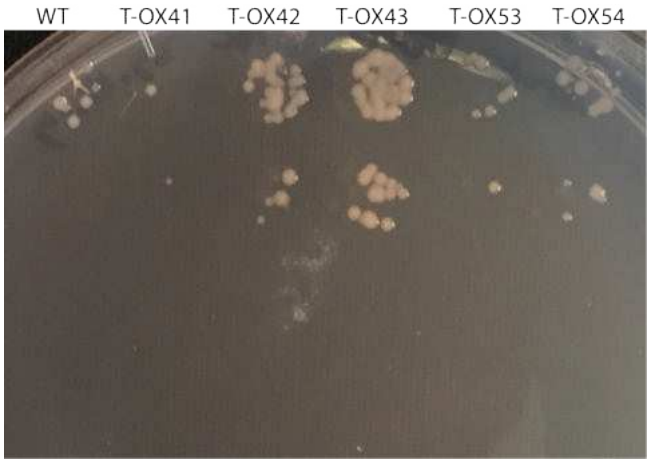

Figure 6.41: Cells treated with 4 mM H_2O_2, plated on YNB-URA and grown at 30 °C for 2 days

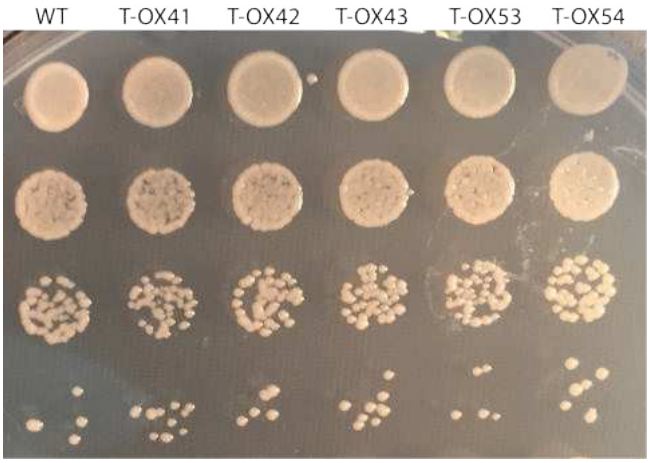

Figure 6.42: Control: cells plated on YNB-URA and grown at 30 °C for 2 days

18. Plate

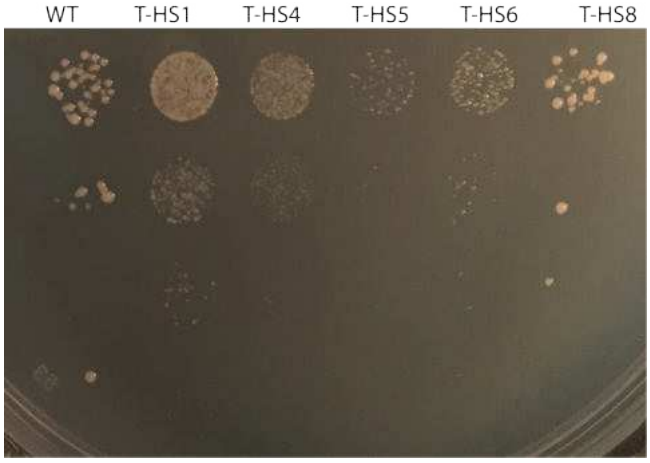

Figure 6.43: Cells treated with 4 mM H_2O_2, plated on YNB-URA and grown at 30 °C for 2 days

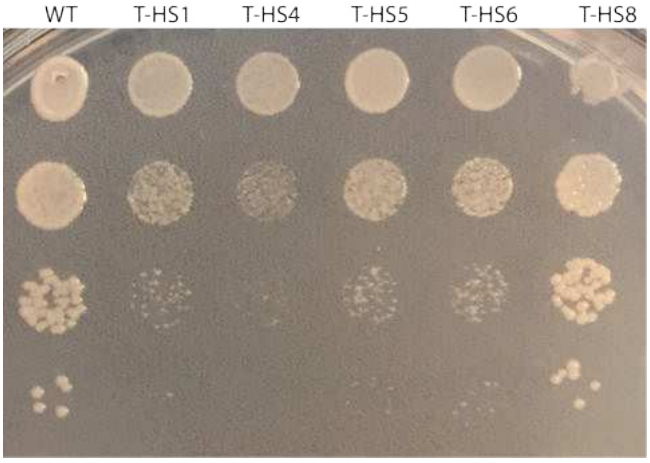

Figure 6.44: Control: cells plated on YNB-URA and grown at 30 °C for 2 days

19. Plate

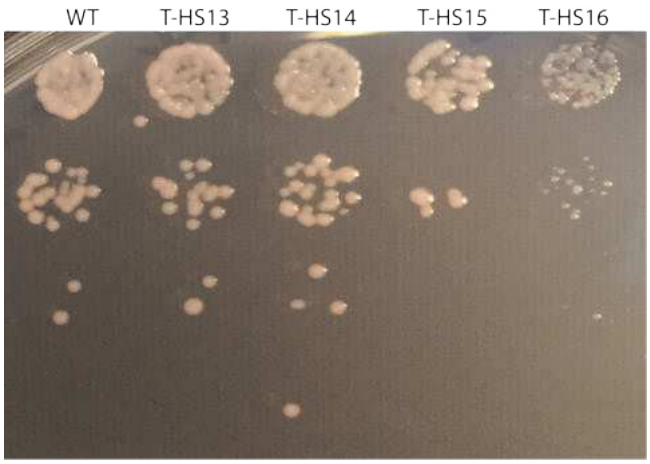

Figure 6.45: Cells treated with 4 mM H_2O_2, plated on YNB-URA and grown at 30 °C for 2 days

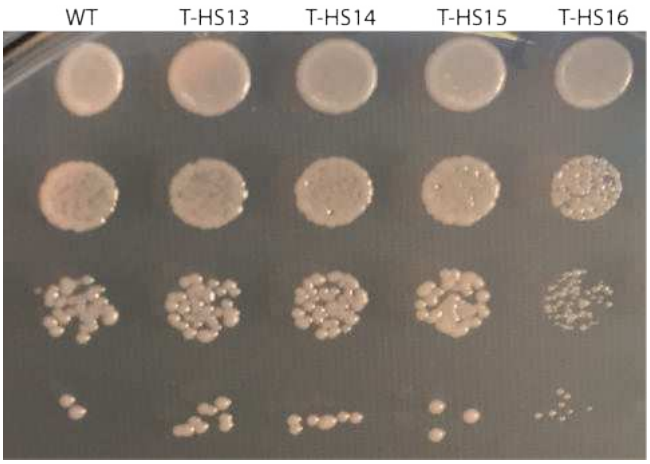

Figure 6.46: Control: cells plated on YNB-URA and grown at 30 °C for 2 days

20. Plate

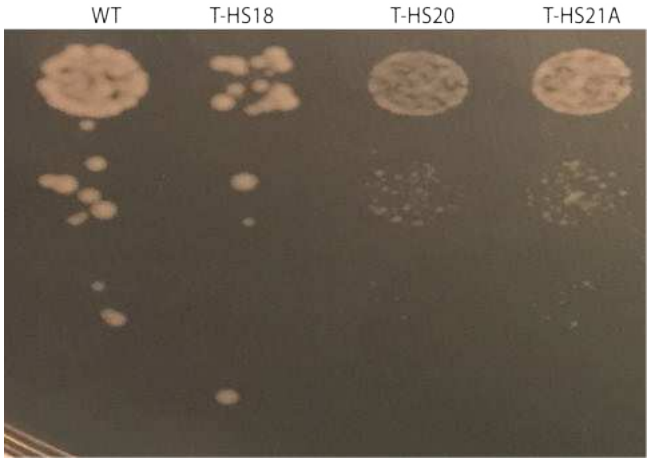

Figure 6.47: Cells treated with 4 mM H_2O_2, plated on YNB-URA and grown at 30 °C for 2 days

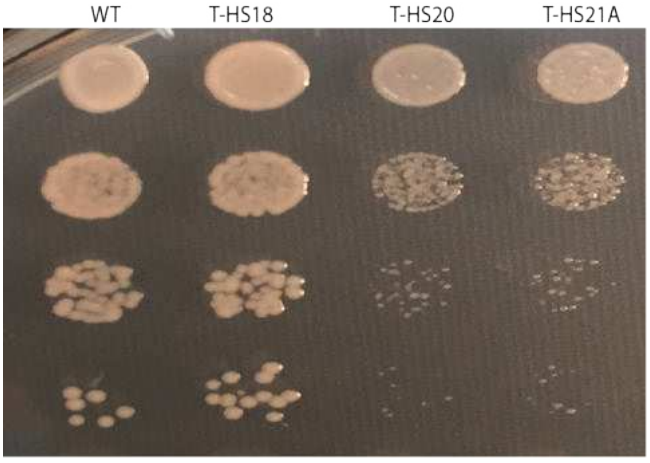

Figure 6.48: Control: cells plated on YNB-URA and grown at 30 °C for 2 days

21. Plate

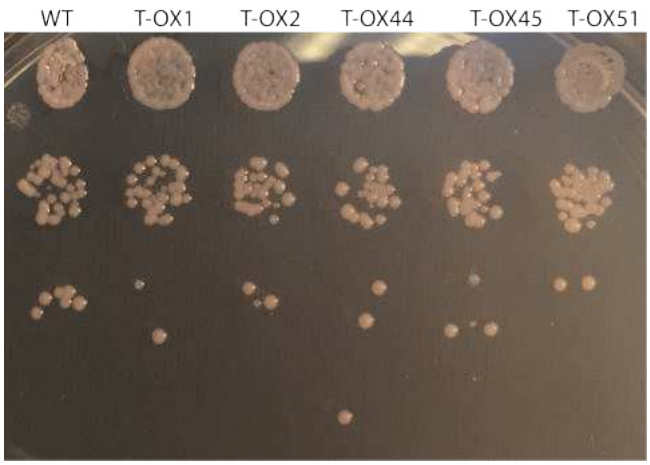

Figure 6.49: Cells treated with 4 mM H_2O_2, plated on YNB-URA and grown at 30 °C for 2 days

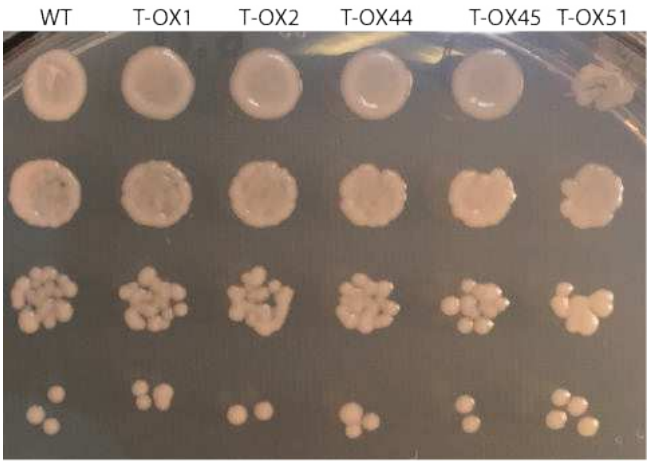

Figure 6.50: Control: cells plated on YNB-URA and grown at 30 °C for 2 days

22. Plate

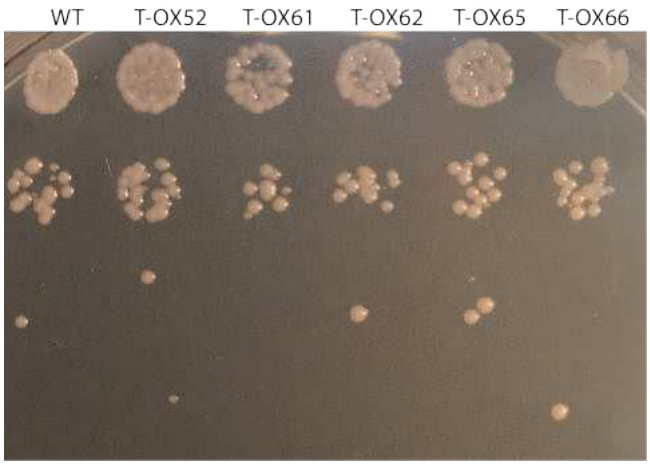

Figure 6.51: Cells treated with 4 mM H_2O_2, plated on YNB-URA and grown at 30 °C for 2 days

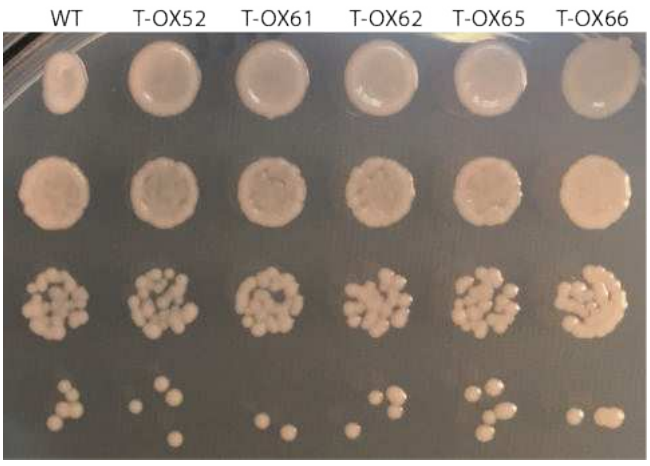

Figure 6.52: Control: cells plated on YNB-URA and grown at 30 °C for 2 days

6.1.4 2nd-Transformants

23. Plate

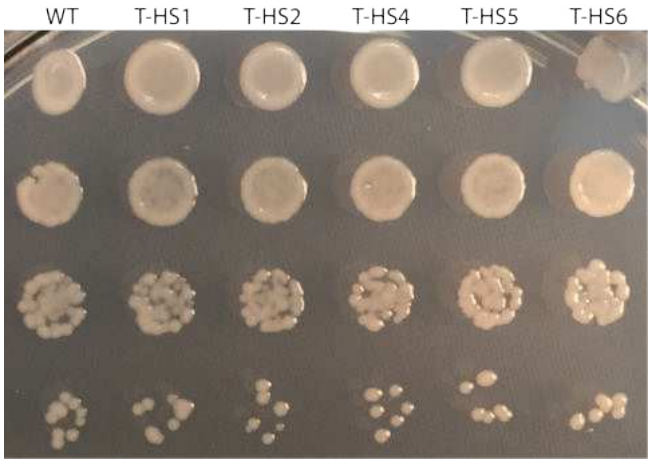

Figure 6.53: Cells plated on YNB-URA and grown at 30 °C for 48 h

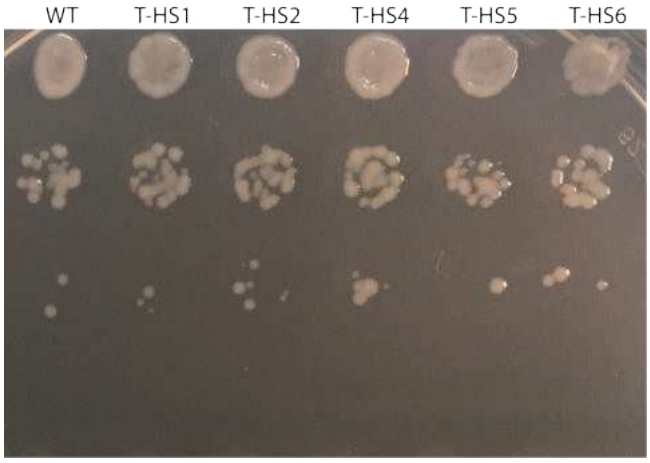

Figure 6.54: Cells treated at 45 °C for 1 h, plated on YNB-URA and grown at 30 °C for 48 h

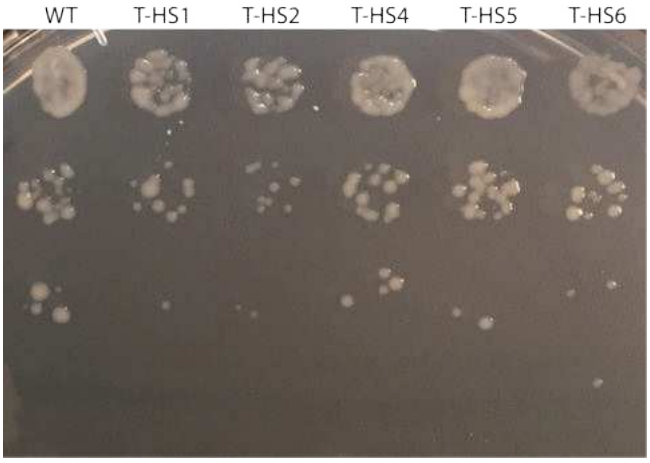

Figure 6.55: Cells treated with 3 mM H_2O_2 for 2 h, plated on YNB-URA and grown at 30 °C for 48 h

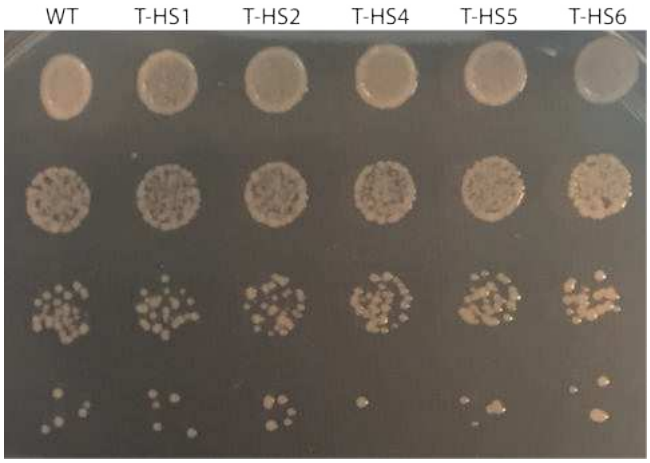

Figure 6.56: Cells plated on YNB-URA supplemented with 1.5 M KCl and grown at 30 °C for 72 h

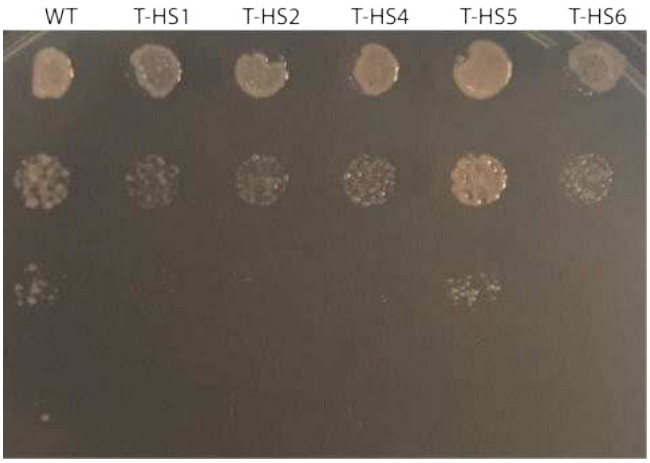

Figure 6.57: Cells plated on YNB-URA supplemented with 1.2 M NaCl and grown at 30 °C for 72 h

24. Plate

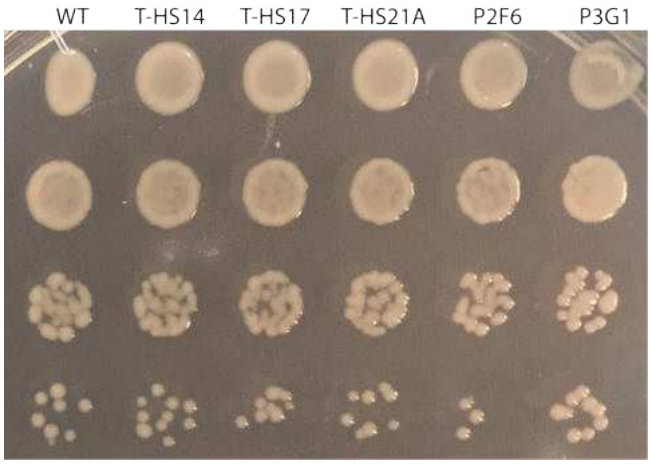

Figure 6.58: Cells plated on YNB-URA and grown at 30 °C for 48 h

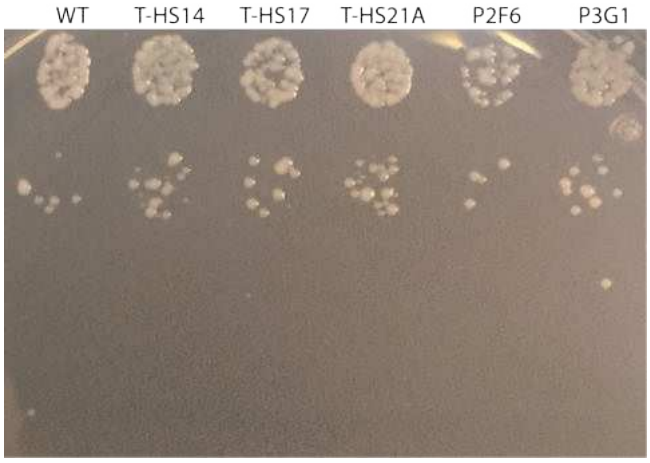

Figure 6.59: Cells treated at 45 °C for 1 h, plated on YNB-URA and grown at 30 °C for 48 h

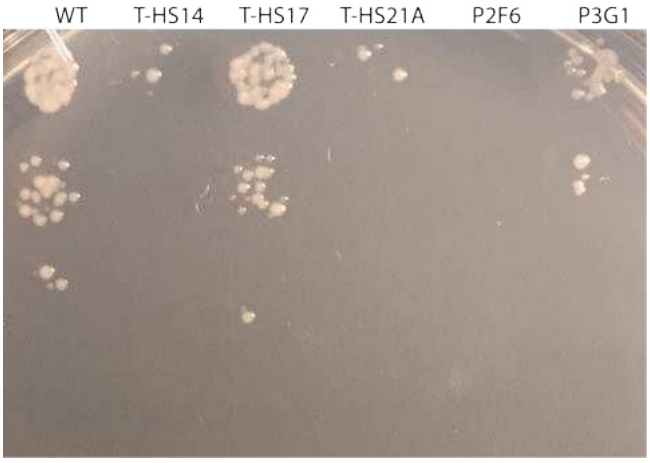

Figure 6.60: Cells treated with 3 mM H_2O_2 for 2 h, plated on YNB-URA and grown at 30 °C for 48 h

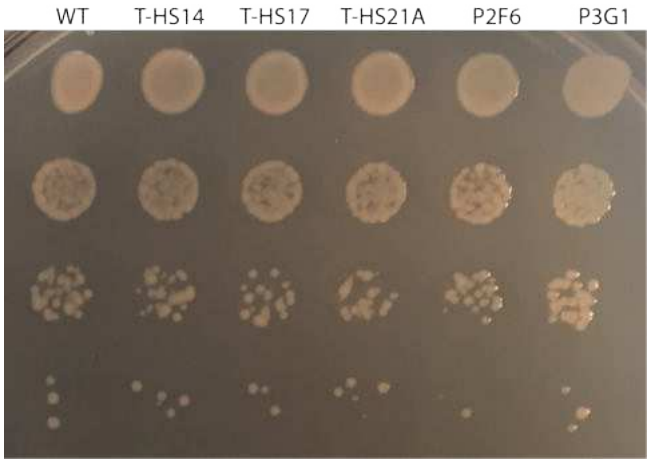

Figure 6.61: Cells plated on YNB-URA supplemented with 1.5 M KCl and grown at 30 °C for 72 h

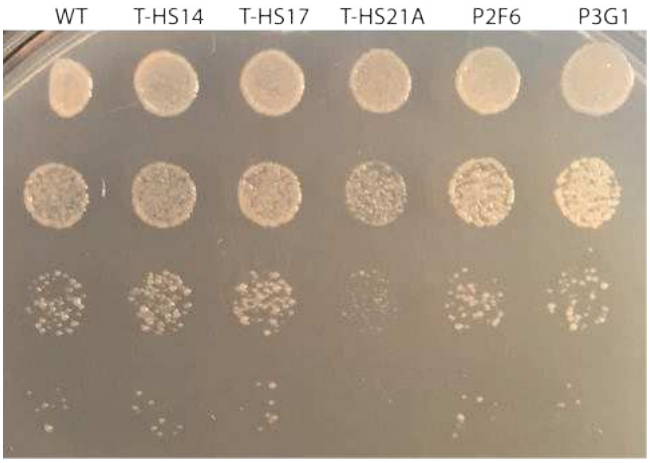

Figure 6.62: Cells plated on YNB-URA supplemented with 1.2 M NaCl and grown at 30 °C for 72 h

25. Plate

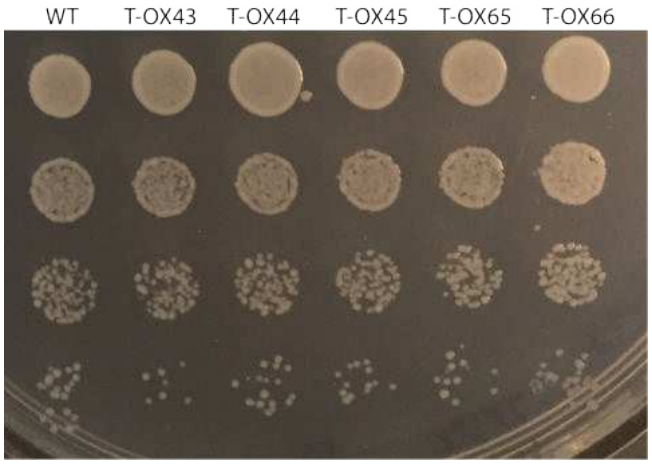

Figure 6.63: Cells plated on YNB-URA and grown at 30 °C for 48 h

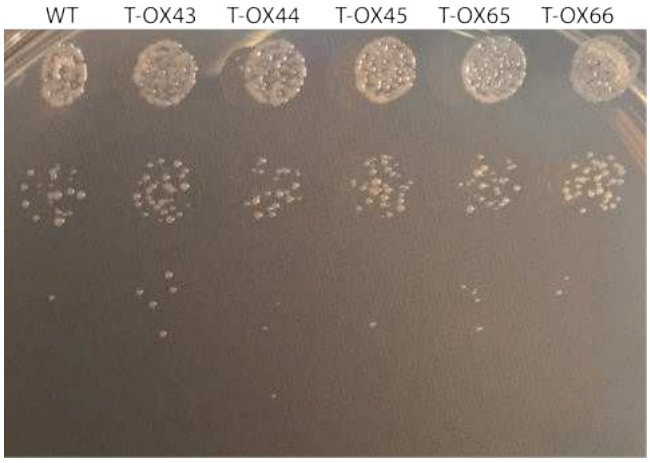

Figure 6.64: Cells treated at 45 °C for 1 h, plated on YNB-URA and grown at 30 °C for 48 h

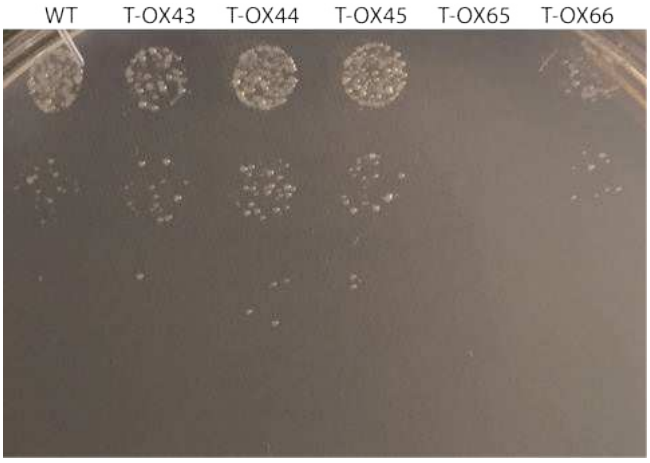

Figure 6.65: Cells treated with 3 mM H_2O_2 for 2 h, plated on YNB-URA and grown at 30 °C for 48 h

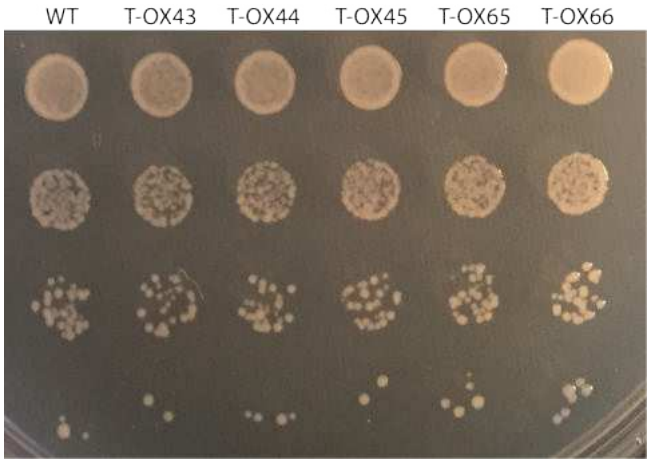

Figure 6.66: Cells plated on YNB-URA supplemented with 1.5 M KCl and grown at 30 °C for 72 h

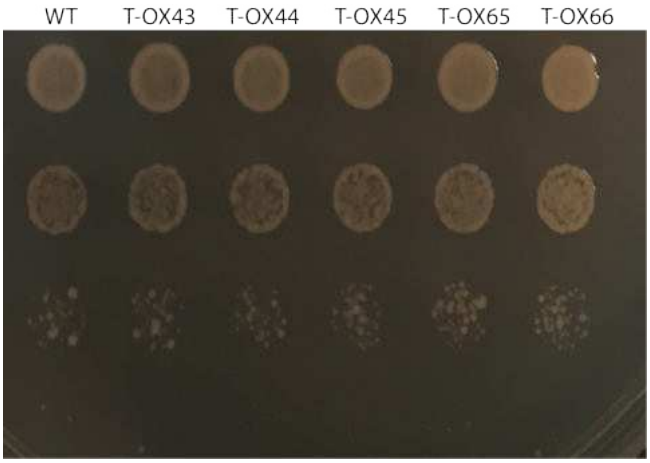

Figure 6.67: Cells plated on YNB-URA supplemented with 1.2 M NaCl and grown at 30 °C for 72 h

6.2 blastx Results

Table 6.1: Sequence and blastx results

T-HS1	length \nt	quality \%	description	query cover \%	E value	per. id. \%
pCM188_47-F	130	28.52	hypothetical protein CWB94_23930 [*Pseudoalteromonas piscicida*]	96	2e-20	95.24
pCM188_51-R	969	55.76	Ub-tTA [synthetic construct]	46	1e-58	97.95
T-HS2	length \nt	quality \%	description	query cover \%	E value	per. id. \%
pCM188_47-F	635	31.87	Nuclear Hormone Receptor family [*Caenorhabditis elegans*]	72	4e-42	57.14
pCM188_51-R	939	57.04	unnamed protein product [*Pneumocystis jirovecii*]	20	2e-36	100.00
T-HS3	length \nt	quality \%	description	query cover \%	E value	per. id. \%
pCM188_51-R	1003	55.61	Ub-tTA [synthetic construct]	44	2e-58	97.95
T-HS4	length \nt	quality \%	description	query cover \%	E value	per. id. \%
pCM188_47-F	457	28.75	-	-	-	-
pCM188_51-R	882	40.00	putative Troponin T [*Hypsibius dujardini*]	49	8e-35	48.95
T-HS5	length \nt	quality \%	description	query cover \%	E value	per. id. \%
pCM188_47-F	1012	54.33	-	-	-	-
pCM188_51-R	984	52.07	-	-	-	-
T-HS13	length \nt	quality \%	description	query cover \%	E value	per. id. \%
pCM188_2111-F	978	51.86	similar to *Drosophila melanogaster* CG9897 [*Drosophila yakuba*]	14	0.30	38.30
pCM188_2445-R	927	39.67	venom S1 protease 18 [*Lethocerus distinctifemur*]	23	0.009	38.46
T-HS14	length \nt	quality \%	description	query cover \%	E value	per. id. \%
pCM188_2111-F	982	51.34	RNB domain containing ribonuclease [*Nitrosospira* sp. Nsp14]	16	2.8	40.00
pCM188_2430-R	910	47.53	phosphoribosyl-aminoimidazole-succinocarboxamide synthase [*Roseburia intestinalis* M50/1]	17	6.3	36.73

Table 6.2: Sequence and blastx results

T-HS17	length \nt	quality \%	description	query cover \%	E value	per. id. \%
pCM188_47-F	957	55.87	-	-	-	-
T-OX41	length \nt	quality \%	description	query cover \%	E value	per. id. \%
pCM188_2131-F	911	52.22	gamma-butyrobetaine dioxygenase [*Candidatus Thioglobus* sp. NP1]	60	0.034	26.06
pCM188_2450-R	556	36.01	PREDICTED: gamma-butyrobetaine dioxygenase-like isoform X3 [*Acropora digitifera*]	98	1e-40	41.94
T-OX42	length \nt	quality \%	description	query cover \%	E value	per. id. \%
pCM188_2131-F	969	52.31	hypothetical protein TSAR_015336 [*Trichomalopsis sarcophagae*]	57	1e-63	68.81
pCM188_2450-R	795	39.65	hypothetical protein M422DRAFT_24623 [*Sphaerobolus stellatus* SS14]	27	7.1	28.99
T-OX43	length \nt	quality \%	description	query cover \%	E value	per. id. \%
pCM188_47-F	1024	54.12	hypothetical protein RvY_05566 [*Ramazzottius varieornatus*]	53	8e-28	52.99
T-OX44	length \nt	quality \%	description	query cover \%	E value	per. id. \%
pCM188_2111-F	987	50.91	myosin regulatory light chain, nonmuscle, putative [*Pediculus humanus corporis*]	60	4e-87	72.25
T-OX45	length \nt	quality \%	description	query cover \%	E value	per. id. \%
pCM188_2111-F	988	51.66	kelch repeat protein [*Aspergillus vadensis* CBS 113365]	38	0.48	33.33
pCM188_2430-R	926	48.08	Kelch-like protein 17 [*Actinomadura* sp. 14C53]	42	5e-04	33.06
T-OX51	length \nt	quality \%	description	query cover \%	E value	per. id. \%
pCM188_2131-F	949	50.99	adiponectin receptor protein 1-like [*Ciona intestinalis*]	60	4e-37	47.88
T-OX52	length \nt	quality \%	description	query cover \%	E value	per. id. \%
pCM188_2111-F	957	50.25	unnamed protein product [*Mus musculus*]	9	1e-04	74.07
pCM188_2430-R	905	46.90	-	-	-	-

Table 6.3: Sequence and blastx results

T-OX53	length \nt	quality \%	description	query cover \%	E value	per. id. \%
pCM188_2131-F	903	51.76	hypothetical protein RvY_11475 [*Ramazzottius varieornatus*]	47	1e-13	37.30
pCM188_2430-R	650	38.62	PDZ and LIM domain protein Zasp-like isoform X1 [*Photinus pyralis*]	31	2e-06	46.77
T-OX62	length \nt	quality \%	description	query cover \%	E value	per. id. \%
pCM188_2131-F	958	50.66	charged multivesicular body protein 5-like [*Eurytemora affinis*]	78	1e-96	67.42
pCM188_2430-R	889	36.28	charged multivesicular body protein 5-like [*Eurytemora affinis*]	63	8e-81	65.84
T-OX65	length \nt	quality \%	description	query cover \%	E value	per. id. \%
pCM188_2131-F	939	51.18	chromosome transmission fidelity protein 8 homolog [*Diabrotica virgifera virgifera*]	37	2.5	30.4
T-OX66	length \nt	quality \%	description	query cover \%	E value	per. id. \%
pCM188_2131-F	889	52.20	Short-chain dehydrogenase/reductase family 42E member 1 [*Hypsibius dujardini*]	47	3e-23	44.72
pCM188_2430-R	916	48.70	short-chain dehydrogenase/reductase family 42E member 1 [*Lingula anatina*]	71	5e-52	44.04
P1E4	length \nt	quality \%	description	query cover \%	E value	per. id. \%
pCM188_47-F	973	54.68	-	-	-	
pCM188_51-R	688	38.56	-	-	-	
P1E5	length \nt	quality \%	description	query cover \%	E value	per. id. \%
pCM188_2111-F	933	52.01	serum paraoxonase/arylesterase 1 [*Strongylocentrotus purpuratus*]	74	9e-16	30.15
pCM188_51-R	-	-	hypothetical protein RvY_05702-1 [*Ramazzottius varieornatus*]	52	1e-15	39.37

Table 6.4: Sequence and blastx results

P1E6	length \nt	quality \%	description	query cover \%	E value	per. id. \%
pCM188_47-F	998	55.20	hypothetical protein RvY_07866 [*Ramazzottius varieornatus*]	62	2e-74	60.00
pCM188_51-R	1015	53.98	inositol oxygenase [*Danio rerio*]	30	2e-45	72.00
P1E8	length \nt	quality \%	description	query cover \%	E value	per. id. \%
pCM188_47-F	968	55.86	DNA excision repair protein ERCC-8 [*Stylophora pistillata*]	84	2e-25	29.24
pCM188_51-R	959	54.58	DNA excision repair protein ERCC-8-like [*Cryptotermes secundus*]	48	8e-19	34.76
P1C12	length \nt	quality \%	description	query cover \%	E value	per. id. \%
pCM188_47-F	949	55.58	hypothetical protein RvY_09030 [*Ramazzottius varieornatus*]	79	3e-74	46.12
pCM188_51-R	658	37.60	hypothetical protein RvY_09030 [*Ramazzottius varieornatus*]	74	2e-47	54.97
P2F6	length \nt	quality \%	description	query cover \%	E value	per. id. \%
pCM188_2111-F	974	52.09	adenosine kinase 2-like isoform X2 [*Limulus polyphemus*]	77	3e-60	46.30
pCM188_2430-R	805	35.25	hypothetical protein AXG93_48s1130 [*Marchantia polymorpha subsp. ruderalis*]	45	6e-30	53.85
P3G1	length \nt	quality \%	description	query cover \%	E value	per. id. \%
pCM188_2111-F	997	51.55	-	-	-	
pCM188_2430-R	991	47.41	hypothetical protein COCSUDRAFT_68340 [Coccomyxa subellipsoidea C-169]	22	0.002	32.88

6.3 Conserved region

Table 6.5: Conserved region search of T-HS1-pCM188_47-F and T-HS1-pCM188_51-R using the tool of NCBI; name of hits; interval on DNA sequence; E value; accession number

primer	name	interval	E value	accession
pCM188_47-F	rap1_RCT super family	3-74	7.20e-06	cl13131
pCM188_51-R	lacZ super family	442-615	4.19e-25	cl35850
pCM188_51-R	DUF155 super family	668-778	3.81e-06	cl00751
pCM188_51-R	PHA03380 super family	42-425	2.98e-10	cl33731

Table 6.6: Conserved region search of T-HS3-pCM188_51-R using the tool of NCBI; name of hits; interval on DNA sequence; E value; accession number

primer	name	interval	E value	accession
pCM188_51-R	lacZ super family	442-615	5.67e-25	cl35850
pCM188_51-R	PHA03380 super family	42-425	3.40e-10	cl33731

Table 6.7: Conserved region search of T-HS13-pCM188_2111-F and -pCM188_2445-R using the tool of NCBI; name of hits; interval on DNA sequence; E value; accession number

primer	name	interval	E value	accession
pCM188_2111-F	Trypsin super family	774-968	1.32e-04	cl27237

Table 6.8: Conserved region search of T-OX41 using the tool of NCBI; name of hits; interval on DNA sequence; E value; accession number

primer	name	interval	E value	accession
pCM188_2131-F	carnitine_bodg super family	306-671	6.15e-05	cl37106
pCM188_2450-R	carnitine_bodg super family	13-555	2.52e-39	cl37106

Table 6.9: Conserved region search of T-OX42 using the tool of NCBI, name of hits, interval on DNA sequence, E value, accession number

primer	name	interval	E value	accession
pCM188_2131-F	FRQ1	181-498	1.64e-16	COG5126
pCM188_2131-F	FRQ1 super family	32-187	1.41e-08	cl34916

Table 6.10: Conserved region search of T-OX42 using the tool of NCBI; name of hits; interval on DNA sequence; E value; accession number

primer	name	interval	E value	accession
pCM188_2131-F	IG_nFLMN	496-762	4.93e-24	smart00557
pCM188_2131-F	Filamin super family	211-471	3e-13	cl27659

Table 6.11: Conserved region search of T-OX44 using the tool of NCBI; name of hits; interval on DNA sequence; E value; accession number

primer	name	interval	E value	accession
pCM188_2111-F	FRQ1	227-673	4.30e-31	COG5126

Table 6.12: Conserved region search of T-OX51 using the tool of NCBI; name of hits; interval on DNA sequence; E value; accession number

primer	name	interval	E value	accession
pCM188_2131-F	HlyIII super family	519-824	2.36e-29	cl03831

Table 6.13: Conserved region search of T-OX53 using the tool of NCBI; name of hits; interval on DNA sequence; E value; accession number

primer	name	interval	E value	accession
pCM188_2430-R	ZM super family	156-233	4.75e-07	cl30972

Table 6.14: Conserved region search of T-OX62 using the tool of NCBI; name of hits; interval on DNA sequence; E value; accession number

primer	name	interval	E value	accession
pCM188_2131-F	Snf7 super family	69-698	6.67e-70	cl21588
pCM188_2430-R	Snf7 super family	317-886	1.37e-59	cl21588

Table 6.15: Conserved region search of P1E6 using the tool of NCBI; name of hits; interval on DNA sequence; E value; accession number

primer	name	interval	E value	accession
pCM188_47-F	MIOX super family	496-948	2.59e-76	cl04959
pCM188_51-R	MIOX super family	694-993	7.88e-59	cl04959

Table 6.16: Conserved region search of P1E8 using the tool of NCBI; name of hits; interval on DNA sequence; E value; accession number

primer	name	interval	E value	accession
pCM188_47-F	WD40 super family	170-937	4.75e-12	cl29593
pCM188_51-R	WD40 super family	496-876	5.02e-06	cl29593

6.4 Similarity to EST database of E. testudo

Table 6.17: T-HS4-pCM188_47-F and -pCM188_51-R blasted against SRX448019 and the resulting hit with query cover, E value, percent identity (per. id.) and accession number

primer	query cover %	E value	per. id. %	accession
pCM188_47-F	100	0.0	93.65	SRA:SRR1141094.434831.2
pCM188_51-R	88	0.0	96.72	SRA:SRR1141094.347171.2

Table 6.18: T-HS5-pCM188_47-F and -pCM188_51-R blasted against SRX448019 and the resulting hit with query cover, E value, percent identity (per. id.) and accession number

primer	query cover %	E value	per. id. %	accession
pCM188_47-F	13	3e-61	100.00	SRA:SRR1141094.189819.2
pCM188_51-R	75	0.0	97.13	SRA:SRR1141094.53292.2

Table 6.19: T-HS13-pCM188_2111-F and -pCM188_2445-R blasted against SRX448019 and the resulting hit with E value query cover, percent identity (per. id.) and accession number

primer	query cover %	E value	per. id. %	accession
pCM188_2111-F	15	8e-67	96.77	SRA:SRR1141094.367160.2
pCM188_2445-R	73	0.0	94.01	SRA:SRR1141094.115558.2

Table 6.20: T-HS14-pCM188_2430-R blasted against SRX448019 and the resulting hit with E value query cover, percent identity (per. id.) and accession number

primer	query cover %	E value	per. id. %	accession
pCM188_2430-R	51	0.0	96.26	SRA:SRR1141094.198643.2

Table 6.21: T-HS17-pCM188_47-F blasted against SRX448019 and the resulting hit with E value query cover, percent identity (per. id.) and accession number

primer	query cover %	E value	per. id. %	accession
pCM188_47-F	82	0.0	97.17	SRA:SRR1141094.379036.2

Table 6.22: T-OX41 blasted against SRX448019 and the resulting hit with E value, query cover, percent identity (per. id.) and accession number

primer	query cover %	E value	per. id. %	accession
pCM188_2131-F	50	0.0	97.76	SRA:SRR1141094.402082.2
pCM188_2450-R	99	0.0	98.37	SRA:SRR1141094.75746.2

Table 6.23: T-OX42 blasted against SRX448019 and the resulting hit with E value, query cover, percent identity (per. id.) and accession number

primer	query cover %	E value	per. id. %	accession
pCM188_2131-F	71	0.0	98.67	SRA:SRR1141094.266974.2
pCM188_2450-R	89	0.0	98.44	SRA:SRR1141094.344205.2

Table 6.24: T-OX43 blasted against SRX448019 and the resulting hit with E value, query cover, percent identity (per. id.) and accession number

primer	query cover %	E value	per. id. %	accession
pCM188_2131-F	79	0.0	98.02	SRA:SRR1141094.363270.2

Table 6.25: T-OX44 blasted against SRX448019 and the resulting hit with E value, query cover, percent identity (per. id.) and accession number

primer	query cover %	E value	per. id. %	accession
pCM188_2111-F	52	0.0	98.87	SRA:SRR1141094.353563.2

Table 6.26: T-OX45 blasted against SRX448019 and the resulting hit with E value, query cover, percent identity (per. id.) and accession

primer	query cover %	E value	per. id. %	accession
pCM188_2111-F	80	0.0	99.26	SRA:SRR1141094.301394.2
pCM188_2430-R	75	0.0	98.93	SRA:SRR1141094.67610.2

Table 6.27: T-OX51 blasted against SRX448019 and the resulting hit with E value, query cover, percent identity (per. id.) and accession

primer	query cover %	E value	per. id. %	accession
pCM188_2131-F	21	3e-75	96.00	SRA:SRR1141094.351641.2

Table 6.28: T-OX52 blasted against SRX448019 and the resulting hit with E value, query cover, percent identity (per. id.) and accession

primer	query cover %	E value	per. id. %	accession
pCM188_2430-R	67	0.0	99.29	SRA:SRR1141094.428453.2

Table 6.29: T-OX53 blasted against SRX448019 and the resulting hit with E value, query cover, percent identity (per. id.) and accession

primer	query cover %	E value	per. id. %	accession
pCM188_2131-F	52	0.0	97.57	SRA:SRR1141094.43055.2
pCM188_2430-R	90	0.0	96.75	SRA:SRR1141094.254832.2

Table 6.30: T-OX62 blasted against SRX448019 and the resulting hit with E value, query cover, percent identity (per. id.) and accession

primer	query cover %	E value	per. id. %	accession
pCM188_2131-F	87	0.0	98.92	SRA:SRR1141094.198423.2
pCM188_2430-R	75	0.0	99.0	SRA:SRR1141094.108853.2

Table 6.31: T-OX65 blasted against SRX448019 and the resulting hit with E value, query cover, percent identity (per. id.) and accession

primer	query cover %	E value	per. id. %	accession
pCM188_2131-F	87	0.0	98.92	SRA:SRR1141094.198423.2
pCM188_2131-F	48	0.0	99.48	SRA:SRR1141094.153001.2

Table 6.32: T-OX62 blasted against SRX448019 and the resulting hit with E value, query cover, percent identity (per. id.) and accession

primer	query cover %	E value	per. id. %	accession
pCM188_2131-F	39	4e-148	98.65	SRA:SRR1141094.395677.2
pCM188_2430-R	72	0.0	94.25	SRA:SRR1141094.320929.2

Table 6.33: P1E6 blasted against SRX448019 and the resulting hit with E value, query cover, percent identity (per. id.) and accession

primer	query cover %	E value	per. id. %	accession
pCM188_47-F	22	2e-97	95.95	SRA:SRR1141094.437615.2
pCM188_51-R	72	0.0	92.69	SRA:SRR1141094.423876.2

Table 6.34: P1E5 blasted against SRX448019 and the resulting hit with E value, query cover in %, percent identity (per. id.) in % and accession number

primer	query cover %	E value	per. id. %	accession
pCM188_2111-F	85	0.0	97.66	SRA:SRR1141094.196987.2
pCM188_51-R	100	0.0	96.31	SRA:SRR1141094.367392.2

Tobias Schierscher

tobias.schierscher@gmx.ch | +43 681 81750231

PERSONAL INFORMATION

Nationality:
Principality of Liechtenstein

born on 1994|12|02
in Grabs | Switzerland

Address:
Aeulestrasse 32
9495 Triesen
Principality of Liechtenstein

SKILLS

COMPUTER AND IT

Windows, ChemDraw, MS Office, Scifinder, Origin, Latex, Adobe Illustrator, R, Linux

LANGUAGES

German (mother tongue)
English (fluent)
French (beginner)

INTERESTS

ACTIVITIES

Jogging, football, hiking, climbing

EDUCATION

MASTER STUDIES "TECHNICAL CHEMISTRY" | TU VIENNA

2018|08 - expected 2020|06
Major in "Biotechnology & Bio-analytics"
Thesis: "Stress-protective Genes from Tardigrades"
supervised by Prof. Per Sunnerhagen
contact: per.sunnerhagen@cmb.gu.se | +46 31 786 3830

BACHELOR STUDIES "TECHNICAL CHEMISTRY" | TU VIENNA

2014|10 - 2018|08
Thesis: "Flavanone-3-β-Hydroxylase Expression in *E. coli*"
supervised by Assoc. Prof. Oliver Spadiut
contact: oliver.spadiut@tuwien.ac.at | +43 1 58801 166473

BORG | FELDKIRCH

2010|09 - 2014|06
upper secondary grammar school with a focus on physics, biology and chemistry

REALSCHULE | SCHAAN

2006|08 - 2010|06

RESEARCH EXPERIENCE

UNIVERSITY OF GOTHENBURG | MSC THESIS "STRESS-PROTECTIVE GENES FROM TARDIGRADES"

2019|08 - 2020|03
S. cerevisiae and *E. coli* transformation, stress response in *S. cerevisiae*, Bioinformatic protein and nucleic acid sequence analysis, phylogenetic analyses, Scan-o-matic, Bioscreen
supervised by Prof. Per Sunnerhagen

TU VIENNA | INTERNSHIP IN BIOCHEMISTRY, MICROBIOLOGY AND GENE TECHNOLOGY

2018|08 - 2018|10
Cultivation of *T. reesei*, homologous recombination, metabolite analysis, Co-Immunoprecipitation, SDS-PAGE, Western Blot
supervised by Dr.rer.nat. Christian Derntl
contact:christian.derntl@tuwien.ac.at | +43 1 58801 166565

TU VIENNA | BSC THESIS "FLAVANONE-3-β-HYDROXYLASE EXPRESSION IN E. COLI"

2017|05 - 2017|08
Recombinant protein expression in *E. coli*, protein purification, HPLC, FACS, shake flask experiments, fermentation
supervised by Assoc. Prof. Oliver Spadiut

WORK EXPERIENCE

SEVERAL STUDENT JOBS

- CEC - Continuing Education Center TU Vienna (2018|09 - 2019|06): seminar responsible (preparation and follow-up; production and duplication of learning materials and scripts)
- MATZKE GmbH Co. KG: bartender
- Wolfgang Flach Gartenbau-Anstalt: landscaper
- Rupert Hoop Zimmerei AG: roofer